NorthWest Research Associates, Inc.
P.O. Box 3027 • Bellevue, WA 98009-3027

NWRA-CR-97-R176 27 February 1998

A Beach Probing System (BPS) for Determining Surf Zone Bathymetry, Currents, and Wave Heights from Measurements Offshore: Phase I - The Prototype Development and Capability Demonstration

Semi-Annual Report #3

Covering the Period 1 April 1997 Through 30 September 1997
For Contract N00014-95-C-0217

Prepared by
Joan Oltman-Shay
James A. Secan
Douglas C. Echert
and
Frank Smith

DISTRIBUTION STATEMENT A
Approved for public release;
Distribution Unlimited

Prepared for
Dr. Thomas Kinder
Program Manager
Office of Naval Research
Ballston Tower One
800 North Quincy Street
Arlington, VA 22217-5660

19980310 157

DTIC QUALITY INSPECTED 4

14508 N.E. 20th Street • Bellevue, WA 98007-3713 • (425) 644-9660 • FAX (425) 644-8422

NWRA-CR-97-R176 27 February 1998

A Beach Probing System (BPS) for Determining Surf Zone Bathymetry, Currents, and Wave Heights from Measurements Offshore: Phase I - The Prototype Development and Capability Demonstration

Semi-Annual Report #3

Covering the Period 1 April 1997 Through 30 September 1997
For Contract N00014-95-C-0217

Prepared by
Joan Oltman-Shay
James A. Secan
Douglas C. Echert
and
Frank Smith

Prepared for
Dr. Thomas Kinder
Program Manager
Office of Naval Research
Ballston Tower One
800 North Quincy Street
Arlington, VA 22217-5660

EXECUTIVE SUMMARY

This report contains both a technical and financial accounting of BPS activities from 1 April 1997 through 30 September 1997. In addition, the project technical objectives and anticipated work for the next six months, and any schedule changes and alerts are outlined. Only the active, technical tasks (Tasks 1-4) are discussed in the Work Performed section; Tasks 5 and 6 are contract options and Task 7 is the management, planning, and reporting task.

The six months reported herein have focused on finalizing the instrument and software design and field deployment strategy, and further developing and testing the inverse model for extracting depth profile estimates from infragravity wave measurements.

A few of the more significant instrument design decisions are:

- We have chosen to use Sontek's Acoustic Doppler Velocimeter (ADV Ocean) as opposed to the Marsh-McBirney electro-magnetic current meter (EMCM);
- The ADV will mount on a pressure case that contains a pressure sensor, flash memory, Tattletale CPU, oven-controlled oscillator, compass/inclinometer, and batteries;
- There is an auxiliary port for the powering and collection of externally mounted instruments such as a conductivity/temperature sensor;
- The sensor package will be deployed mounted on the anchor pipe without the ability for in-situ adjustments of the package on the pipe.

Further description and discussion of the instrument and mounting design can be found in Section 1.4.2.

Influencing instrument design and array deployment methods is the error associated with array-element position measurement and clock synchronization. An analysis of these errors is presented in Section 1.1.3 of this report.

In September 1997 we traveled to Duck, NC, to participate in the instrument deployment of Reggie Beach's surf zone sensors and to discuss instrument design and deployment strategies with the Field Research Facility (FRF) staff and other PIs at the Duck field site. The lessons learned influenced our final instrument and deployment design. Our notes from that trip are summarized in Section 1.2.2.

In August 1997 we successfully deployed and tested our prototype instrument designs in the field (Copalis Beach, Washington). A report of this test is presented in Section 1.2.3, followed by an outline of objectives and sensor deployment strategy for the next Copalis Beach field test (Section 1.2.4).

Finally, our study of the inverse method is described in Section 1.1.2 where the Template Matching Technique (TMT), discussed in detail in the Semi-Annual Report #2 (May 1997), is

now applied to nonplanar depth profiles. To determine the accuracy and stability of the TMT plane-beach approximation, we studied depth profiles from the beaches of Torrey Pines, CA; Santa Barbara, CA; and Duck, NC. The perturbation expansion of the infragravity edge wave solution, also discussed in the Semi-Annual Report #2, was further studied to address the accuracy of its solution when given TMT-estimated plane beach profile approximations as a zeroth-order depth profile and the difference between the plane beach and true depth profile as the first-order depth profile input. A comparison of the perturbation-equation edge wave solutions with solutions from the full equations was made to investigate the reasonableness of using the perturbation equations for the inverse model.

An integral component of this report are the previous Semi-Annual Reports and the documentation of the BPS hardware and software designs and operation plans (listed below). These latter BPS documents are "living" documents in that they will be undergoing modifications, additions, and enhancements throughout the life of the project. Please note that documents and/or volumes shown with an asterisk are not available at this date. Other referenced material follows the list of BPS Documents.

List of BPS Documents

BPS Semi-Annual Report #1 (Oct. 1996, NWRA-CR-96-R160)

BPS Semi-Annual Report #2 (May 1997, NWRA-CR-97-R164)

BPS Software Documentation (NWRA-CR-96-R0156)

- Vol. I. On-shore Software Design Specification
- Vol. II. In-situ Software Design Specification
- Vol. III. Array Controller Software Design Specification*

BPS Hardware Documentation (NWRA-CR-96-R161)

- Vol. I. Instrument Design Specification
- Vol. II. Field Deployment Hardware Design Specification*

BPS Bench Testing Documentation (NWRA-CR-98-xxxx)*

- Vol. I. Bench Test Specification
- Vol. II. Bench Test Results (Array 1)
- Vol. III. Bench Test Results (Array 2)

BPS Concept Testing Software Documentation (NWRA-CR-98- xxxx)*

- Vol. I. Concept-Testing Software Design Specification
- Vol. II. Concept-Testing GUI Design Specification

BPS Concept of Field Operations Documentation (NWRA-CR-98-xxxx)*

- Vol. I. Field Campaign #1 - Concept of Operations
- Vol. II. Field Campaign #2 - Concept of Operations
- Vol. III. Field Campaign #3 - Concept of Operations

Other Referenced Material

Evergreen Pacific, 1996, *Evergreen Pacific Tide Guide 1997,* Evergreen Pacific Publishing Ltd., Seattle, WA.

Falques, A. and V. Iranzo, 1992, "Edge waves on a longshore shear flow," Physics of Fluids, A4, pp. 2169-2190.

Howd, P.A., A.J. Bowen, and R.A. Holman, 1992, "Edge waves in the presence of strong longshore currents," J. Geophys. Res., vol. 97, C7, pp. 11,357-11,371.

Oltman-Shay, J.M. and P.A. Howd, 1993, "Edge Waves in Nonplanar Bathymetry and Alongshore Currents: A Model and Data Comparison," J. Geophys. Res., v. 98, C2, pp. 2495-2507.

Putrevu, U., and J. Oltman-Shay, 1997, "Influence Functions for Edge Wave Propagation Over a Nonplanar Bottom Bathymetry," Phys. of Fluids, v. 10 (1), pp. 330-332.

Thornton, E.B. and R.T. Guza, 1986, "Surf zone longshore currents and random waves: field data and models," J. Phys. Oceaongr., vol. 16, 7, pp. 1165-1178.

USGS (1994) "Copalis Beach, WA, 7.5 minute topographic map," No. 47124-A2-TF-024, United States Geological Survey, based on aerial photographs taken 1990.

TABLE OF CONTENTS

LIST OF FIGURES

LIST OF TABLES

1.0 WORK PERFORMED 1 APRIL 1997 – 30 SEPTEMBER 1997

1.1 Task 1: Concepts and Algorithm Development

1.1.1 Overview

In the Semi-Annual Report #2 (May 1997), we listed the Task-1 milestones and objectives to be met by the end of the six-month reporting period. These are listed again below.

1) Continue the testing of the Template Matching Technique (TMT) as an inverse method for obtaining depth profile estimates from offshore infragravity edge wave observations.
2) Compare the (infragravity) edge wave perturbation expansion solution against numerical solutions, investigating issues such as the effect of the choice of the zeroth-order beach slope on the first-order correction.
3) Study the magnitude and nature of the deviations from a plane-beach solution of both the edge wave dispersion and cross-shore solutions for various natural depth profiles and for a range of offshore measurement locations.
4) Design an inverse solution for the first-order correction to the plane-beach approximation.
5) Design the array geometry and offshore placement for Field Campaign #1.
6) Complete the design phase of the concept-testing GUI (which consists of a GUI, batch-processing script, and a conflicts executive); start implementation of code.
7) Update the BPS Concept Testing Software Documentation.

Presented below is a brief discussion of the status of these efforts with an outline of the results or a direction to the locations in this report with more detailed discussions.

1) Continue the testing of the Template Matching Technique (TMT).

   We ported the TMT code from Matlab (on a PC) to Fortran (on a Sun Ultra). The BPS operational code will be in Fortran on a PC. We have modified the TMT matching search to assume that the depth of measurement is known and have continued our study of the uniqueness, stability, and resolution of the TMT estimates using simulated data for planar depth profiles and for profiles from Torrey Pines (CA), Leadbetter (CA), and Duck (NC) beaches. The results of this work are discussed in Section 1.1.2 (The Inverse Method).

2) Compare the (infragravity) edge wave perturbation expansion solution against numerical solutions, and
3) Study the magnitude and nature of the deviations from a plane beach solution of both the edge wave dispersion and cross-shore solutions for various natural depth profiles and for a range of offshore measurement locations.

We applied the TMT to edge wave spectra, simulated for nonplanar depth profiles such as those from Duck, NC, etc. (see item 1 above), to obtain plane-beach slope approximations to the nonplanar depth profiles. Estimated beach slopes for each of the edge wave spectra were then used as the zeroth-order depth profile input for the perturbation expansion equation and the difference between the true depth profile and the zeroth-order planar beach was the first-order depth profile input. Comparisons were then made between the exact edge wave solutions (using the numerical method of Falques and Iranzo, 1992) and the perturbation equation solutions. These comparisons are discussed in detail in Section 1.1.2.2.

4) Design an inverse solution for the first-order correction to the plane-beach approximation.

   We are delaying this until Summer 1998. From our study of the TMT and perturbation expansion (items 1-3 above), we decided to first look at a two-slope fit of the depth profile using the TMT and study the quality of the perturbation expansion with those TMT estimates as the zeroth-order depth profile.

5) Design the array geometry and offshore placement for Field Campaign #1.

   Our first study of the TMT and perturbation expansion (items 1-3 above) suggests that the best depths for placement of the array are in 3 to 5m depth of water. Therefore, we are using those depths in our preliminary design of the array placement. However, we will be revisiting this with the two-slope TMT study. Thus far we have also only used one array geometry. Once we have completed the two-slope TMT study with this same geometry, we will study other geometries.

6) Complete the design phase of the concept-testing GUI; start implementation of code.

   Thus far, implementation of the code has been in the form of Perl Scripts used to automated our Monte Carlo tests of the TMT. A more complete description of this and the Java interface will be documented at a later date.

7) Update the BPS Concept Testing Software Documentation.

   This will be done at a later date.

1.1.2 The Inverse Method

This section reports on the progress of the development of the BPS inverse method. The objective of this method is to estimate the nearshore depth profile from wavenumber-frequency (k-f) spectral measurements of the offshore infragravity edge wave field (surface gravity waves like sea and swell but with longer periods and wavelengths). The measurements are assumed to be from an alongshore-aligned array of bottom-mounted current and pressure sensors. As discussed in detail in the BPS Semi-Annual Report #2 (May 1997), the approach we have chosen to study is a two-stage procedure.

In the first stage we apply the Template Matching Technique (TMT) to the k-f spectrum estimated from the alongshore array of current meter data. The output from the TMT is an

approximation to the true depth profile between the array and the shoreline.

In the second stage we use the TMT depth profile approximation and the measured k-f spectrum to estimate differences in the true depth profile from the TMT approximation. This estimation may be done by applying inverse methods to a perturbation expansion of the edge wave equations, where the first-order (inverse) solution can be the TMT-estimated depth profile and the second-order solution is the perturbations in depth about that profile.

1.1.2.1 The Template-Matching Technique

As its name implies, this technique matches measured k-f spectral parameters (i.e., data matrices) against a library of true k-f spectral parameters (i.e., test templates). The k-f spectral parameters that define the test template are obtained from a solution of the edge wave equations. The k-f test templates are built from a range of nearshore depth profile and offshore observation location inputs to the edge wave equations. Both edge wave dispersion and cross-shore variance structure information are in the k-f templates. The template is a 2-D (k-f) matrix of numbers. The k,f matrix element location that satisfies the edge wave dispersion solution is given a value of one. All other elements are zero. The cross-shore structure of the alongshore velocity variance is included by filtering out edge wave mode dispersion solutions (zeroing matrix element values) for modes that are relatively too weak to be observed; this decision is based on our experience with the behavior of our k-f spectral analysis tools and sensor array geometries. For the test template, we are presently setting the k,f matrix element of an edge wave mode to zero if the relative alongshore velocity variance of that mode is less than 0.9 times the mode with maximum velocity variance at the same frequency, f. The optimal method of mimicking the filtering of edge wave modes as observed by limited, offshore phase arrays and spectral analysis methods will be more closely studied at a later date. Further discussion of the TMT can be found in the BPS Semi-Annual Report #2 (May 1997).

1.1.2.1.1 Plane-slope beach results with depth known a priori

In the BPS Semi-Annual Report #2 (May 1997), we presented the results from the matching of data matrices, built from the edge wave spectra simulated for plane-slope (planar) beaches, to a TMT library of test templates built from edge wave spectra simulating spectra from different planar beaches. The depth of measurement was not assumed to be known. Here we present the TMT matching results for the scenario where depth of the array is assumed to be known from the pressure-sensor measurements.

The TMT was tested for a series of different depths (2-10 m at 1 m increments) and plane beach slopes (0.005 to 0.1 at 0.005 increments). Figures 1.1-1 through 1.1-4 compare TMT-estimated slopes against the true slope for spectra simulated for 2, 5, 8, and 10m measurement depths. For each slope/depth combination, 99 stochastic realizations (48 degrees of freedom) were run with a broadband Noise-to-Signal Ratio (NSR) of 0.05 and an array geometry simulating a 5-element array that spans 260m. The circles in the figures denotes the median TMT slope estimate and the error bars span one standard deviation about the median. Significant improvement was noted

when a-priori depth was assumed known.

Several important points can be made of these planar beach tests:

1) With a-priori depth known, the TMT method is exceptionally accurate when the measurement location is at a depth <8 meters. For a measurement depth of 2 meters, it was 100% accurate in all the simulation runs (Figure 1.1-1). With larger measurement depths, the deterioration of the accuracy of the measurement can be traced to the "collapse" of the measured edge wave spectrum to lower wavenumbers (longer wavelengths) for the simulated array geometry (5-element array with a maximum span of 260m; Figures 1.1-5 through 1.1-7).

   It appears that with our present implementation of the TMT, the resolution of the templates may be limited by the estimate of the half-power bandwidth of the peak in k-f space. We are simulating a half-power bandwidth that is typically observed in archival field data (0.002 m^{-1}) with similar array geometries. The TMT uses the estimated half-power bandwidth to define the nonzero k,f elements in the data matrix. For measurement depths >8m, the total range of alongshore wavenumbers are only of order ± 0.005 m^{-1}. Thus, as the measurement depth increases, it becomes increasingly difficult to distinguish between different slope estimates (compare Figures 1.1-5 through 1.1-7). One solution may be to use ¼-power bandwidths of the peaks to define the nonzero k,f elements in the data matrices.

2) In the BPS Semi-Annual Report #2 (May 1997), it was noted that there is a slight upward bias in the slope estimation which can be seen by plotting a histogram of TMT estimates. This bias is likely due to energy in the higher modes bleeding into the estimation of the k-f peak location. This higher mode number energy will cause the k estimate to be biased low and thus the slope estimate to be biased high. This bias is not as clear in these tests where depth of measurement is known a priori. However, we will continue to study estimator bias as the technique develops.

3) Potential improvements of the TMT plane beach approximation are worthy of investigation.

   a) Reducing the effect of the measurement scenario on the ½-power bandwidth estimate with changes in array geometry and a better handling of bandwidth smearing caused by e.g., tidal changes in water depth;

   b) Using ¼-power bandwidth instead ½-power bandwidth to define nonzero matrix elements in the data matrices;

   c) Building the data matrices using only k-f peaks of relatively high energy in the infragravity frequency band instead of the dominant peak in each frequency;

   d) Matching the measured the wavenumber bin of the peak power against a test template library that accounts for peak shifts due to the presence of multiple modes at a given frequency. For instance, building the test template library from a simulation of 10 or more edge wave modes with >400 degrees of freedom.

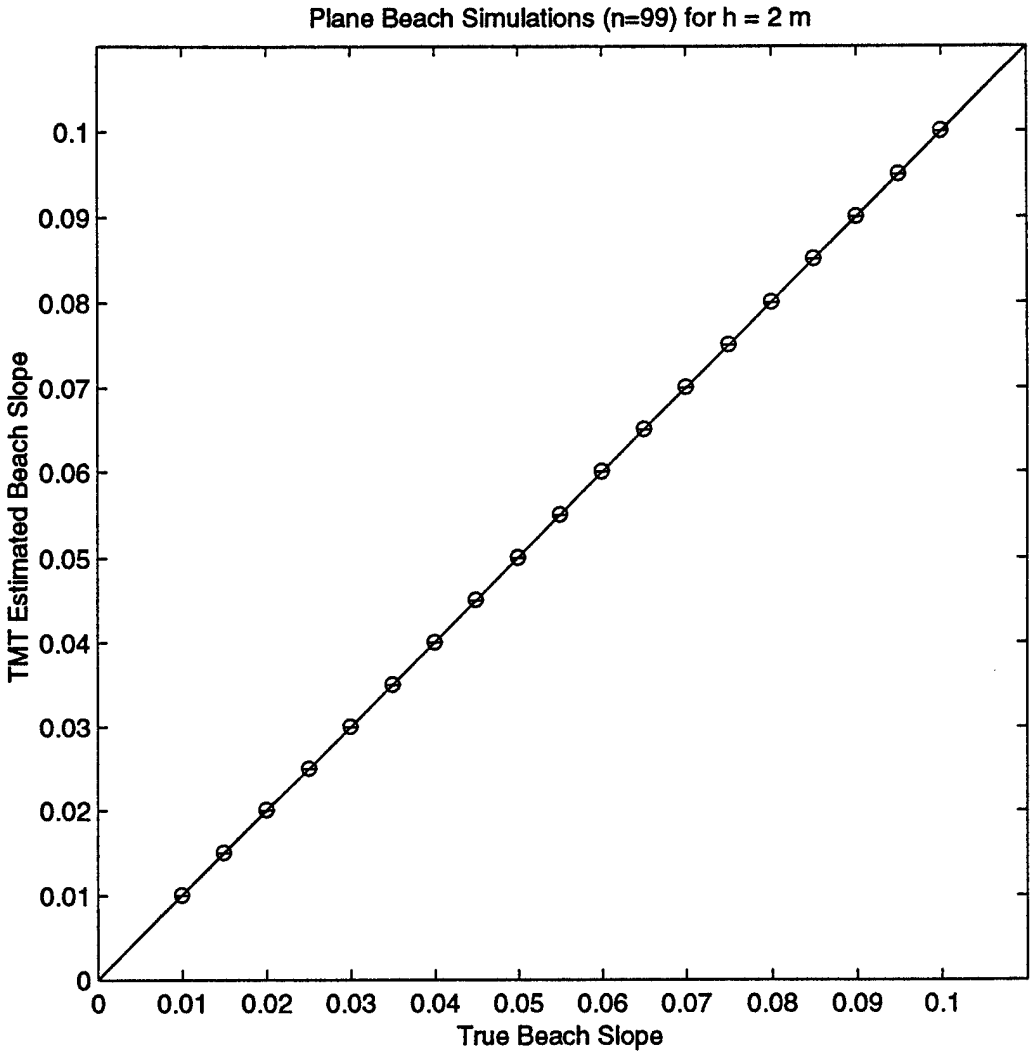

Figure 1.1-1. Comparison between TMT-estimated and true planar beach slopes for 99 stochastic realizations and a measurement depth of 2m. The circle denotes the median TMT estimate; the vertical bar spans one standard deviation. A bar within the circle boundaries denotes zero standard deviation.

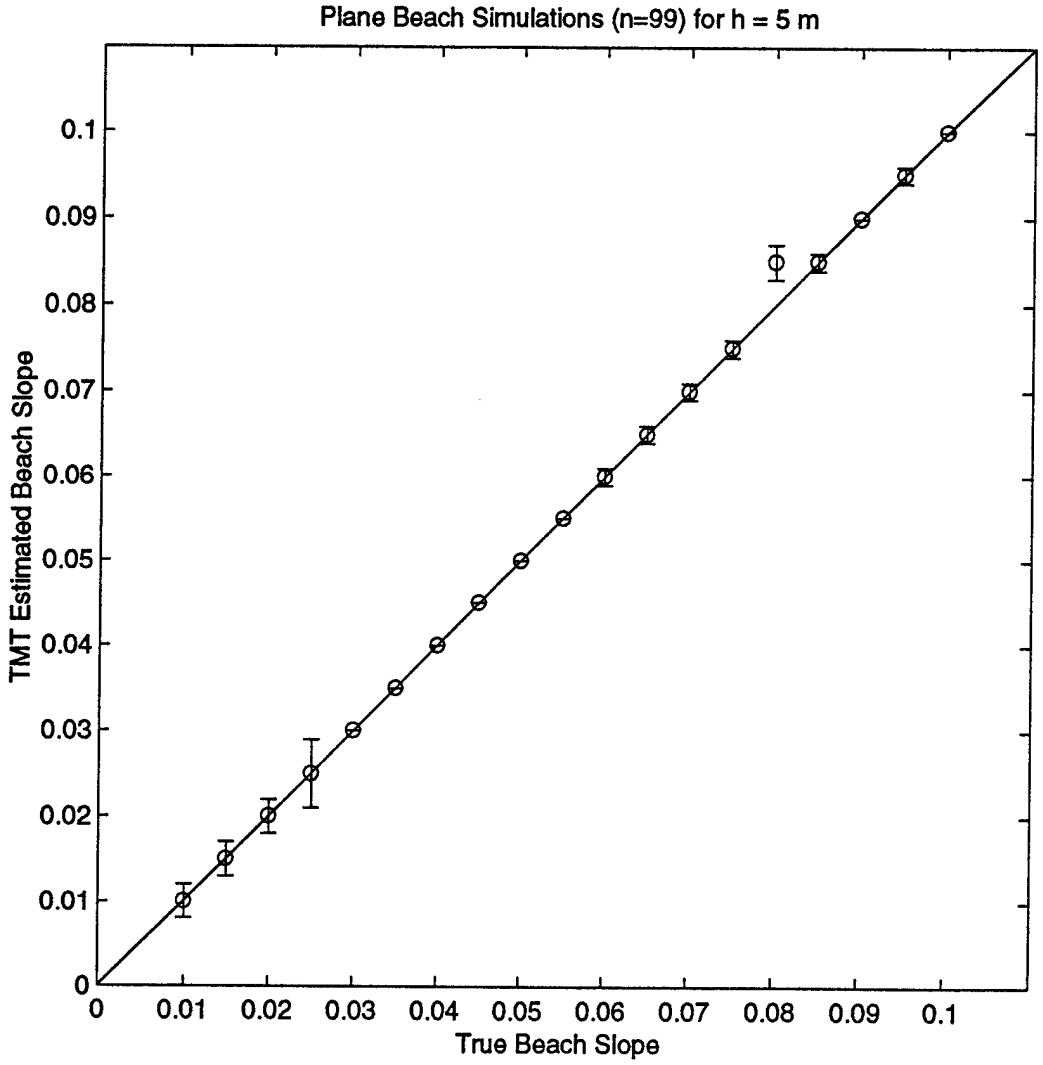

Figure 1.1-2. Same as 1.1-1, except a 5m instead of a 2m measurement depth.

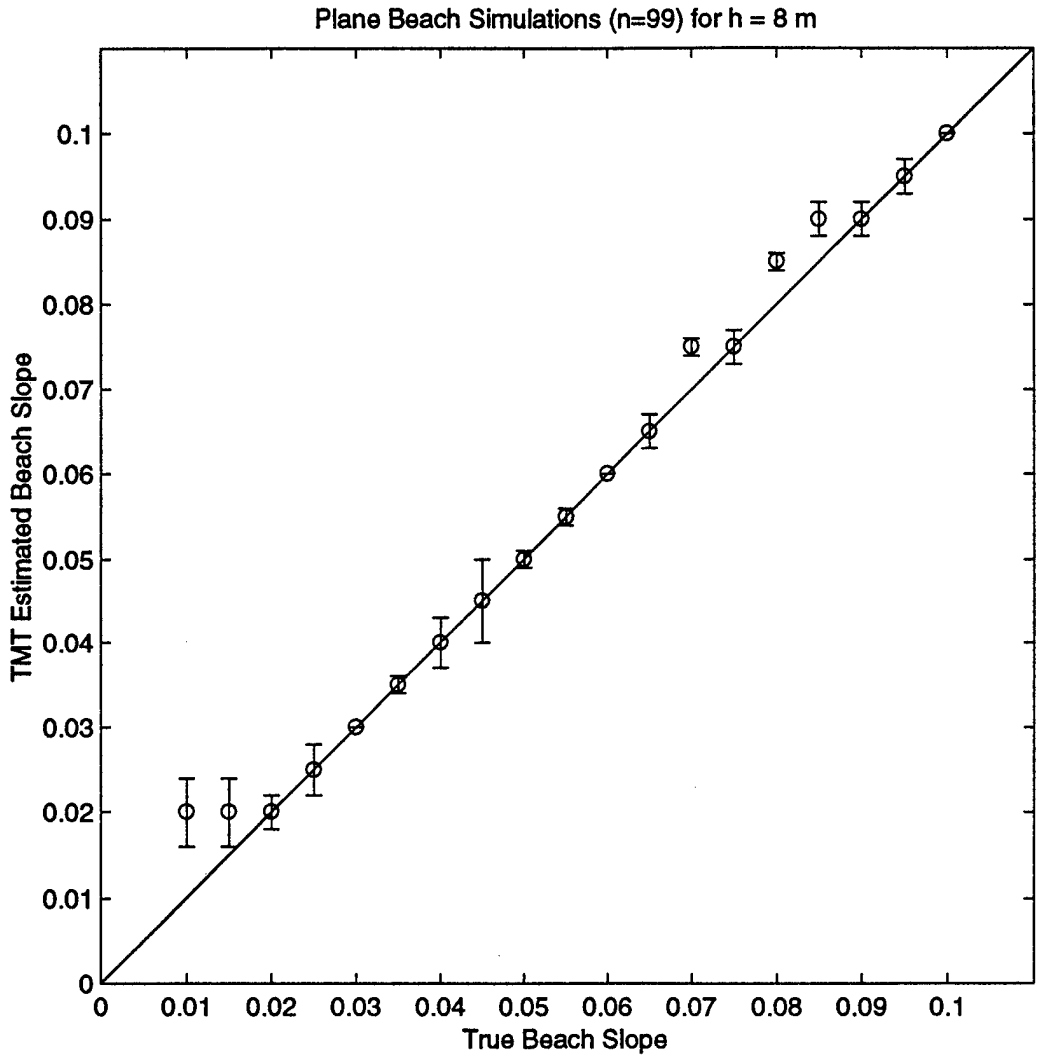

Figure 1.1-3. Same as 1.1-1, except an 8m instead of a 2m measurement depth.

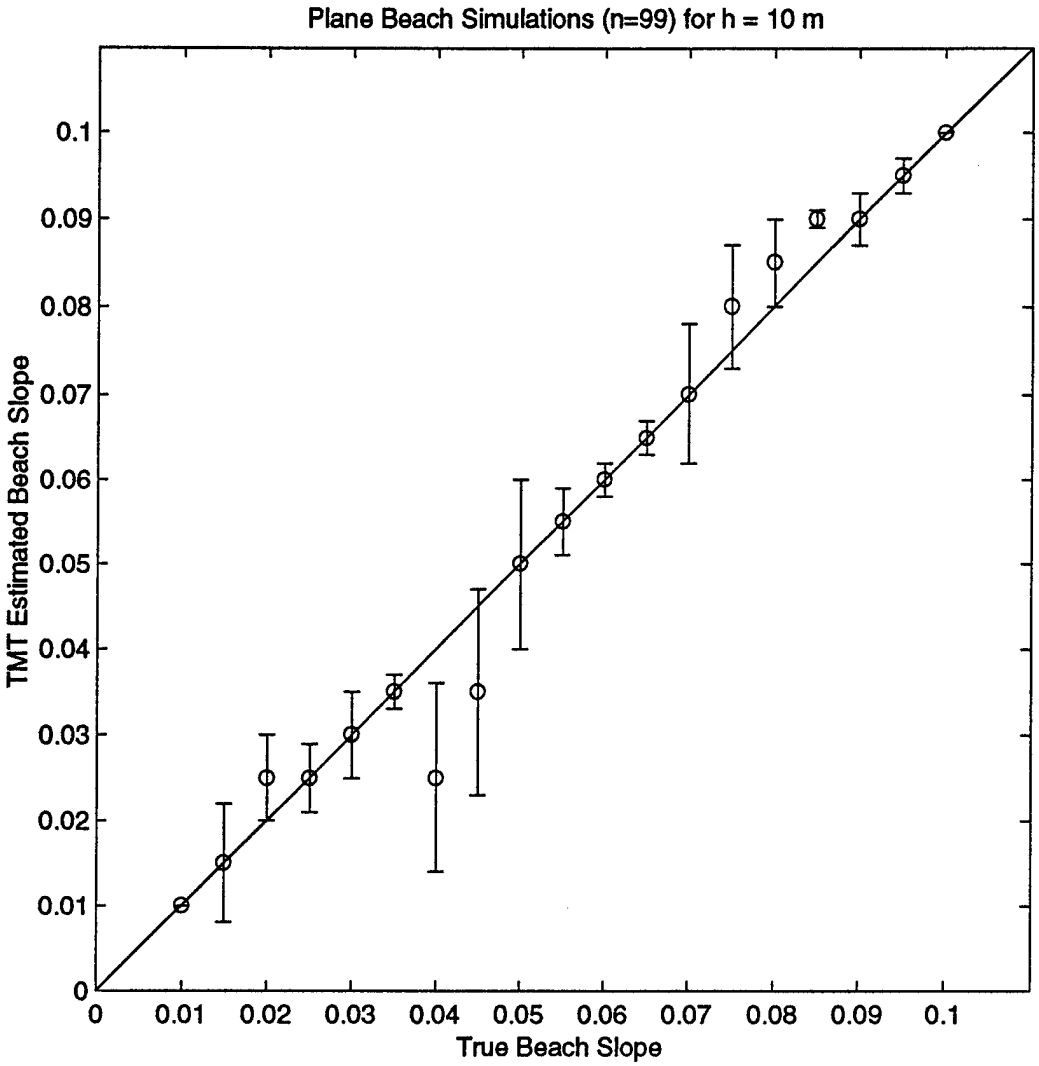

Figure 1.1-4. Same as 1.1-1, except a 10m instead of a 2m measurement depth.

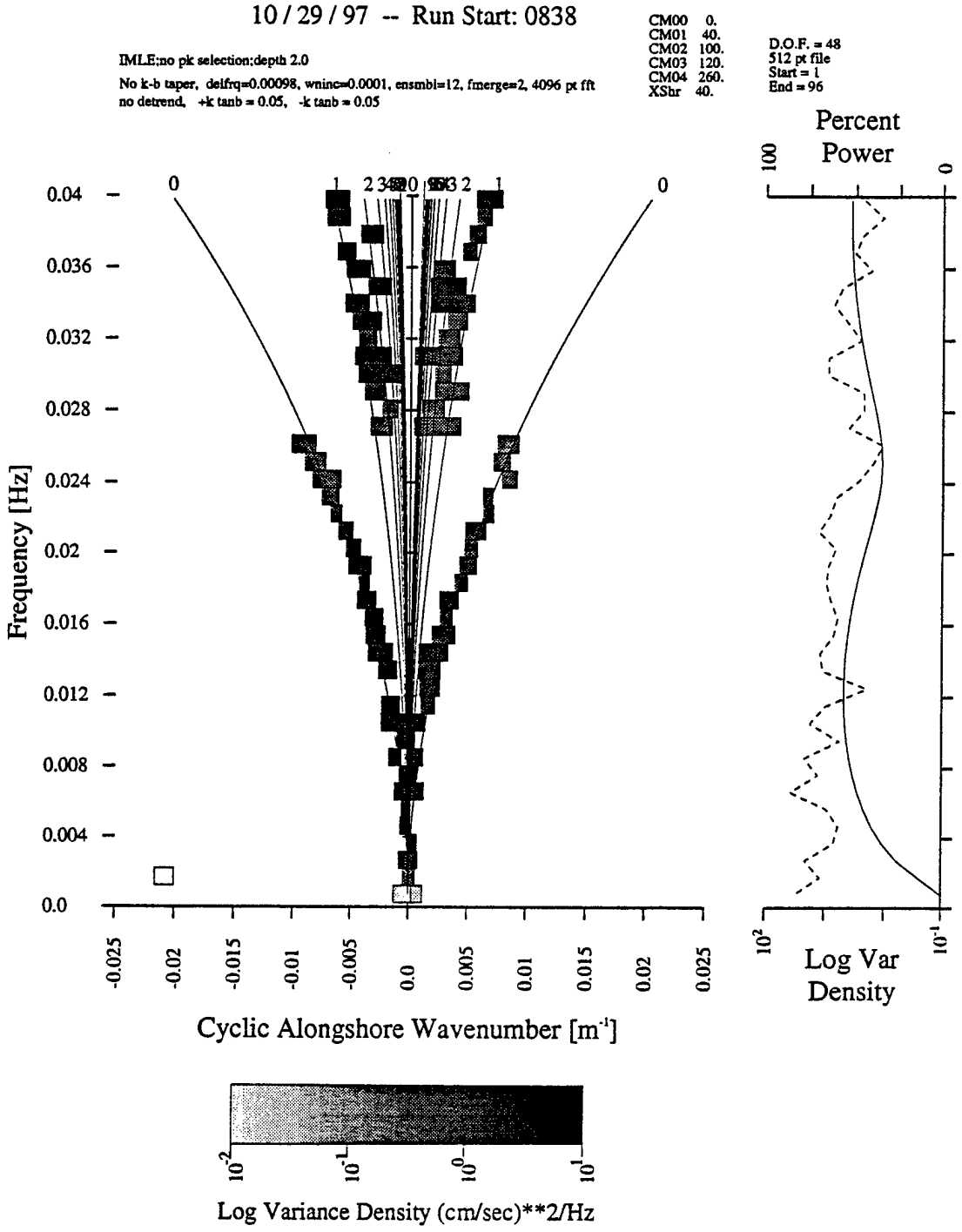

Figure 1.1-5. A wavenumber-frequency (*k-f*) spectrum for a planar beach with a 0.05 slope simulating measurement by a 5-element array (260m length) in 2m depth of water. The width of the boxes spans the half-power bandwidth of the wavenumber peak, the solid lines labeled 0, 1, 2, etc. are the plane beach dispersion solutions for modes 0, 1, 2, etc. The side panel shows the power-density spectrum (solid line) and the percent total power displayed in the *k-f* spectra (dashed line) (48 D.O.F., 0.05 NSR).

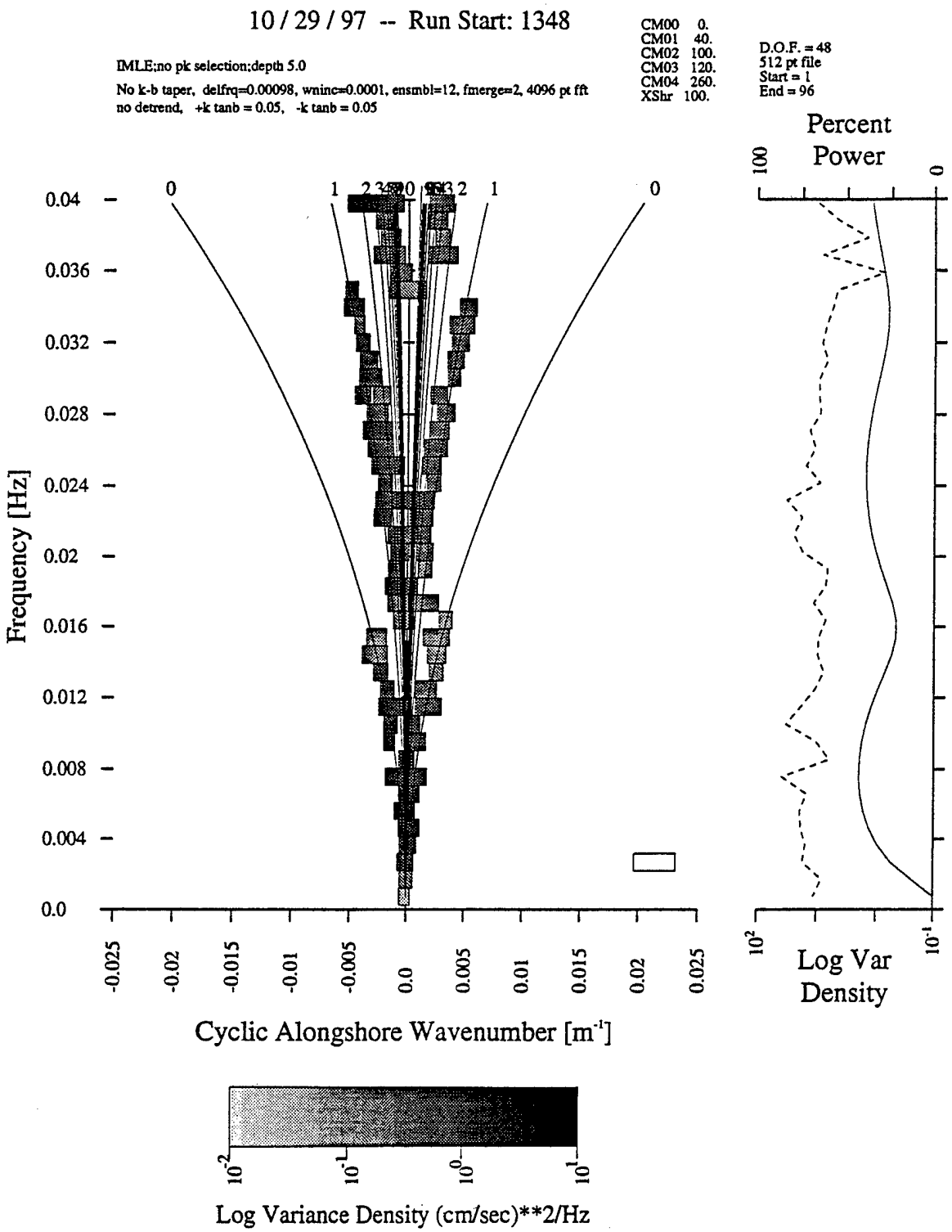

Figure 1.1-6. Same as 1.1-5, except a 5m measurement depth.

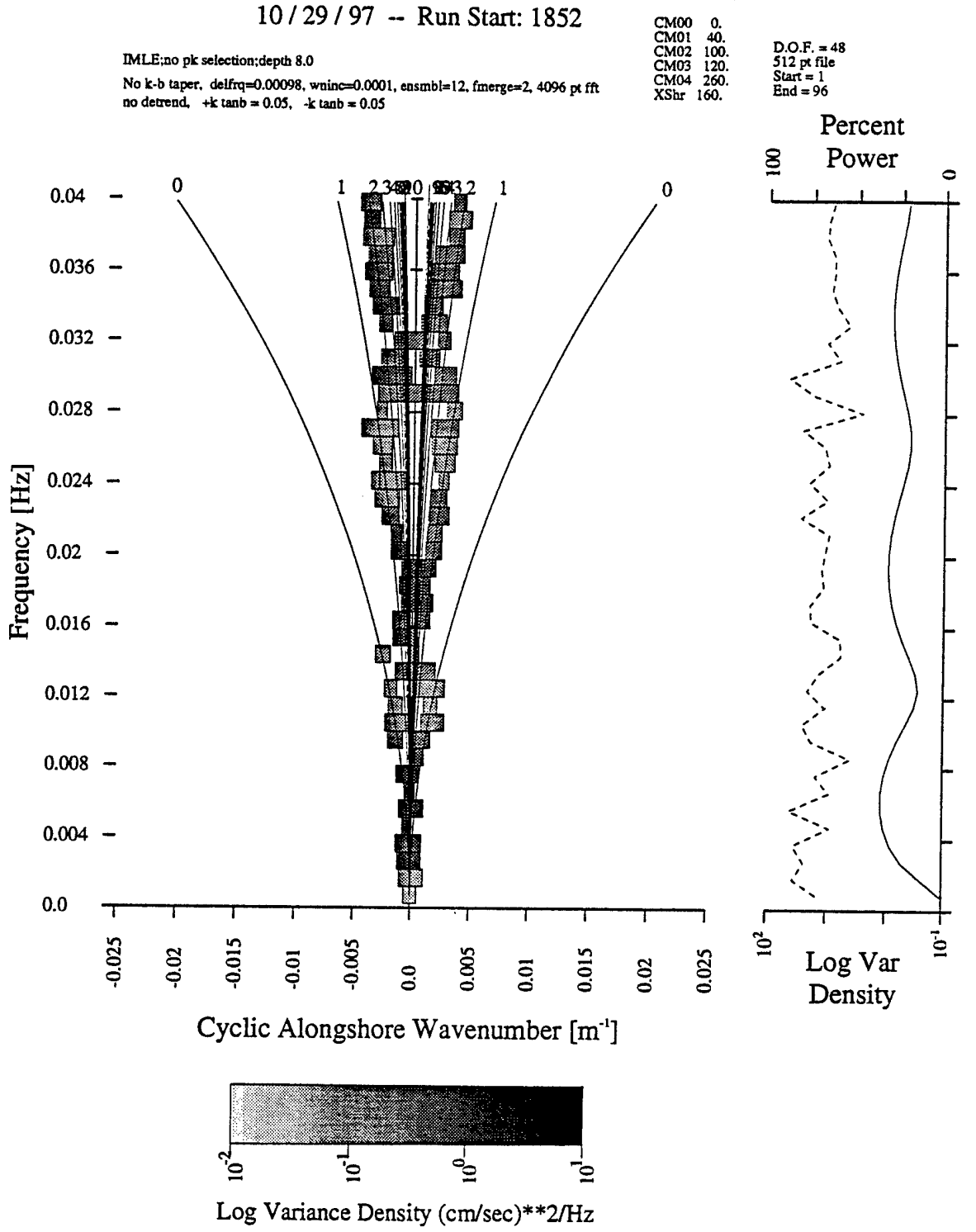

Figure 1.1-7. Same as 1.1-5, except an 8m measurement depth.

1.1.2.1.2 Nonplanar beaches - Torrey Pines, Santa Barbara, and Duck beaches

Testing has begun on the TMT using k-f spectra simulated for three nonplanar depth profiles from three beaches. The three profiles chosen are from Duck, NC (Samson and Delilah 1990 experiment), Santa Barbara, CA (NSTS 1980 experiment), and Torrey Pines, CA (NSTS 1978 experiment). These profiles were chosen for their distinct characteristics (Duck is barred, TP is planar with a steep foreshore, SB is four-sloped: steep to shallow to steep to shallow).

As described above, the TMT matches measured (or simulated) k-f spectra against a library of true k-f spectra. In our present implementation of the TMT, the TMT library consists only of plane beach spectra and, thus, by matching the nonplanar beach profiles against the test library we are attempting to make a planar approximation to the nonplanar profile. This estimate could be used as the zeroth order model (m_0) in the perturbation expansion (2^{nd} Semi-Annual Report, May 97). Again 100 stochastic realizations were simulated for each of the measurement depths (from 1 to 10 meters). The statistics from these tests are shown in Table 1.1-1. All three beaches are remarkably stable (small standard deviation) in their estimates.

The mean slope estimate at the two nearly planar beaches (TP & SB) do not vary as much as Duck with measurement depth. The standard deviation of the slope estimate is also smaller at TP and SB than at Duck. The median TMT depth profile from each of these three depth profiles is plotted against the true depth profile in Figures 1.1-8 through 1.1-10. There are three TMT estimates for each of the three "real" nonplanar depth profiles, one for each of three measurement depths (2, 5, and 8m). The fit of the TMT-estimated depth profile with TP and SB profiles is excellent. Duck is degraded by the extreme difference in the slope of the depth profile shoreward and seaward of ~150m. All the beaches demonstrate the TMT sensitivity to the nearshore (shoreline to ~100m) slope.

Table 1.1-1. Statistics of the TMT slope estimations from 100 stochastic realizations of *k-f* spectral measurements simulated for Torrey Pines (TP), Santa Barbara (SB), and Duck beach profiles and array measurement locations in 2 to 10m depth.

Model Name	Depth of Array (m)	X-Shore Loc. (m)	Median Slope	Mean Slope	Standard Deviation	Extrema (Max)	Extrema (Min)
TP	2	94	0.03	0.03	0	0.03	0.03
TP	3	134	0.03	0.03	0	0.03	0.03
TP	4	172	0.03	0.03	0.001	0.03	0.025
TP	5	216	0.03	0.024	0.006	0.03	0.01
TP	6	260	0.025	0.025	0.001	0.03	0.025
TP	7	300	0.025	0.025	0	0.025	0.025
TP	8	345	0.025	0.025	0.001	0.035	0.025
TP	9	390	0.025	0.025	0	0.025	0.025
TP	10	432	0.025	0.025	0.001	0.035	0.025
SB	2	40	0.055	0.055	0	0.055	0.055
SB	3	66	0.055	0.055	0	0.055	0.055
SB	4	88	0.055	0.055	0	0.055	0.055
SB	5	105	0.055	0.054	0.002	0.055	0.05
SB	6	120	0.055	0.055	0.001	0.055	0.05
SB	7	140	0.055	0.055	0.001	0.055	0.05
SB	8	186	0.05	0.05	0	0.05	0.05
SB	9	274	0.04	0.04	0.001	0.045	0.04
SB	10	372	0.035	0.035	0.005	0.04	0.015
Duck	2	79	0.045	0.044	0.002	0.045	0.04
Duck	3	111	0.04	0.04	0	0.04	0.04
Duck	4	147	0.035	0.035	0.001	0.04	0.035
Duck	5	278	0.03	0.023	0.008	0.03	0.01
Duck	6	413	0.02	0.021	0.004	0.03	0.015
Duck	7	561	0.02	0.02	0.005	0.03	0.015
Duck	8	709	0.02	0.019	0.005	0.035	0.015
Duck	9	857	0.02	0.021	0.006	0.035	0.015
Duck	10	1018	0.015	0.015	0.001	0.025	0.015

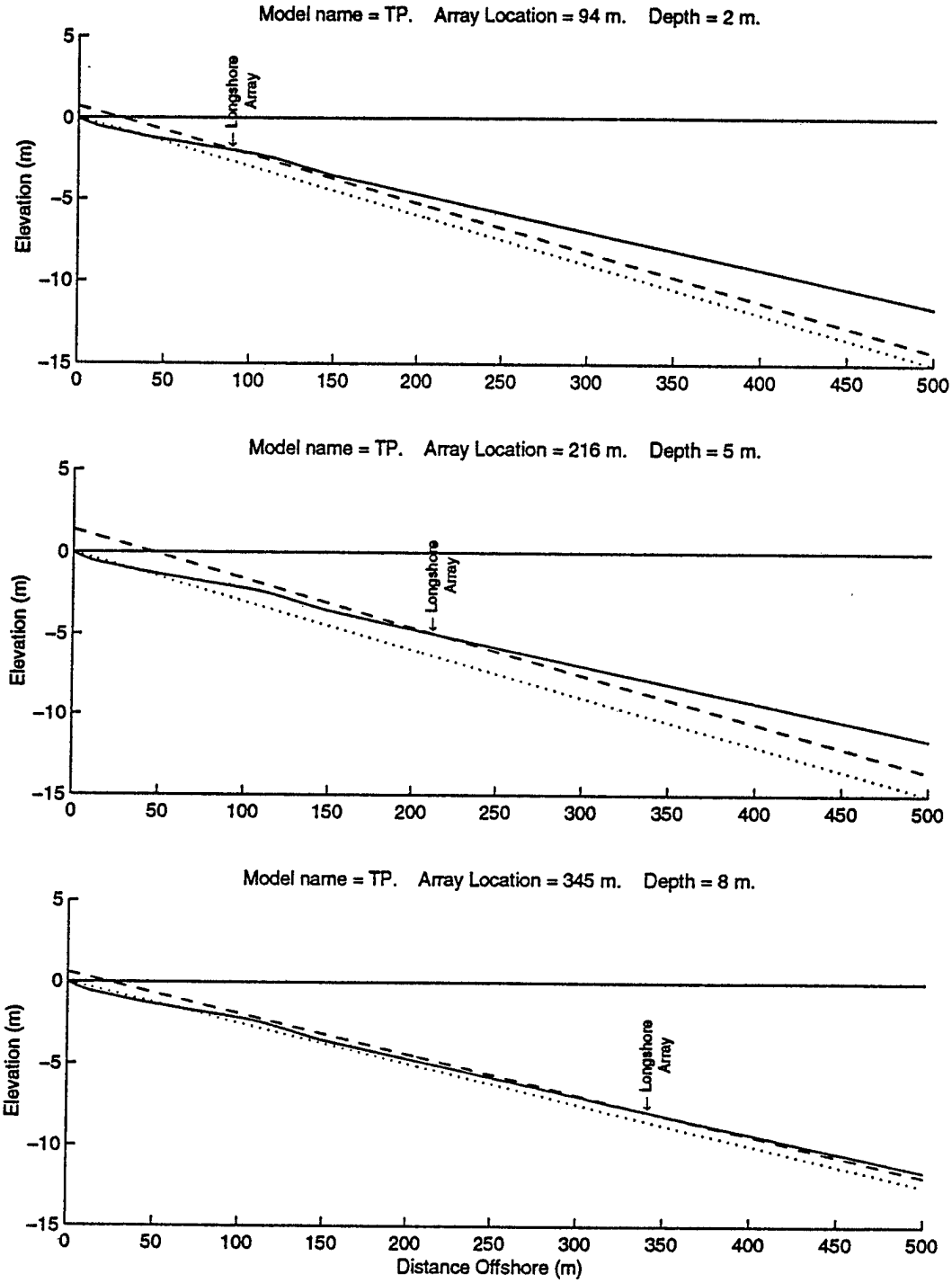

Figure 1.1-8. Torrey Pines Beach. Comparison of estimated (dot and dashed line) and true (solid line) depth profiles. TMT estimates were from measurements simulated for 2, 5 and 8m depth. The dashed line is constrained by the measurement depth. The dotted line is constrained to be zero at the shoreline (D.O.F. = 48, NSR = 0.05).

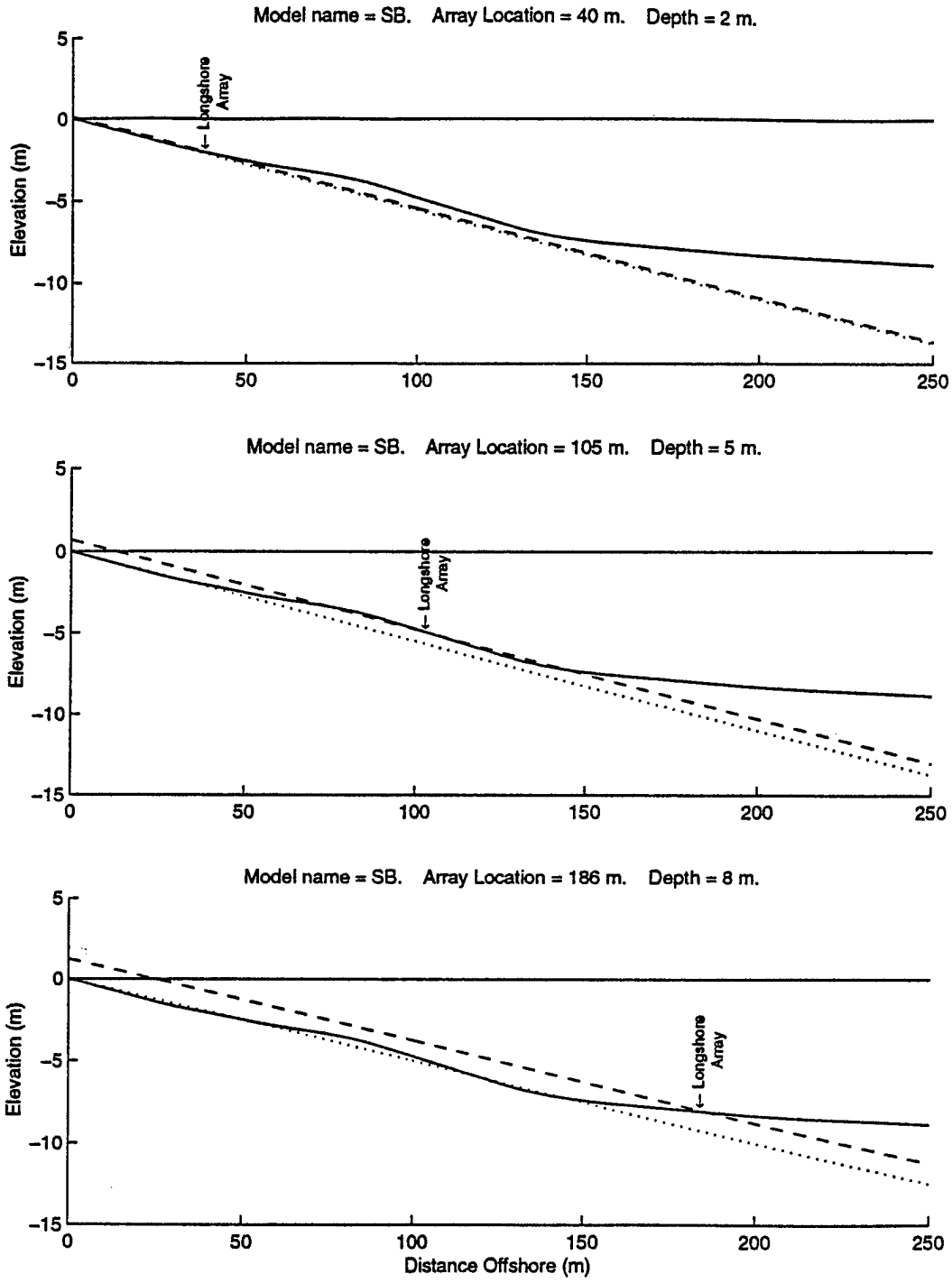

Figure 1.1-9. Santa Barbara Beach. See Figure 1.1-8 for description.

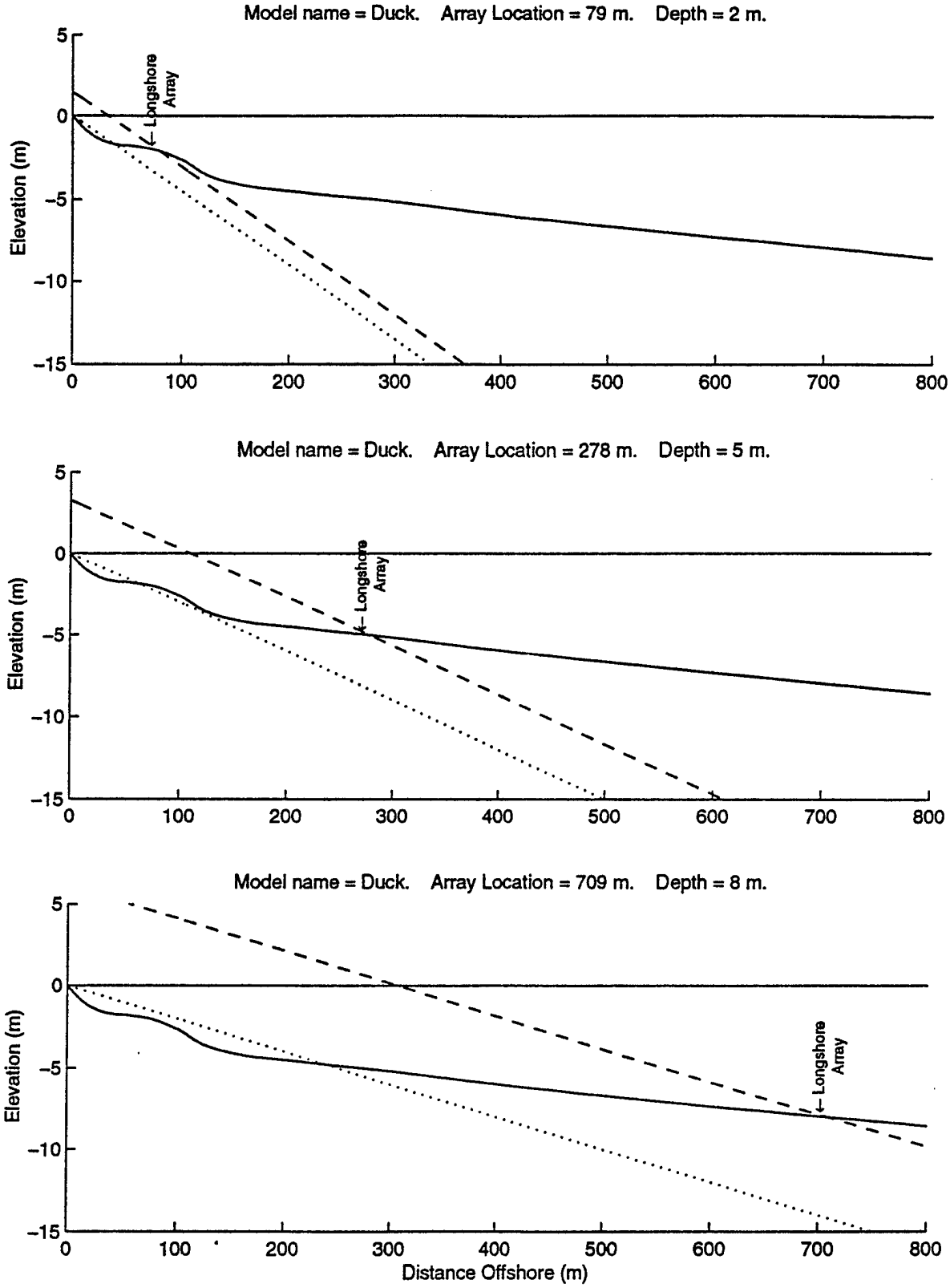

Figure 1.1-10. Duck Beach. See Figure 1.1-8 for description.

1.1.2.2 The Perturbation Expansion Solution – the effect of the zeroth-order depth profile approximation on the solution

The objective of this effort is to investigate the accuracy of the perturbation solutions for different zero-order planar approximations of the depth profile. In the BPS Semi-Annual Report #2 (May 1997), the infragravity wave solution sensitivity to nearshore depth profile features (such as steep foreshores, bars and troughs) was explored using a perturbation expansion of the edge wave equations. The depth profile and concomitant wave solutions were broken into two parts with the depth profile broken into a zeroth-order planar depth profile and a first-order perturbation about that profile. The results were encouraging; the infragravity solution showed sensitivity to nearshore depth profile features that we could exploit in an inverse model. We now want to know whether we can use an inverse model built on this perturbation equation to obtain nonplanar features in the depth profile. Our motivation for using the perturbation equations instead of the full equations is the computational speed and the easy integration with the TMT estimate. The next question then is whether the perturbation equation solution is accurate (a close approximation to the solution from the full equations) in the scenario we would employ it.

To address this, we applied the TMT to edge wave spectra simulated for the nonplanar depth profiles, from the Torrey Pines, Santa Barbara, and Duck beaches, to obtain plane beach slope approximations (Section 1.1.2.1.2). The median TMT-estimated planar beach slopes for each of the edge wave spectra were used as the zeroth-order depth profile input for the perturbation expansion equation and the difference between the true depth profile and the zeroth-order planar beach was the first-order depth profile input. Comparisons were made between the exact edge wave solutions (using the numerical method of Falques and Iranzo, 1992) and the solutions from the perturbation equation.

Table 1.1-2 lists the typical fractional errors of the perturbation solution from the full equation solution. Both the error in the dispersion solutions ($\Delta f/f_{TRUE}$) and the alongshore velocity variance solutions ($\Delta v^2/v^2_{TRUE}$) were examined. Differences between the perturbation solutions and the exact solutions were always found, the largest difference on each beach occurring in the alongshore velocity variance. Santa Barbara beach had the least error, and Duck had the most error.

Table 1.1-2. Typical fractional error of perturbation solution.

Typical fractional errors of the perturbation (PERT) solution from the full equation (TRUE) solution. The dispersion solution error, monitored with frequency, is $\Delta f/f_{TRUE}$, where $\Delta f = f_{TRUE}-f_{PERT}$. The cross-shore variance solution error, monitored with alongshore variance, is $\Delta v^2/v^2_{TRUE}$, where $\Delta v^2=v^2_{TRUE}-v^2_{PERT}$.

Beach	Range of Array Depths (m)	Median TMT Planar Slope	$\Delta f/f_{TRUE}$	$\Delta v^2/v^2_{TRUE}$
TP	2 - 6	0.03	0.04	0.20
SB	2 - 6	0.055	0.01	0.07
DUCK	2 - 6	0.03-0.045	0.15	0.50

Figures 1.1-11 through 1.1-19 step through the perturbation error analysis for an array measurement depth of ~4m on each of the three beaches. Other depths show, in general, similar results. The median TMT-estimated beach slope for this depth at each beach (Table 1.1-1) is used for the zeroth-order depth profile in the perturbation equation. The estimated depth profiles are plotted against the true depth profile for each beach in Figures 1.1-11, -14, and -17. The best fit of the TMT planar depth profile close to shore is for the Santa Barbara (SB) beach (Figure 1.1-14). The higher error in the TP perturbations solutions (Figures 1.1-12, -13) over those from a similar planar beach, SB (Figures 1.1-15, -16), is consistent with the observations of Oltman-Shay and Howd (1993) and Putrevu and Oltman-Shay (1997); the edge wave equations are more sensitive to shoreline features, like the steep foreshore at TP, than offshore features, like the terrace on the SB depth profile. If the TMT plane-beach approximation does not closely approximate the shoreline depth profile, then a large correction may be required to the zeroth-order solution. The difference between the zeroth- and first-order depth profile (h_0 and h_1, respectively) at this location may also be too large to be suitable for the perturbation expansion equation. One or both of these difficulties appears to occur with the TP depth profile. The ratio of the h_1/h_0 near the shoreline at TP is approximately one, violating the perturbation ordering, whereas the ratio at SB is reasonably small (compare Figures 1.1-11 and 1.1-14). Thus, the inherent sensitivity of the edge wave equations to the shoreline features and the violation of the perturbation ordering with the TMT planar estimate for h_0 make TP, a very planar beach, almost unsuitable for application of the perturbation equations.

Examination of the change in $\Delta f/f_{TRUE}$ with frequency further supports these conclusions. The trend of $\Delta f/f_{TRUE}$ with frequency at TP shows an increase with frequency (Figures 1.1-12). The higher-frequency edge waves are trapped closer to shore where h_0 does not approximate the steep foreshore well. However, the SB trend of the $\Delta f/f_{TRUE}$ error with frequency shows a decreased error with increased frequency (Figure 1.1-15). Here, the foreshore is closely approximated by the h_0, and the high-frequency edge waves close to shore are traveling on that closely

approximated section of beach. However, the lower-frequency edge waves are traveling over the offshore bathymetry that diverges from h_0 (Figure 1.1-14), thus increasing the error at these frequencies relative to the higher frequencies. Interestingly, the trend of $\Delta f / f_{TRUE}$ with frequency using the Duck depth profile goes both ways, perhaps in response to the nonmonotonic depth profile.

The results of this perturbation solution study clearly indicate that if we intend to use the perturbation expansion equations to obtain corrections to the TMT-estimated depth profile, then we are going to have to do a better job estimating the depth profile near the shoreline with the TMT. To that end, we are now investigating the enhancement of the TMT library of test templates to include two slope beaches where the nearshore slope, offshore slope, and depth of slope break are the free parameters. Clearly, a concern here is uniqueness of the solution. To further constrain the solution we are also investigating adding to the inverse problem the measurement of the infragravity wave travel time from the array to the shore and back. This information could be obtained from any and each of the sensor array elements.

One final side note: we have yet to address the effect of longshore currents on the TMT and perturbation estimates. In depths greater than 3 to 4m, we believe that the doppler-like shift of the infragravity *k-f* spectra will be negligible, and therefore the TMT library of test templates does not need to be modified. However, we will nonetheless investigate this. In shallower depths, we will investigate splitting the *k-f* spectrum into + and -*k* (up- and downcoast) parts and estimating a TMT depth profile from each half spectrum.

The corrections to the TMT estimate, using the perturbation equations, may be affected by the presence of a longshore current at greater depths than the TMT. The work of Howd et al. (1992) shows that infragravity edge waves respond to a longshore current as a sand bar or trough, dependent on the propagation direction. Therefore, we may be able to use inverse methods on each wavenumber half of the k-f spectrum to obtain longshore current magnitude and direction, separate from the effects of the topography. This infragravity wave-derived longshore current information would enhance that obtained from the Thornton and Guza (1986) longshore current model applied to the measured wind wave directional spectrum and depth profile. In particular, it could be used to calibrate the model.

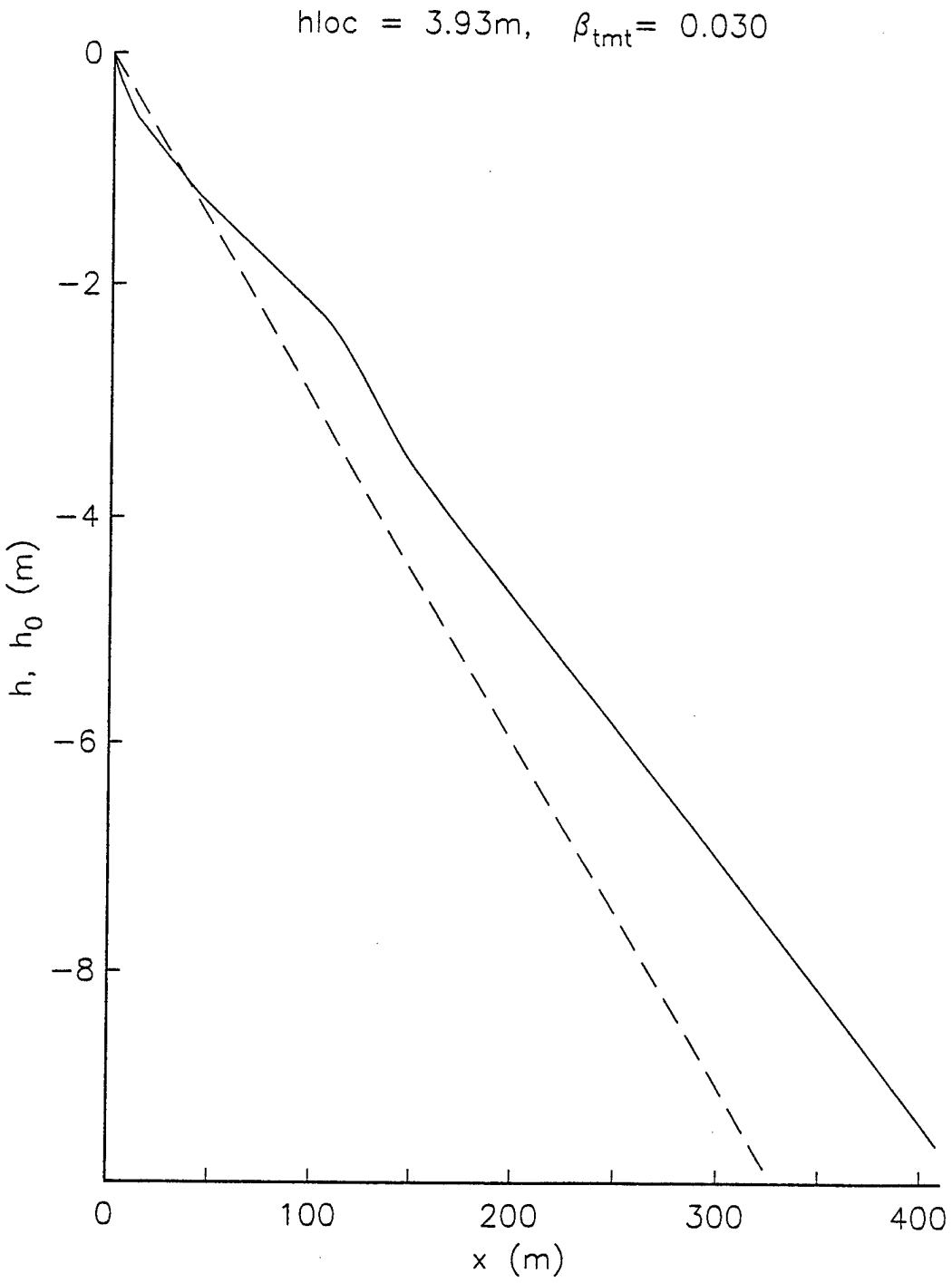

Figure 1.1-11. Torrey Pines Beach. A comparison between the median TMT-estimated (h_0) planar depth profile (0.030 slope, dashed line) and the true (h) depth profile (i.e., measured, solid line). The TMT-estimate is for an array measurement depth of approximately 4m.

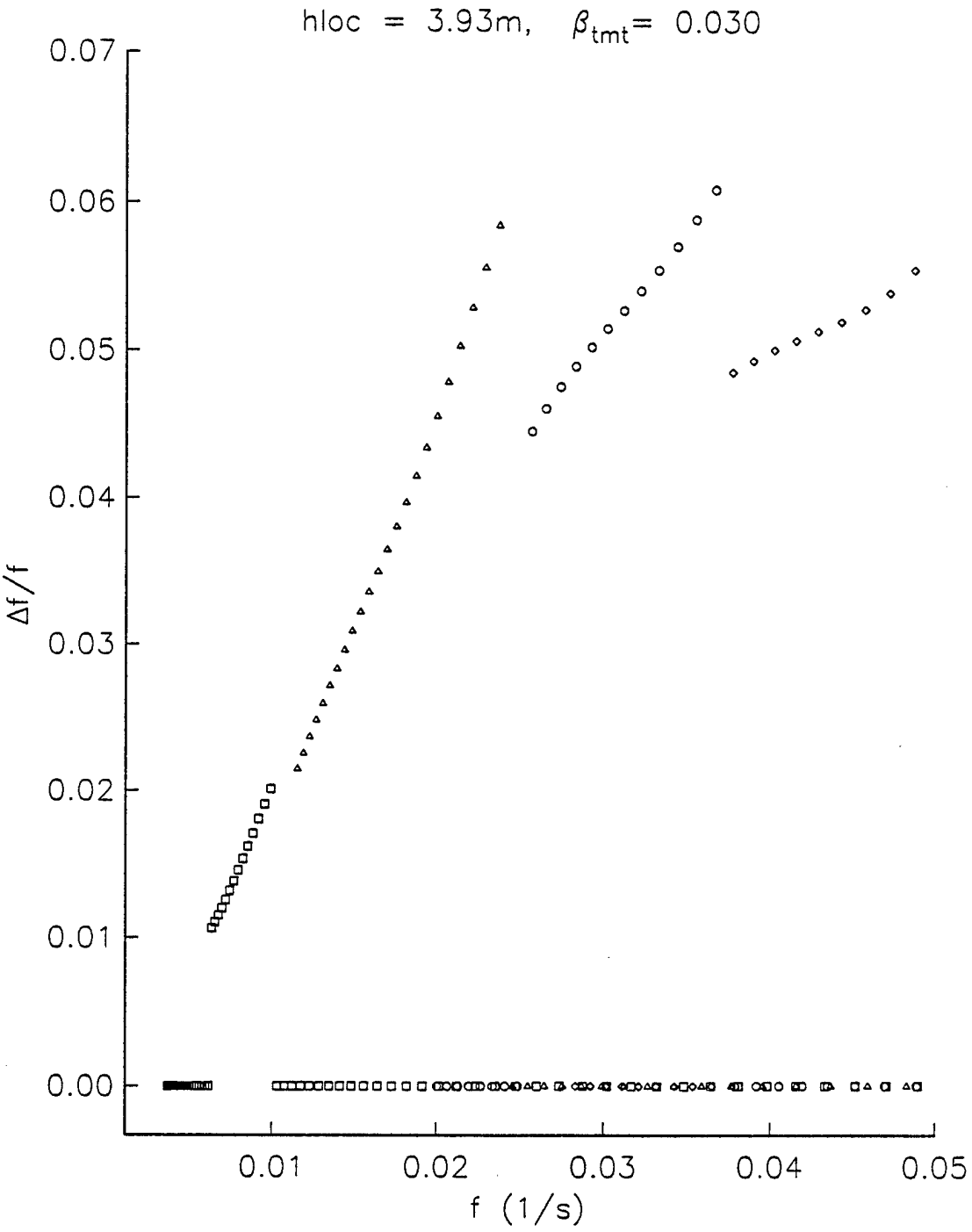

Figure 1.1-12. Torrey Pines Beach. A measure of the dispersion error in the perturbation expansion equation for the TMT-estimated zeroth-order depth profile in Figure 1.1-11. Shown is the fractional difference, $\Delta f / f_{TRUE}$, where $\Delta f = f_{PERT} - f_{TRUE}$, f_{PERT} is the perturbation solution, and f_{TRUE} is the full-equation solution.

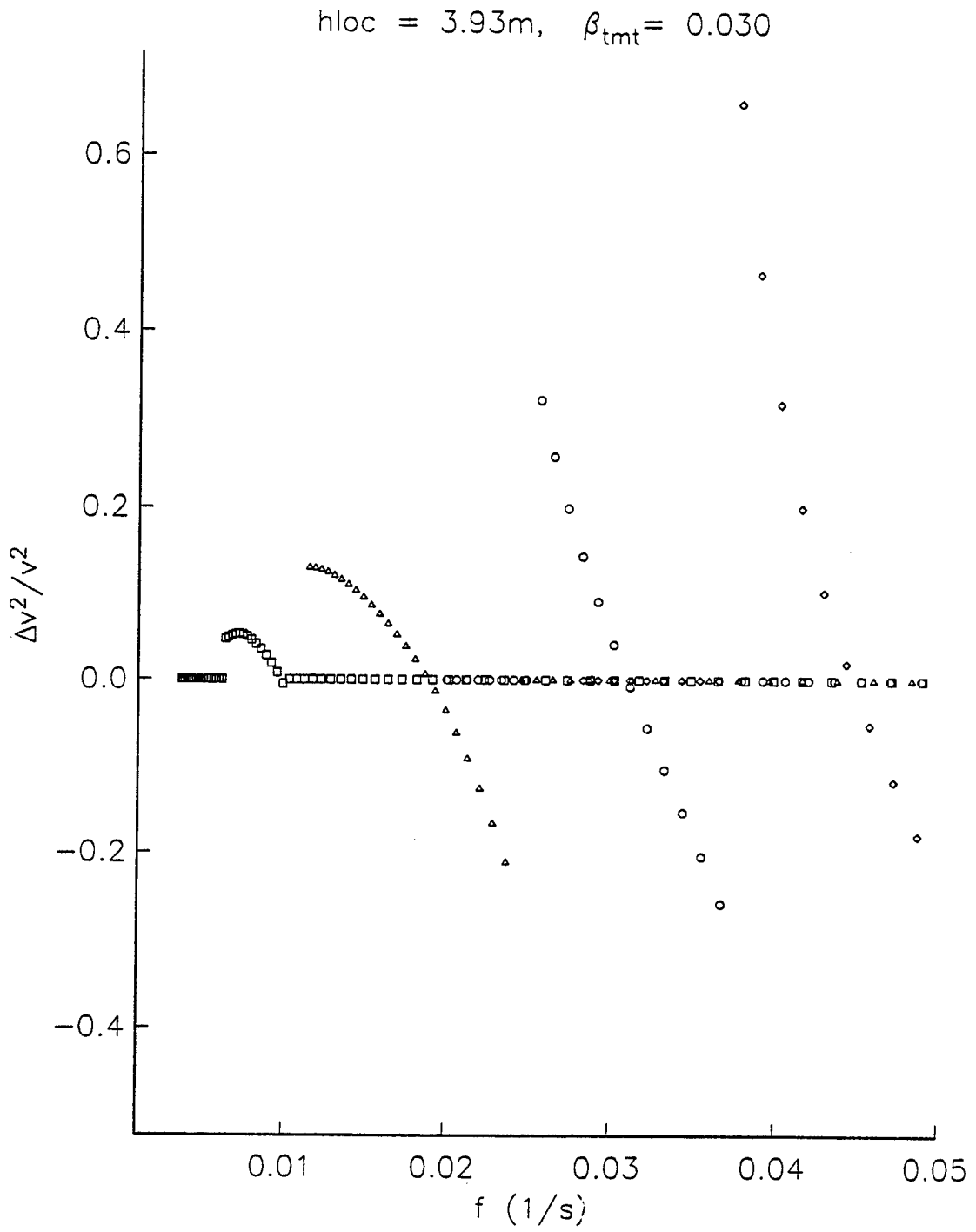

Figure 1.1-13. Torrey Pines Beach. A measure of the cross-shore variance error in the perturbation expansion equation for the TMT-estimated zeroth-order depth profile in Figure 1.1-11. Shown is the fractional difference, $\Delta v^2 / v^2_{TRUE}$, where $\Delta v^2 = v^2_{PERT} - v^2_{TRUE}$, v^2_{PERT} is the perturbation solution, and v^2_{TRUE} is the full-equation solution.

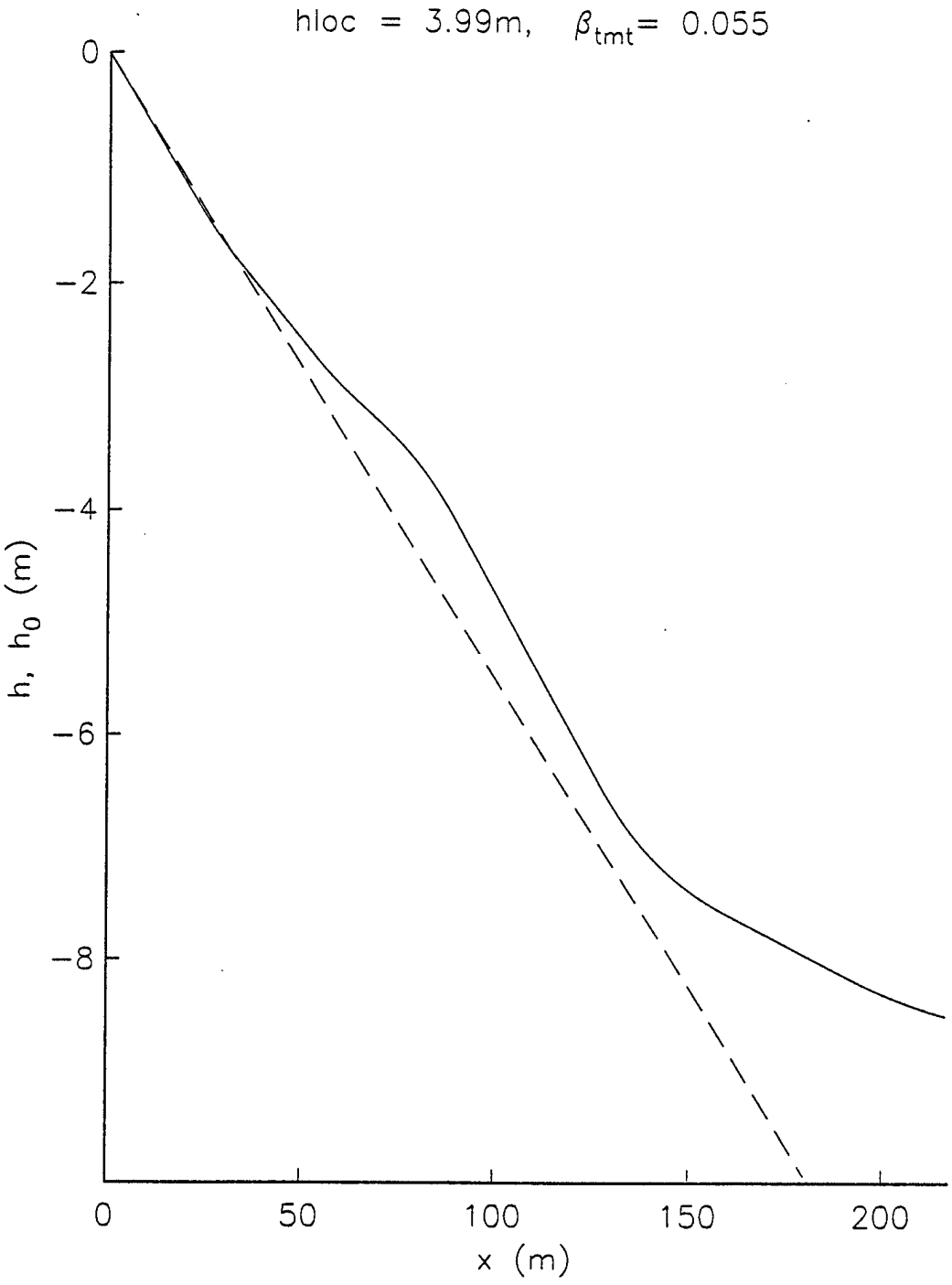

Figure 1.1-14. Santa Barbara Beach. A comparison between the median TMT-estimated (h_0) planar depth profile (0.055 slope, dashed line) and the true (h) depth profile (i.e., measured, solid line). The TMT-estimate is for an array measurement depth of approximately 4m.

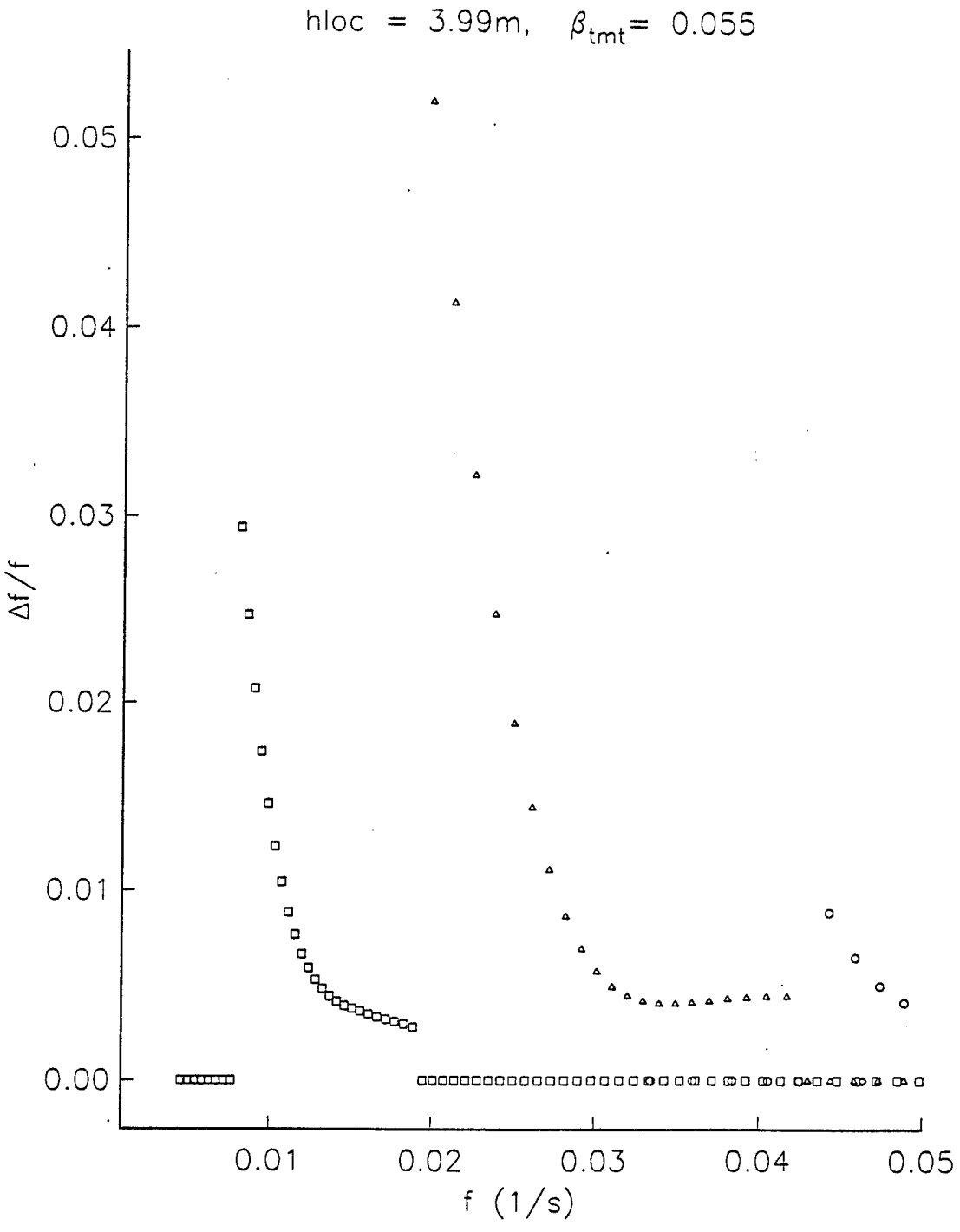

Figure 1.1-15. Santa Barbara Beach. A measure of the dispersion error in the perturbation expansion equation for the TMT-estimated zeroth-order depth profile in Figure 1.1-14. Shown is the fractional difference, $\Delta f/f_{TRUE}$, where $\Delta f = f_{PERT}-f_{TRUE}$, f_{PERT} is the perturbation solution, and f_{TRUE} is the full-equation solution.

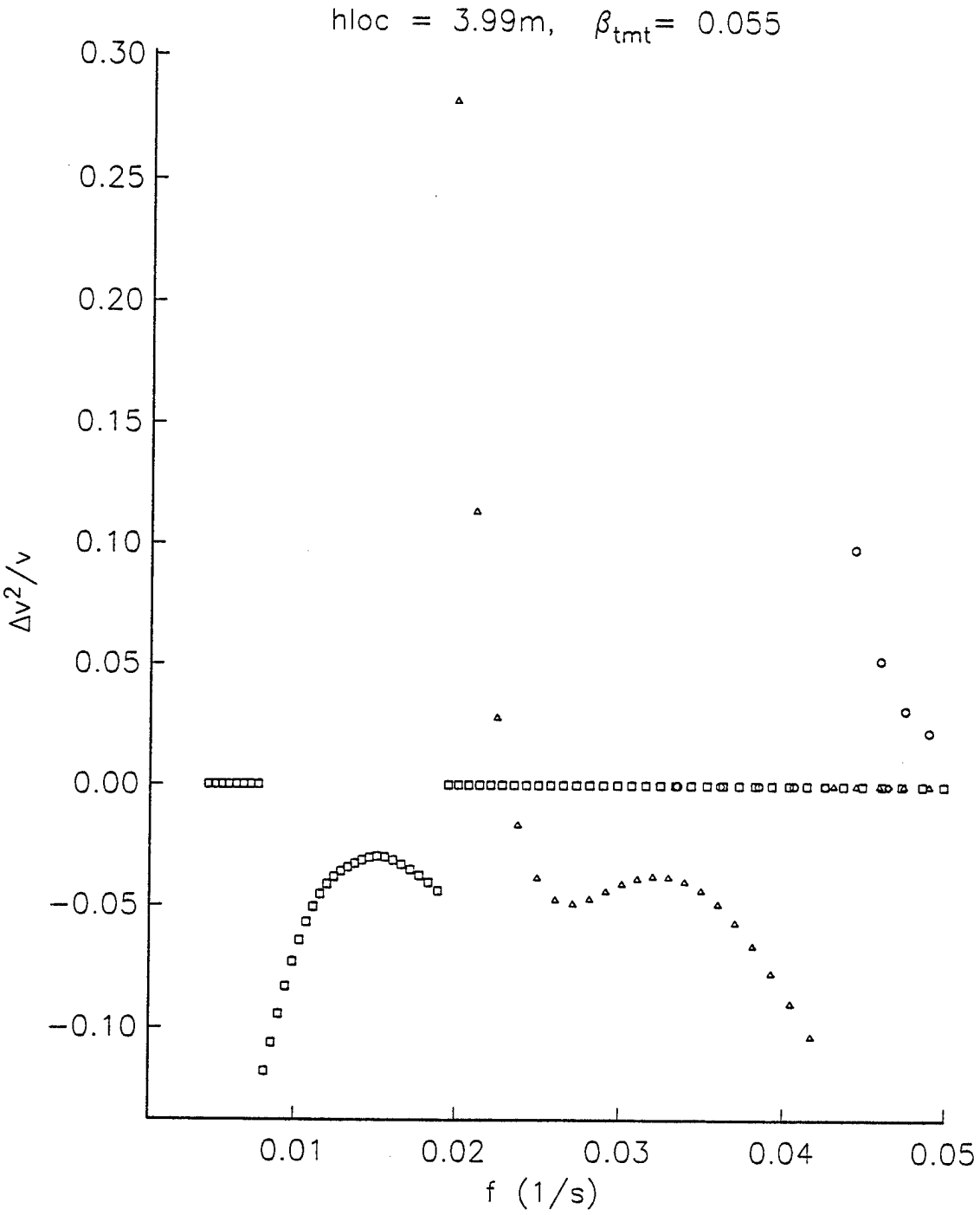

Figure 1.1-16. Santa Barbara Beach. A measure of the cross-shore variance error in the perturbation expansion equation for the TMT-estimated zeroth-order depth profile in Figure 1.1-14. Shown is the fractional difference, $\Delta v^2 / v^2_{TRUE}$, where $\Delta v^2 = v^2_{PERT} - v^2_{TRUE}$, v^2_{PERT} is the perturbation solution, and v^2_{TRUE} is the full-equation solution.

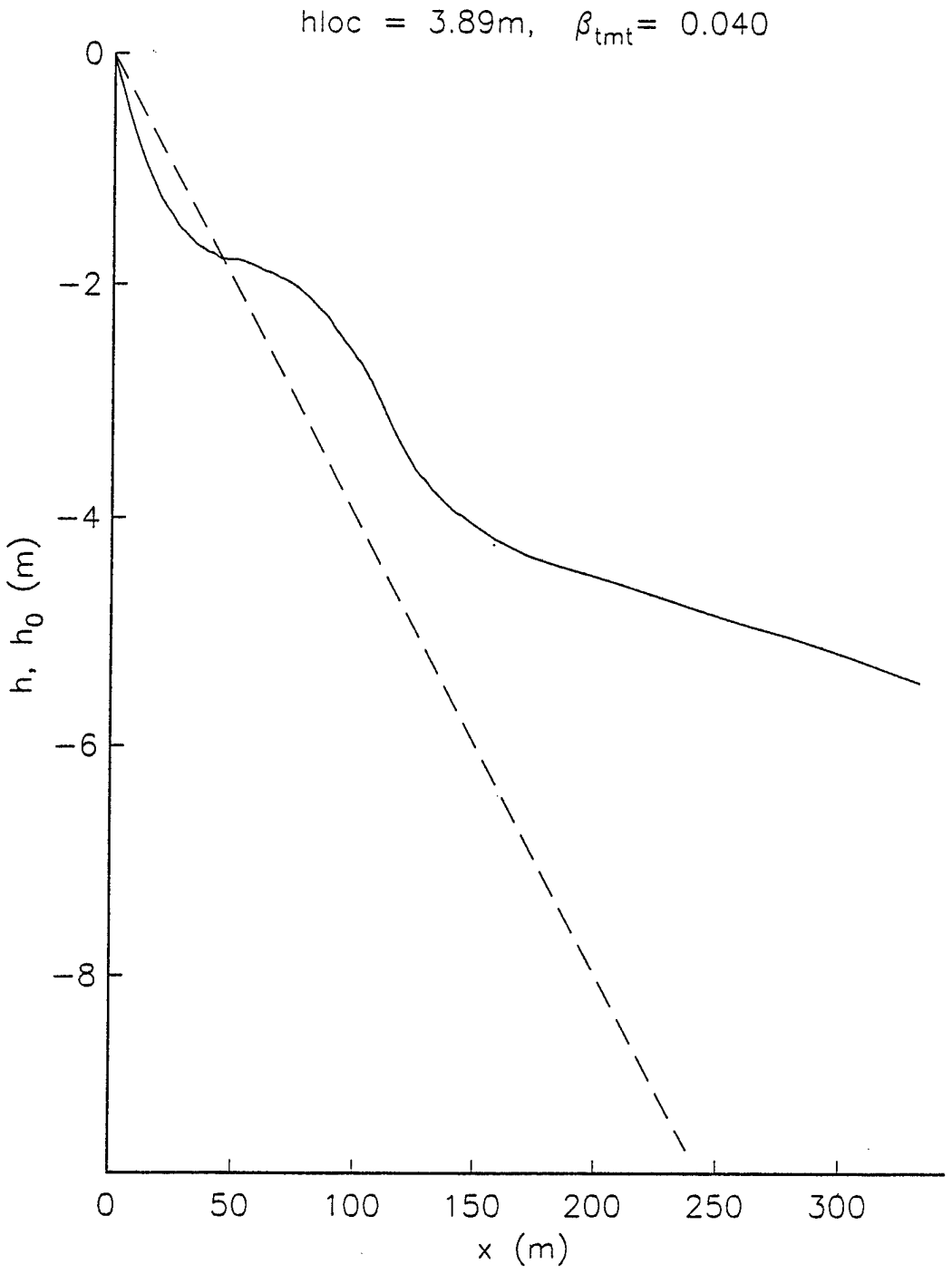

Figure 1.1-17. Duck Beach. A comparison between the median TMT-estimated (h_0) planar depth profile (0.040 slope, dashed line) and the true (h) depth profile (i.e., measured, solid line). The TMT-estimate is for an array measurement depth of approximately 4m.

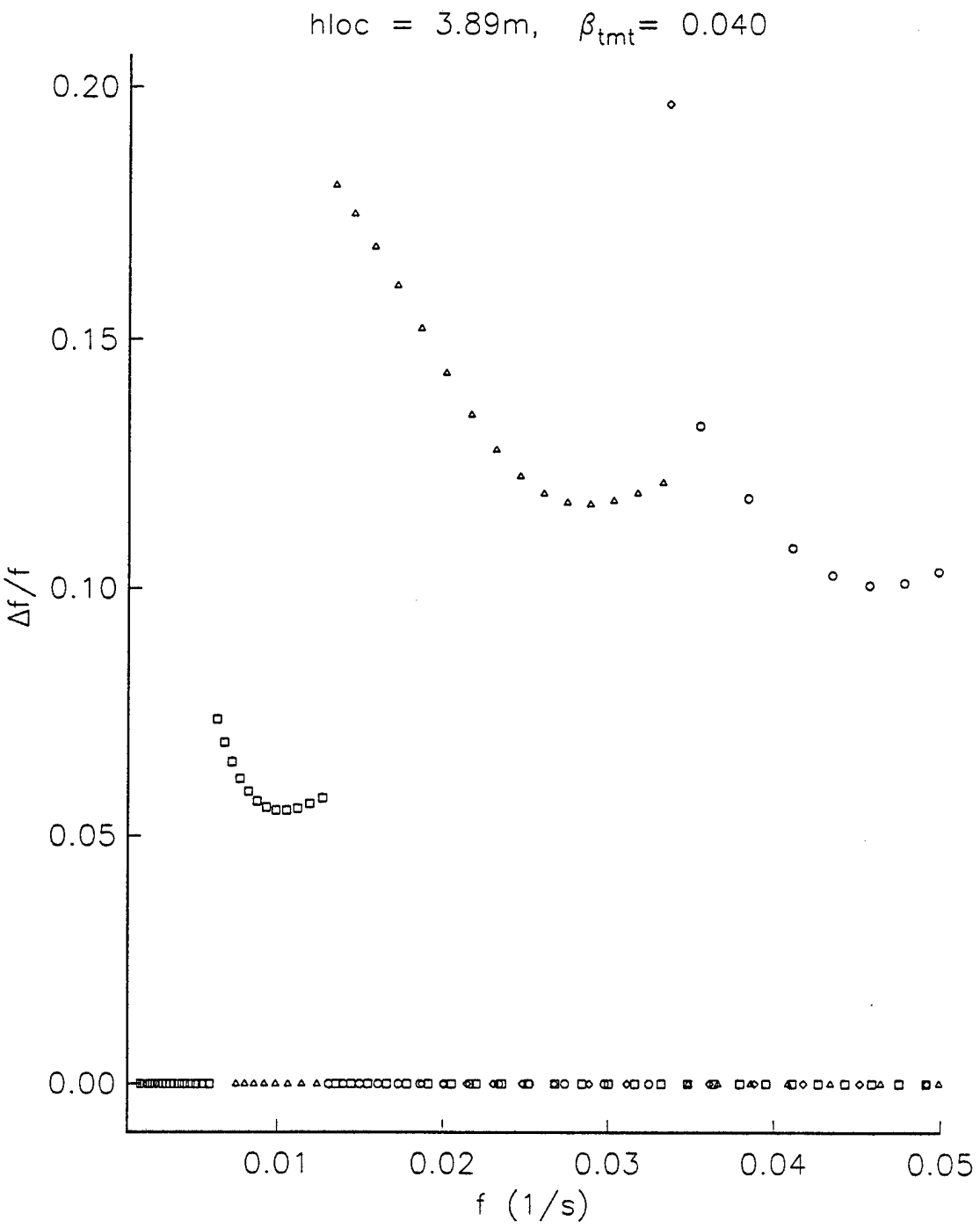

Figure 1.1-18. Duck Beach. A measure of the dispersion error in the perturbation expansion equation for the TMT-estimated zeroth-order depth profile in Figure 1.1-17. Shown is the fractional difference, $\Delta f/f_{TRUE}$, where $\Delta f = f_{PERT}-f_{TRUE}$, f_{PERT} is the perturbation solution, and f_{TRUE} is the full-equation solution.

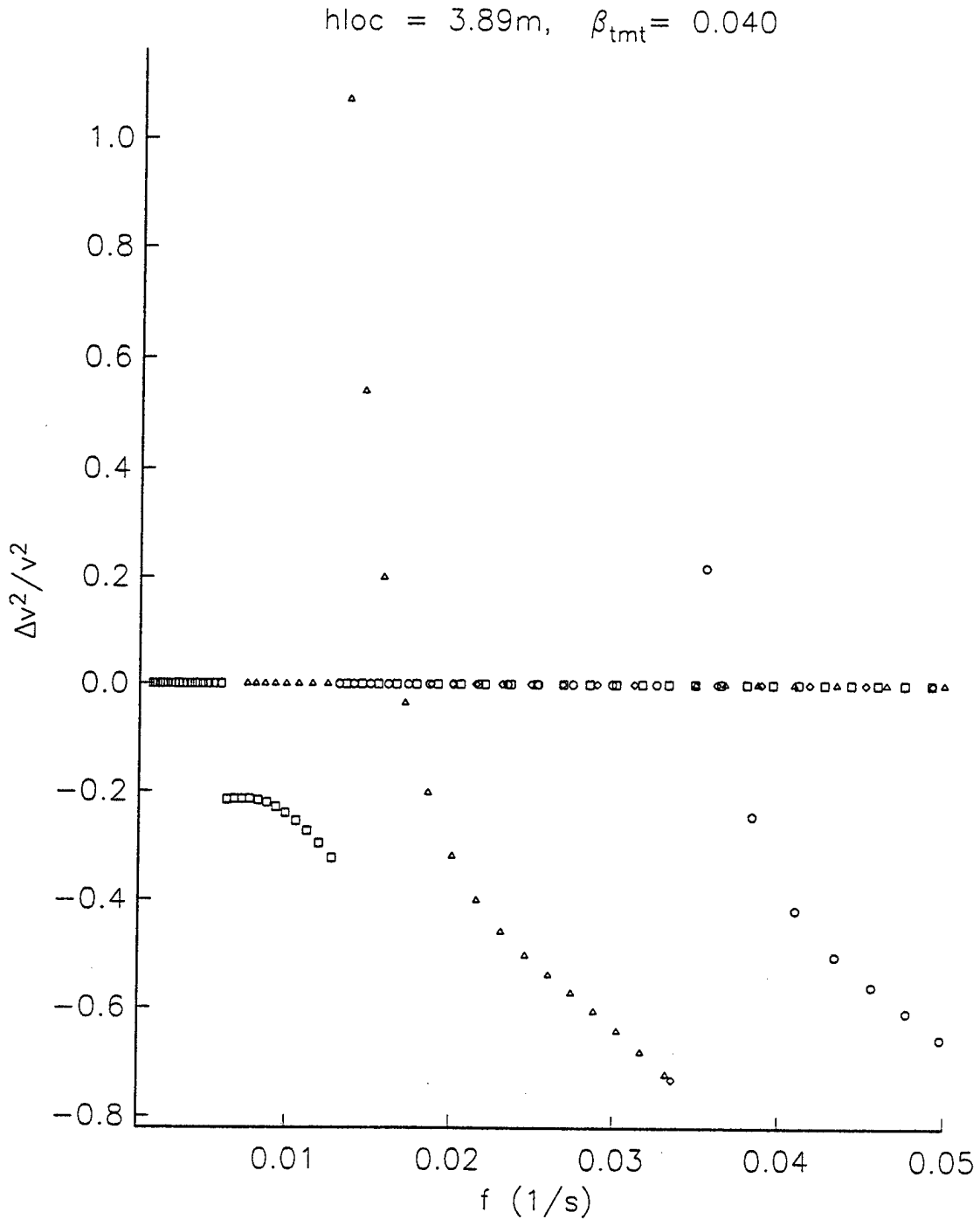

Figure 1.1-19. Duck Beach. A measure of the cross-shore variance error in the perturbation expansion equation for the TMT-estimated zeroth-order depth profile in Figure 1.1-17. Shown is the fractional difference, $\Delta v^2 / v^2_{TRUE}$, where $\Delta v^2 = v^2_{PERT} - v^2_{TRUE}$, v^2_{PERT} is the perturbation solution, and v^2_{TRUE} is the full-equation solution.

1.1.3 Array Element Position and Synchronization Error Analysis

In this section, the issue of clock synchronization amongst the array elements (sensor packages) and the measurement accuracy of the array element position are addressed. The consequences of the error are examined in terms of the estimate degradation of both the wind wave direction and the infragravity (IG) wavenumber. Addressing these errors is important for design of the sensor package (i.e., required clock accuracy) and the concept of operations for both data collection (resetting of clocks) and array deployment (methods and time).

Assume the following:

$\delta t \equiv$ clock error between two sensors,

$\delta y \equiv$ alongshore sensor separation measurement error,

$\Delta y \equiv$ alongshore sensor separation,

$\delta\varphi \equiv$ phase error between two sensors,

$\varphi_T \equiv$ true phase between two sensors,

$\varphi_m \equiv$ measured phase between two sensors,

$\theta_T \equiv$ true angle of incidence of the wave train,

$\theta_m \equiv$ measured angle of incidence of the wave train,

$k_{y_T} \equiv$ true alongshore wavenumber of the infragravity (IG) wave, and

$k_{y_m} \equiv$ measured alongshore wavenumber of the infragravity (IG) wave.

Further assume a coordinate system where y is directed alongshore and x is directed offshore. Wind wave trains with oblique angles of incidence to the beach are at nonzero degrees off the x axis, the beach normal; wind wave trains normal to the beach travel along the x axis.

1.1.3.1 Clock Synchronization Error

Wind Wave Directional Error

The true phase difference between two sensors, due to the approach of an oblique wave train, varies with the alongshore wavenumber, k_y, of the incident wave train and the sensor alongshore separation, Δy, as

$$\varphi_T = 2\pi k_y \Delta y. \qquad (1)$$

The true direction of the wave train, θ_T, is obtained from the phase between two sensors when the total wavenumber, k ($= k_y^2 + k_x^2$), and the sensor alongshore separation, Δy, are known,

$$\theta_T = \sin^{-1}\left(\frac{k_{y_T}}{k}\right) = \sin^{-1}\left(\frac{\varphi_T}{2\pi k\Delta y}\right). \quad (2)$$

Therefore, the true phase between two sensors can alternatively be expressed as a function of the direction and total wavenumber of the wave train and the sensor separation as

$$\varphi_T = 2\pi k\Delta y \sin\theta_T. \quad (3)$$

The measured phase between two sensors will be subject to errors in the synchronization of the clocks used to collect data for each of the two sensors as well as error due to stochastic noise, signal noise, and sensor-position measurement. The phase error between two sensors due to clock synchronization error can be expressed as

$$\delta\varphi = 2\pi\left(\frac{\delta t}{T}\right) = 2\pi f\delta t, \quad (4)$$

where $T(f)$ is the period (frequency) of the wave train.

The measured phase, φ_m, is therefore

$$\varphi_m = \varphi_T \pm \delta\varphi = 2\pi k\Delta y \sin\theta_T \pm 2\pi f\delta t\ . \quad (5)$$

Therefore, applying equation 2,

$$\theta_m = \sin^{-1}\left(\frac{\varphi_m}{2\pi k\Delta y}\right) = \sin^{-1}\left(\sin\theta_T \pm \frac{f\delta t}{k\Delta y}\right). \quad (6)$$

From the wind wave dispersion we have

$$(2\pi f)^2 = g2\pi k\tanh(2\pi kh), \quad (7)$$

where g is the gravitational constant.

Using the shallow water assumption, the dispersion relation reduces to

$$f^2 = gk^2h. \quad (8)$$

Therefore, with substitution of equation 8 into 6, an expression for the measured angle of incidence that does not vary with frequency or wavenumber of the wave train is

$$\theta_m = \sin^{-1}\left(\sin\theta_T \pm \frac{\delta t\sqrt{gh}}{\Delta y}\right). \quad (9)$$

Table 1.1-3 is a spreadsheet applying equation 9 for clock errors of 10, 50, and 100ms, in a water depth of 5m, and with sensor separations of 20 and 50m. In 5m depth, a 0.14Hz wave has a 50m total wavelength and a .35Hz wave has a 20m wavelength. The errors in θ_m vary from 0.08

Table 1.1-3. Wave direction (theta) estimation error associated with clock synchronization errors of 10, 50, and 100ms.

10ms clock error - 5m water depth - 50m sensor separation

Clock Error	Snsr Sep	Water Depth	Theta True	Theta Meas.	Theta Error
0.01	50	5	0	0.080	0.080
0.01	50	5	5	5.081	0.081
0.01	50	5	10	10.082	0.082
0.01	50	5	20	20.085	0.085
0.01	50	5	30	30.093	0.093
0.01	50	5	40	40.105	0.105
0.01	50	5	60	60.161	0.161
0.01	50	5	80	80.474	0.474

50ms clock error - 5m water depth - 50m sensor separation

0.05	50	5	0	0.401	0.401
0.05	50	5	5	5.403	0.403
0.05	50	5	10	10.408	0.408
0.05	50	5	20	20.428	0.428
0.05	50	5	30	30.465	0.465
0.05	50	5	40	40.526	0.526
0.05	50	5	60	60.813	0.813
0.05	50	5	80	82.664	2.664

100ms clock error - 5m water depth - 50m sensor separation

0.1	50	5	0	0.803	0.803
0.1	50	5	5	5.807	0.807
0.1	50	5	10	10.816	0.816
0.1	50	5	20	20.857	0.857
0.1	50	5	30	30.932	0.932
0.1	50	5	40	41.056	1.056
0.1	50	5	60	61.647	1.647
0.1	50	5	80	87.219	7.219

Note: in 5m depth, a 0.14Hz wave has a 50m wavelength and a .35Hz wave has a 20m wavelength

10ms clock error - 5m water depth - **20m** sensor separation

Clock Error	Snsr Sep	Water Depth	Theta True	Theta Meas.	Theta Error
0.01	20	5	0	0.201	0.201
0.01	20	5	5	5.202	0.202
0.01	20	5	10	10.204	0.204
0.01	20	5	20	20.214	0.214
0.01	20	5	30	30.232	0.232
0.01	20	5	40	40.263	0.263
0.01	20	5	60	60.404	0.404
0.01	20	5	80	81.231	1.231

50ms clock error - 5m water depth - 20**m** sensor separation

0.05	20	5	0	1.004	1.004
0.05	20	5	5	6.008	1.008
0.05	20	5	10	11.021	1.021
0.05	20	5	20	21.072	1.072
0.05	20	5	30	31.166	1.166
0.05	20	5	40	41.323	1.323
0.05	20	5	60	62.073	2.073
0.05	20	5	80	75.305	4.695

100ms clock error - 5m water depth - 20**m** sensor separation

0.1	20	5	0	2.008	2.008
0.1	20	5	5	7.019	2.019
0.1	20	5	10	12.045	2.045
0.1	20	5	20	22.151	2.151
0.1	20	5	30	32.346	2.346
0.1	20	5	40	42.674	2.674
0.1	20	5	60	64.298	4.298
0.1	20	5	80	71.763	8.237

to 8.24 degrees. The more normal the incidence angle of the wave train to the beach, the smaller the error. If we assume incidence angles of less than 60 degrees off the beach normal, then a 50ms error in the clocks will result in errors less than 1 degree for sensors separations greater than 50m and less than 2 degrees for separation greater than 20m.

Wind wave directional arrays are typically designed with a minimum sensor separation of 5 to 10m. The alongshore coherence of the incident wave is on the order of 100m. Therefore, critical information is contained in the phase between sensors separated by 5m to 50m. If we are striving for 1 to 2 degree accuracy in wave direction, then we need a clock-synchronization accuracy better than 50ms.

Infragravity (IG) Wave Wavenumber Error

The true phase difference, φ_T, between two sensors, due to the incidence of an IG wave, varies with the true alongshore wavenumber, k_{y_T}, of the IG wave and the sensor alongshore separation, Δy, as

$$\varphi_T = 2\pi k_{y_T} \Delta y. \tag{10}$$

The phase error between two sensors due to clock synchronization error can be expressed as

$$\delta\varphi = 2\pi\left(\frac{\delta t}{T}\right) = 2\pi f \delta t, \tag{11}$$

where $T(f)$ is the period (frequency) of the IG wave. The measured phase is therefore

$$\varphi_m = \varphi_T \pm \delta\varphi = 2\pi\left(k_{y_T}\Delta y \pm \delta t f\right), \tag{12}$$

and the measured alongshore wavenumber, k_{y_m}, is

$$k_{y_m} = \frac{\varphi_m}{2\pi\Delta y} = k_{y_T} \pm \frac{f\delta t}{\Delta y}. \tag{13}$$

The error in the measured phase is therefore

$$\delta k_y = \pm\frac{f\delta t}{\Delta y}, \tag{14}$$

$$\text{and the \% error in } k_{y_m} = 100 \times \left|\frac{\delta k_y}{k_{y_T}}\right| = 100\left|\frac{f\delta t}{\Delta y k_{y_T}}\right|. \tag{15}$$

For IG edge waves on a planar depth profile

$$(2\pi f)^2 = g2\pi k_{y_T}(2n+1)\beta, \tag{16}$$

where n is the mode number and β is the beach slope.

Substituting equation 16 in equation 15 to remove k_{y_T}, the percent error in k_{y_m} is

$$100 \times \left| \frac{\delta t g(2n+1)\beta}{2\pi f \Delta y} \right|. \tag{17}$$

Spreadsheets were used to apply equation 17 for clock errors of 10ms (Table 1.1-4), 50ms (Table 1.1-5), and 100ms (Table 1.1-6). For each clock-error table, two beach slopes, 0.02 and 0.06, two IG frequencies, 0.01 and 0.03Hz, and two IG modes, 0 and 1 are applied. The alongshore wavelength, λ, is calculated, and three sensor separations are examined, 1/2λ, 1/4λ, and 1/8λ. For clock error of 10ms (Table 1.2-4), the percent error in k_{y_m} varies from 0.02 to 0.24 percent, increasing for higher frequencies and smaller sensor separations. The error is shown to be independent of mode number when sensor separation is defined in terms of the IG alongshore wavelength.

For clock error of 50ms (Table 1.1-5), the percent error varies from 0.1 to 1.2 percent. For clock error of 100ms (Table 1.1-6) the percent error varies from 0.2 to 2.4 percent. If we are requiring no more than 1 to 2 percent error in the k_y measurement, then a clock error better than 100ms is required.

Table 1.1-4. Percent error in wavenumber (ky) estimation associated with 10 ms clock synchronization error.

Clock Error	f	β	n	ky	λ	Δy (=1/2 λ)	δky	λ+δλ	δλ	% error in ky
0.01	0.01	0.06	0	0.001066	937.74	468.87	2.13279E-07	937.5534	0.19	0.02
0.01	0.01	0.06	1	0.000355	2813.22	1406.61	7.10928E-08	2812.66	0.56	0.02
0.01	0.01	0.02	0	0.003199	312.58	156.29	6.39836E-07	312.5178	0.06	0.02
0.01	0.01	0.02	1	0.001066	937.74	468.87	2.13279E-07	937.5534	0.19	0.02
0.01	0.03	0.06	0	0.009598	104.19	52.10	5.75852E-06	104.131	0.06	0.06
0.01	0.03	0.06	1	0.003199	312.58	156.29	1.91951E-06	312.3929	0.19	0.06
0.01	0.03	0.02	0	0.028793	34.73	17.37	1.72756E-05	34.71032	0.02	0.06
0.01	0.03	0.02	1	0.009598	104.19	52.10	5.75852E-06	104.131	0.06	0.06

Clock Error	f	β	n	ky	λ	Δy (=1/4 λ)	δky	λ+δλ	δλ	% error in ky
0.01	0.01	0.06	0	0.001066	937.74	234.44	4.26557E-07	937.366	0.37	0.04
0.01	0.01	0.06	1	0.000355	2813.22	703.31	1.42186E-07	2812.098	1.12	0.04
0.01	0.01	0.02	0	0.003199	312.58	78.15	1.27967E-06	312.4553	0.12	0.04
0.01	0.01	0.02	1	0.001066	937.74	234.44	4.26557E-07	937.366	0.37	0.04
0.01	0.03	0.06	0	0.009598	104.19	26.05	1.1517E-05	104.0686	0.12	0.12
0.01	0.03	0.06	1	0.003199	312.58	78.15	3.83901E-06	312.2057	0.37	0.12
0.01	0.03	0.02	0	0.028793	34.73	8.68	3.45511E-05	34.68952	0.04	0.12
0.01	0.03	0.02	1	0.009598	104.19	26.05	1.1517E-05	104.0686	0.12	0.12

Clock Error	f	β	n	ky	λ	Δy (=1/8 λ)	δky	λ+δλ	δλ	% error in ky
0.01	0.01	0.06	0	0.001066	937.74	117.22	8.53114E-07	936.9913	0.75	0.08
0.01	0.01	0.06	1	0.000355	2813.22	351.65	2.84371E-07	2810.974	2.25	0.08
0.01	0.01	0.02	0	0.003199	312.58	39.07	2.55934E-06	312.3304	0.25	0.08
0.01	0.01	0.02	1	0.001066	937.74	117.22	8.53114E-07	936.9913	0.75	0.08
0.01	0.03	0.06	0	0.009598	104.19	13.02	2.30341E-05	103.944	0.25	0.24
0.01	0.03	0.06	1	0.003199	312.58	39.07	7.67803E-06	311.8319	0.75	0.24
0.01	0.03	0.02	0	0.028793	34.73	4.34	6.91022E-05	34.64799	0.08	0.24
0.01	0.03	0.02	1	0.009598	104.19	13.02	2.30341E-05	103.944	0.25	0.24

Table 1.1-5. Percent error in wavenumber (ky) estimation associated with 50 ms clock synchronization error.

Clock Error	f	β	n	ky	λ	Δy (=1/2 λ)	δky	λ+δλ	δλ	% error in ky
0.05	0.01	0.06	0	0.001066	937.74	468.87	1.06639E-06	936.8041	0.94	0.1
0.05	0.01	0.06	1	0.000355	2813.22	1406.61	3.55464E-07	2810.412	2.81	0.1
0.05	0.01	0.02	0	0.003199	312.58	156.29	3.19918E-06	312.268	0.31	0.1
0.05	0.01	0.02	1	0.001066	937.74	468.87	1.06639E-06	936.8041	0.94	0.1
0.05	0.03	0.06	0	0.009598	104.19	52.10	2.87926E-05	103.8818	0.31	0.3
0.05	0.03	0.06	1	0.003199	312.58	156.29	9.59753E-06	311.6454	0.93	0.3
0.05	0.03	0.02	0	0.028793	34.73	17.37	8.63778E-05	34.62726	0.10	0.3
0.05	0.03	0.02	1	0.009598	104.19	52.10	2.87926E-05	103.8818	0.31	0.3
Clock Error	f	β	n	ky	λ	Δy (=1/4 λ)	δky	λ+δλ	δλ	% error in ky
0.05	0.01	0.06	0	0.001066	937.74	234.44	2.13279E-06	935.8692	1.87	0.2
0.05	0.01	0.06	1	0.000355	2813.22	703.31	7.10928E-07	2807.608	5.62	0.2
0.05	0.01	0.02	0	0.003199	312.58	78.15	6.39836E-06	311.9564	0.62	0.2
0.05	0.01	0.02	1	0.001066	937.74	234.44	2.13279E-06	935.8692	1.87	0.2
0.05	0.03	0.06	0	0.009598	104.19	26.05	5.75852E-05	103.572	0.62	0.6
0.05	0.03	0.06	1	0.003199	312.58	78.15	1.91951E-05	310.716	1.86	0.6
0.05	0.03	0.02	0	0.028793	34.73	8.68	0.000172756	34.524	0.21	0.6
0.05	0.03	0.02	1	0.009598	104.19	26.05	5.75852E-05	103.572	0.62	0.6
Clock Error	f	β	n	ky	λ	Δy (=1/8 λ)	δky	λ+δλ	δλ	% error in ky
0.05	0.01	0.06	0	0.001066	937.74	117.22	4.26557E-06	934.0049	3.74	0.4
0.05	0.01	0.06	1	0.000355	2813.22	351.65	1.42186E-06	2802.015	11.21	0.4
0.05	0.01	0.02	0	0.003199	312.58	39.07	1.27967E-05	311.335	1.25	0.4
0.05	0.01	0.02	1	0.001066	937.74	117.22	4.26557E-06	934.0049	3.74	0.4
0.05	0.03	0.06	0	0.009598	104.19	13.02	0.00011517	102.9579	1.24	1.2
0.05	0.03	0.06	1	0.003199	312.58	39.07	3.83901E-05	308.8738	3.71	1.2
0.05	0.03	0.02	0	0.028793	34.73	4.34	0.000345511	34.31931	0.41	1.2
0.05	0.03	0.02	1	0.009598	104.19	13.02	0.00011517	102.9579	1.24	1.2

Table 1.1-6. Percent error in wavenumber (ky) estimation associated with 100 ms clock synchronization error.

Clock Error	f	β	n	ky	λ	Δy (=1/4 λ)	δky	λ+δλ	δλ	% error in ky
0.1	0.01	0.06	0	0.001066	937.74	468.87	2.13279E-06	935.8692	1.87	0.2
0.1	0.01	0.06	1	0.000355	2813.22	1406.61	7.10928E-07	2807.608	5.62	0.2
0.1	0.01	0.02	0	0.003199	312.58	156.29	6.39836E-06	311.9564	0.62	0.2
0.1	0.01	0.02	1	0.001066	937.74	468.87	2.13279E-06	935.8692	1.87	0.2
0.1	0.03	0.06	0	0.009598	104.19	52.10	5.75852E-05	103.572	0.62	0.6
0.1	0.03	0.06	1	0.003199	312.58	156.29	1.91951E-05	310.716	1.86	0.6
0.1	0.03	0.02	0	0.028793	34.73	17.37	0.000172756	34.524	0.21	0.6
0.1	0.03	0.02	1	0.009598	104.19	52.10	5.75852E-05	103.572	0.62	0.6

Clock Error	f	β	n	ky	λ	Δy (=1/4 λ)	δky	λ+δλ	δλ	% error in ky
0.1	0.01	0.06	0	0.001066	937.74	234.44	4.26557E-06	934.0049	3.74	0.4
0.1	0.01	0.06	1	0.000355	2813.22	703.31	1.42186E-06	2802.015	11.21	0.4
0.1	0.01	0.02	0	0.003199	312.58	78.15	1.27967E-05	311.335	1.25	0.4
0.1	0.01	0.02	1	0.001066	937.74	234.44	4.26557E-06	934.0049	3.74	0.4
0.1	0.03	0.06	0	0.009598	104.19	26.05	0.00011517	102.9579	1.24	1.2
0.1	0.03	0.06	1	0.003199	312.58	78.15	3.83901E-05	308.8738	3.71	1.2
0.1	0.03	0.02	0	0.028793	34.73	8.68	0.000345511	34.31931	0.41	1.2
0.1	0.03	0.02	1	0.009598	104.19	26.05	0.00011517	102.9579	1.24	1.2

Clock Error	f	β	n	ky	λ	Δy (=1/8 λ)	δky	λ+δλ	δλ	% error in ky
0.1	0.01	0.06	0	0.001066	937.74	117.22	8.53114E-06	930.2985	7.44	0.8
0.1	0.01	0.06	1	0.000355	2813.22	351.65	2.84371E-06	2790.896	22.33	0.8
0.1	0.01	0.02	0	0.003199	312.58	39.07	2.55934E-05	310.0995	2.48	0.8
0.1	0.01	0.02	1	0.001066	937.74	117.22	8.53114E-06	930.2985	7.44	0.8
0.1	0.03	0.06	0	0.009598	104.19	13.02	0.000230341	101.7514	2.44	2.4
0.1	0.03	0.06	1	0.003199	312.58	39.07	7.67803E-05	305.2542	7.33	2.4
0.1	0.03	0.02	0	0.028793	34.73	4.34	0.000691022	33.91713	0.81	2.4
0.1	0.03	0.02	1	0.009598	104.19	13.02	0.000230341	101.7514	2.44	2.4

1.1.3.2 Alongshore Position Error

Wind Wave Directional Error

As was discussed in section 1.1.3.1, the true phase difference between two sensors, due to the approach of an oblique wave train, varies with the alongshore wavenumber, k_y, of the incident wave train and the sensor alongshore separation, Δy, as

$$\varphi_T = 2\pi k_y \Delta y. \tag{18}$$

The true direction of the wave train, θ_T is obtained from the phase between two sensors when the total wavenumber, k (= $k_y^2 + k_x^2$), and the sensor alongshore separation, Δy, are known,

$$\theta_T = \sin^{-1}\left(\frac{k_{y_T}}{k}\right) = \sin^{-1}\left(\frac{\varphi_T}{2\pi k \Delta y}\right). \tag{19}$$

Therefore, the true phase between two sensors can alternatively be expressed as a function of the wave direction and total wavenumber of the wave train and the sensor separation as

$$\varphi_T = 2\pi k \Delta y \sin\theta_T. \tag{20}$$

The measured phase between two sensors will be subject to errors in the sensor alongshore-position measurement. The phase error between two sensors due to position-measurement error can be expressed as

$$\delta\varphi = 2\pi k_{y_T} \delta y. \tag{21}$$

The measured phase, φ_m, is therefore

$$\varphi_m = \varphi_T \pm \delta\varphi = 2\pi k_{y_T}(\Delta y \pm \delta y). \tag{22}$$

Applying equation 19,

$$\theta_m = \sin^{-1}\left(\frac{\varphi_m}{2\pi k \Delta y}\right) = \sin^{-1}\left(\frac{k_{y_T}(\Delta y \pm \delta y)}{k\Delta y}\right) = \sin^{-1}\left(\frac{k_{y_T}}{k} \pm \frac{k_{y_T}}{k}\frac{\delta y}{\Delta y}\right), \text{ and}$$

$$\theta_{error} = \theta_m - \theta_T = \sin^{-1}\left(\frac{k_{y_T}}{k}\left[1 \pm \frac{\delta y}{\Delta y}\right]\right) - \theta_T. \tag{23}$$

Since $\frac{k_{y_T}}{k} = \sin\theta_T$,

$$\theta_{error} = \sin^{-1}\left(\sin\theta_T\left[1 \pm \frac{\delta y}{\Delta y}\right]\right) - \theta_T. \tag{24}$$

Equation 24 provides us with an expression for the error in the measured wave direction as a function of the true direction and the ratio of the alongshore separation measurement error to the true separation. Table 1.1-7 is a spreadsheet applying equation 24 for position errors of 0.1, 0.2, 0.5, and 1.0m. The incident waves are in 5m water depth and sensor separations are 20 and 50m. In 5m depth, a 0.14Hz wave has a 50m total wavelength and a .35Hz wave has a 20m wavelength. The errors in θ_m vary from 0.000 to 10.682 degrees. The more normal the incidence angle of the wave train, the smaller the error. If we assume incidence angles of less than 60 degrees, then a 0.5m error in the position measurement will result in errors less than 1 degree for sensor separations greater than 50m and less than 2 degrees for separations greater than 20m.

Wind wave directional arrays are typically designed to have a minimum sensor separation of 5 to 10m. The alongshore coherence of the incident wave is on the order of 100m. Therefore, critical information is contained in the phase between sensors separated by 5m to 50m. If we are striving for 1 to 2 degree accuracy in wave direction, then we need an alongshore separation measurement accuracy of better than 0.5m.

Infragravity (IG) Wave Wavenumber Error

As was discussed in Section 1.1.3.1, the true phase difference, φ_T, between two sensors, due to the incidence of an IG wave varies with the true alongshore wavenumber, k_{y_T}, of the IG wave and the sensor alongshore separation, Δy, as

$$\varphi_T = 2\pi k_{y_T} \Delta y. \tag{25}$$

The true wavenumber of the IG wave can therefore be expressed in terms of the true phase difference and the sensor separation,

$$k_{y_T} = \frac{\varphi_T}{2\pi \Delta y}. \tag{26}$$

The measured phase, φ_m, between two sensors will be subject to errors in the sensor alongshore position measurement,

$$\delta\varphi = 2\pi k_{y_T} \delta y\,. \tag{27}$$

The measured phase is therefore

$$\varphi_m = \varphi_T \pm \delta\varphi = 2\pi k_{y_T} (\Delta y \pm \delta y)\,, \tag{28}$$

and applying equation 26, the measured alongshore wavenumber, k_{y_m}, is

$$k_{y_m} = \frac{\varphi_m}{2\pi \Delta y} = \frac{2\pi k_{y_T} (\Delta y \pm \delta y)}{2\pi \Delta y} = k_{y_T} \pm \frac{\delta y}{\Delta y} k_{y_T}\,, \tag{29}$$

Table 1.1-7. Wave direction (theta) estimation error associated with sensor position measurement errors of 10, 20, 50, and 100 cm.

0.1m alongshore position error - 5m water depth - 50m sensor separation

Position Error	Snsr Sep	Water Depth	Theta True	Theta Meas.	Theta Error
0.1	50	5	0	0.000	0.000
0.1	50	5	5	5.010	0.010
0.1	50	5	10	10.020	0.020
0.1	50	5	20	20.042	0.042
0.1	50	5	30	30.066	0.066
0.1	50	5	40	40.096	0.096
0.1	50	5	60	60.199	0.199
0.1	50	5	80	80.672	0.672

0.2m position error - 5m water depth - 50m sensor separation

0.2	50	5	0	0.000	0.000
0.2	50	5	5	5.020	0.020
0.2	50	5	10	10.040	0.040
0.2	50	5	20	20.083	0.083
0.2	50	5	30	30.132	0.132
0.2	50	5	40	40.193	0.193
0.2	50	5	60	60.399	0.399
0.2	50	5	80	81.396	1.396

0.5m position error - 5m water depth - 50m sensor separation

0.5	50	5	0	0.000	0.000
0.5	50	5	5	5.050	0.050
0.5	50	5	10	10.101	0.101
0.5	50	5	20	20.209	0.209
0.5	50	5	30	30.331	0.331
0.5	50	5	40	40.482	0.482
0.5	50	5	60	61.008	1.008
0.5	50	5	80	84.074	4.074

Note: in 5m depth, a 0.14Hz wave has a 50m wavelength and a .35Hz wave has a 20m wavelength

1.0m position error - 5m water depth - 50m sensor separation

Position Error	Snsr Sep	Water Depth	Theta True	Theta Meas.	Theta Error
1	50	5	0	0.000	0.000
1	50	5	5	5.100	0.100
1	50	5	10	10.202	0.202
1	50	5	20	20.418	0.418
1	50	5	30	30.664	0.664
1	50	5	40	40.968	0.968
1	50	5	60	62.049	2.049
1	50	5	80	74.821	5.179

0.1m position error - 5m water depth - **20m** sensor separation

Clock Error	Snsr Sep	Water Depth	Theta True	Theta Meas.	Theta Error
0.1	20	5	0	0.000	0.000
0.1	20	5	5	5.025	0.025
0.1	20	5	10	10.051	0.051
0.1	20	5	20	20.104	0.104
0.1	20	5	30	30.166	0.166
0.1	20	5	40	40.241	0.241
0.1	20	5	60	60.500	0.500
0.1	20	5	80	81.782	1.782

0.2m position error - 5m water depth - **20m** sensor separation

0.2	20	5	0	0.000	0.000
0.2	20	5	5	5.050	0.050
0.2	20	5	10	10.101	0.101
0.2	20	5	20	20.209	0.209
0.2	20	5	30	30.331	0.331
0.2	20	5	40	40.482	0.482
0.2	20	5	60	61.008	1.008
0.2	20	5	80	84.074	4.074

0.5m position error - 5m water depth - **20m** sensor separation

0.5	20	5	0	0.000	0.000
0.5	20	5	5	5.125	0.125
0.5	20	5	10	10.253	0.253
0.5	20	5	20	20.522	0.522
0.5	20	5	30	30.830	0.830
0.5	20	5	40	41.213	1.213
0.5	20	5	60	62.583	2.583
0.5	20	5	80	73.778	6.222

1.0m position error - 5m water depth - **20m** sensor separation

Clock Error	Snsr Sep	Water Depth	Theta True	Theta Meas.	Theta Error
1	20	5	0	0.000	0.000
1	20	5	5	5.251	0.251
1	20	5	10	10.506	0.506
1	20	5	20	21.046	1.046
1	20	5	30	31.668	1.668
1	20	5	40	42.448	2.448
1	20	5	60	65.412	5.412
1	20	5	80	69.320	10.680

where the error in the measured phase is $\delta k_y = \pm \frac{\delta_y}{\Delta y} k_{yr}$. (30)

Therefore, the percent error in k_y is dependent only on the ratio of the measurement error to the alongshore separation distance.

$$\%\,\textbf{error}\, k_y = 100 \times \frac{\delta k_y}{k_{yr}} = 100 \frac{\delta y}{\Delta y}. \quad (31)$$

Table 1.1-8 presents the results from applying equation 31 to a range of sensor separations and separation measurement errors. A measurement error of 0.50m yields a percent error in k_y of 0.3 to 10% for a range of sensor separations of 200 to 5m, respectively. Arrays used to measure IG waves typically have minimum sensor separations of 10m and maximum lengths of several hundred meters. The waves are coherent over one wavelength and wavelengths of interest are several hundred meters to 1km. Therefore, if we are requiring no more than 1 to 2 percent error in the k_y measurement, then an alongshore separation measurement error better than 0.5m is required.

Table 1.1-8 Percent error in wavenumber (k_y) estimation error associated with sensor position measurement errors of 10, 20, 50, and 100 cm.

	Measurement Error			
Δy	0.10m	0.20m	0.50m	1.0m
5m	2.0%	4.0%	10.0%	20.0%
10	1.0%	2.0%	5.0%	10.0%
20	0.5%	1.0%	2.5%	5.0%
60	0.2%	0.3%	0.8%	1.7%
100	0.1%	0.2%	0.5%	1.0%
150	0.07%	0.2%	0.3%	0.7%
200	0.05%	0.1%	0.3%	0.5%

1.2 Task 2: Field Campaign #1 – Depth Profile and Current Resolution

1.2.1 Overview

In the April 1997 Semi-Annual Report, we listed the Task 2 milestones and objectives to be met by the end of the six-month reporting period. These are listed again below.

1) Complete logistics preparation for the Sensor Package Field Test.
2) Perform an ocean test of a limited-element (Sensor Package) BPS Station complete with Array Controller and Onshore Processor.
3) Set up visit to Duck NC to coordinate with the FRF staff for Field Campaign #1 and obtain logistic information (lodging and transportation).

Presented below is a brief discussion of the status of these efforts with an outline of the results or a direction to the locations in this report with more detailed discussions.

1) Complete logistics preparation for the Sensor Package Field Test, and
2) Perform an ocean test of a limited-element (Sensor Package) BPS Station.

   Done, and the field test was a success. On our first time out to the field we collected good pressure and current meter data from two proto-type Sensor Packages. A description of the field site, logistics, data acquired, problems, and lessons learned is presented in Section 1.2.3.

3) Set up visit to Duck NC to coordinate with the FRF staff for Field Campaign #1 and obtain logistic information (lodging and transportation).

   The visit took place in early September when Reggie Beach's nearshore array was being deployed. We actively participated in that deployment and talked to FRF staff and other nearshore experimentalists about their methods and approach. A summary of what we learned can be found below in Section 1.2.2.

1.2.2 Notes from the September 1997 Visit to Duck, NC

In Summer/Fall of 1997, the Field Research Facility at Duck, NC, hosted a large nearshore field experiment called SandyDuck. Joan Oltman-Shay, Skip Echert, and Andrew Cookson visited the field site during deployment activities. The visit was timed to coincide with the surf zone deployment of Reggie Beach's instrumentation because their deployment requirements are similar to the BPS requirements and the activities could be easily viewed from shore. Presented below are the notes taken after participation in deployment and after conversations with scientists and engineers at the field site. The notes are organized in general topics such as cable, mounting, deployment, etc.

1.2.2.1 Cables

- Reggie Beach (ONR/OSU) uses neoprene-covered electric cable that is anchored loosely every 33m or so (the distance was determined by the amount of post they had available). Anchored loosely means that the cable is on one side of the mooring post and the strain relief wire (¼-inch nylon-covered wire rope) is on the other. A problem with neoprene cable is that it floats. It is therefore difficult to deploy in a longshore current, and it does not bury into the sand. It also does not have much tensile strength.
- To deploy the cable, they strung the relief cable between the mooring posts and then fastened the neoprene to this using plastic cable ties. They placed the wire rope on one side of the post and the neoprene cable on the other. The two are attached together on each side of the post with rope, allowing the cables to slip up and down on the post (Figure 1.2-1).
- One reason the FRF does not like unsupported neoprene is that it is difficult to remove if it gets buried. It can't take hard pulling. Even supporting it with wire rope may only partially facilitate recovery of the wire rope. The neoprene may be pulled away.

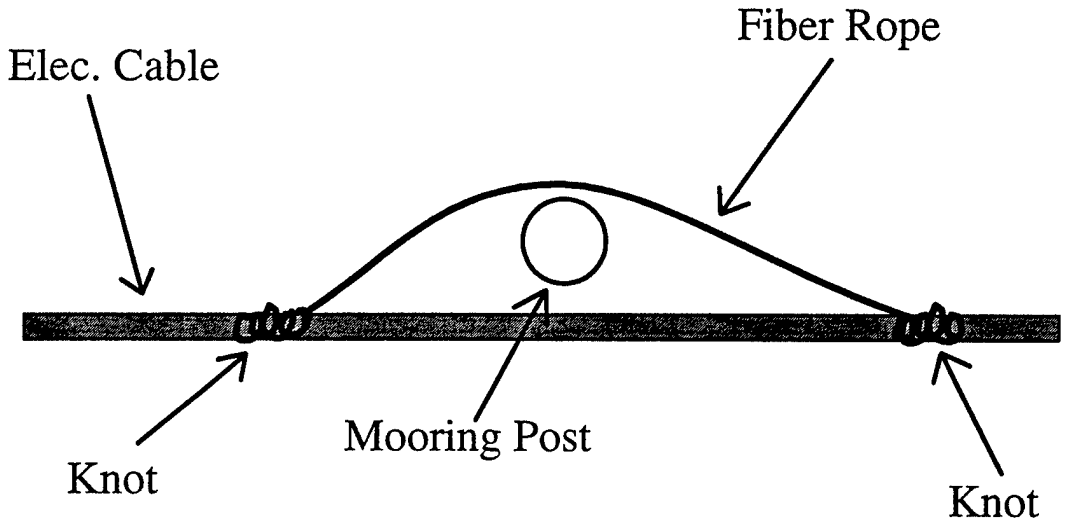

Figure 1.2-1. Illustration of method for anchoring electric cable to mooring post.

- There was considerable discussion among Rex Johnson, Walt Waldorf, Reggie Beach, and Dan Conley about methods to strain-relieve the neoprene cables to the mooring posts. It was a given that rope was to be used. Rex said that multiple clove hitches on a cable can result in uneven strain relief and bends or even tangles in the cable. He recommended tying the rope to the pipe with a bowline and then using a "modified prussik knot" to tie the rope to the cable (Figure 1.2-1). The modified prussik knot is a string of spaced wraps around the cable with the end looped back to the beginning of the knot (nearest to the pipe) and tied there "using any knot" (e.g., two half-hitches). This is the method used for Reggie's instruments. Rex showed us a pre-tied bowline that can be used to expedite tying the bowline around a post.

1.2.2.2 Mounting

- Reggie is using 2 3/8 inch irrigation pipe for his mooring posts. It is lightweight and strong enough according to Reggie. (Bill Birkemeier of the FRF is not sure of that.) The pipes are 21 feet long and will be inserted 16 feet into the sediments. They had two fins at the bottom end of the pipe to stop the pipe from rotating. The 21-foot length is the FRF standard for mooring posts in the surf zone.
- The FRF jets through the pipe for installation. From the FRF's Coastal Amphibious Buggy (CRAB), Reggie's team used a 10' long extension pipe (from the FRF) to extend the reach of the jetted pipe. The extension pipe was screwed to the mooring pipe, the mooring pipe jetted in, then the extension pipe unscrewed and removed. There was no need for a diver to disconnect the hose end from the jetted pipe with this method. The winch cable was marked with tape at the desired insertion depth.
- If jetting out is necessary, it requires a separate jetting pipe.
- Walt Waldorf (works for Reggie/OSU) warned that the screws on stainless hose clamps are usually not stainless.
- Bill Birkemeier (Chief, FRF) said that if we use the standard mooring posts that they use for mounting instruments, the FRF would have extension pipes with hose fittings of many lengths (and therefore deployment depths) for jetting in our posts.

1.2.2.3 Deployment

- Reggie's group deploys with all sensors plugged in. Each sensor is cabled to the trailer onshore. There is no junction box.
- Reggie's team pulled cable initially the same way as we did at Copalis Beach (Section 1.2.3) – each person takes a length on his/her shoulder and walks out. They needed to pull all of the cable out from the trailer and leave the extra flaked out on the beach, to be pulled out during instrument installation. Once the first person reached the beach, the folks spread the cable out by pulling hand over hand.
- For two cables going out to the same instrument pipe, Reggie's group black-taped the wet ends together every 10 - 15 feet using 3-5 wraps of Scotch 33.
- Reggie's group had shade/rain shields for work area outside the trailers. The September sun is harsh and rain is likely. They had shipping crates that open up on one side and also serve as shelf storage.
- The CRAB has a winch and short low arm on the upper deck to lift items to the working level. Total throw from the sand to the top of the winch is about 31 feet.
- Most jetting at the FRF is done with the CRAB. The majority of the work is done with a particular (about 2" dia.) galvanized pipe endorsed by the FRF.
- The FRF folks commonly use the through-the-pipe method of jetting in pipes. Each mooring pipe connects temporarily to an extension pipe, which the FRF has in various lengths. The extension pipe used by Reggie's team screwed onto the mooring pipe.

- The winch line lowers the jetted pipe/extension pipe combination during jetting. Reggie's pipes needed a little hand pushing to get full insertion. The heavier FRF pipe may need none. For recovery, the CRAB often can pull the pipes out without jetting.
- Bill Birkemeier and Bill Grog (FRF) suggested that we could have the array junction box cables come in to shore either at the north property line or at the end of the pier. Either place has fiber optic network cable from the trailer back to the FRF building where we could set up the Onshore Array Controllers and Processors.
- Contract versus NWRA divers:

  ⇒ Three to four contract divers cost about $1200/day plus expenses.

  ⇒ AAUS (American Association of Underwater Scientists) – Dive organization mentioned by Walt Waldorf (OSU) that allows divers to legally dive on any university ship/facility, or participate in any university or other program. Walt teaches the program down at Oregon State. We need to find out more and consider taking the UW program. Divers to be trained are Matt, Andrew, Joan, and Skip.

1.2.2.4 Sontek Acoustic Doppler Velocimeters

- Kent Hathaway and Dan (both from FRF) were using a ss metal halo they designed and fabricated to protect the arms of the Sontek. It attached to the shaft of the Sontek.
- Kent was told by Sontek to average for at least 100ms.
- Steve Elgar (WSU/Scripps) does not worry about Sontek synchronization with the pressure sensor. He uses Paros pressure sensors that do a 100msec frequency averaging to determine the pressure and 400ms averaging of the Sonteks. He claims that the pressure and current meter data are 'synchronous enough.'
- Steve Elgar also mentioned to Sontek his desire to have in-field repair kits for the Sontek. In particular, he has found out from Ramon (President of Sontek) that it is not difficult to replace the Sontek arms. However, it is not clear yet if Sontek is willing to sell and train us on the repair kits.
- Kent's Sonteks have zinc clamps around the probe trunk.
- Kent has successfully transmitted (both ways) at 9600 baud, down 1500m of cable (7 ply) using RS422.
- Kent was having problems with spikes when running three Sonteks simultaneously in a small (5-foot diameter) tank. He probably had lots of acoustic reverberation. He did not have problems with a 1 to 30cm/sec dynamic range, but did at 0 to 100cm/sec range. *More on this below.*
- Craig Huhta from Sontek was at Duck. He helped us understand Kent's problem better and the basics on how a Sontek works:

  ⇒ The field Sontek uses a 5MHz acoustic signal (the lab version uses 10MHz signal). It sonifies a 1cm cubed volume 18 cm above the main probe head.

⇒ There is a variable frequency of the 5MHz pulse packets. This frequency changes with the dynamic range setting. I believe (Joan) that there is a 300Hz sampling frequency of the pulse pairs for a dynamic range of 0 to 200cm/sec.

⇒ To estimate the velocity, they look at the phase change (range = +/- pi) between the pulse pairs. For a larger dynamic range, the accuracy goes down because +/- pi is now ranging from 0 to 200cm/sec instead of 0 to 30cm/sec. However, they compensate some by decreasing the time between pulse packets (e.g., increasing the frequency from 100Hz to 300Hz) – smaller dynamic ranges have smaller pulse frequencies (larger maximum delta time). This is why Kent's problem only occurred for the larger dynamic ranges. By lowering the dynamic range, the pulse frequency was also automatically lowered and the reverberation noise was reduced.

* Note: the bad data that result from measuring velocities outside the dynamic range is because of aliasing...exceeding the +/- pi phase values and wrapping into values less than pi. With a lot of work one can unravel the data using velocity tracking methods, but it is difficult and not always perfect, especially for rapidly changing environments like a bore fields.

- We found out from Peter Howd (USGS/Univ of Florida) and from Steve Elgar (Scripps/WA State) that Sontek has been extending their instrumentation to both autonomous (stand alone) systems and to shore-attached, synchronous (RS485) systems.

⇒ USGS is having autonomous Sensor Packages fabricated by Sontek. These systems will have a Sontek current meter, compass and inclinometer, internal batteries, flash memory recording, clocking, and ports for pressure sensors and other sensors(?). The nominal cost to USGS is $20,000 per package (this does not include the pressure sensor; USGS will be buying Paros sensors).

* Sontek's design uses the existing CPU in the Sontek main probe for managing the internal data collection and timing. They will place the flash memory, sensor port(s), compass and inclinometer in a small cylindrical package attached to the CM probe. The batteries will be in a separate container, with cables between the two containers. This allows the Sontek probe to be placed close to the ocean bottom, upside down on a extension pipe or a separate pipe.

⇒ Steve Elgar and Army Corps WES are having Sontek current meter sensor arrays designed and fabricated by Sontek. The intention here is to have power, clock, and data archival onshore. Sontek has written code for RS485 communications.

* Steve Elgar is testing a two-sensor package array at Duck. So far it looks like the RS485 software is working fine. His major complaint is that Ramon insisted on using 16-prong Impulse plugs. It is very difficult to plug in underwater 16-prong plugs. They are also very expensive.

1.2.2.5 Beach Surveying and Sensor Positioning

- Mike Lefler (FRF) is in charge of the CRAB surveying.

- Mike thought we could do a mini grid (20 lines with 25m spacing out to 6m depth) in 6 to 7 hours.
- The CRAB Survey (GPS) system has 2cm accuracy in x,y,z.
- Mike felt that he could achieve 10cm accuracy in sensor placement. This number probably does not account for survey rod listing in deep water. Steve Elgar was of the opinion that 0.3 to 1.0m accuracy was more likely – even with post-deployment underwater measurement by divers.
- The accuracy of the CRAB positioning system negates the need for surveying in the sensor locations before placement of the sensors (two end pipes with taut wire between and rings identifying sensor pipe placement locations – as per Mike Clifton's deployment strategy). We can now instead position and deploy packages in the same outing.

1.2.2.6 Sonteks: Who is doing what

- Steve Elgar and Britt Raubenheimer, SIO
  ⇒ They have two sensors, one ocean and one lab. They are using the Sontek RS485 system to an on-shore PC. The software in the on-shore PC was created by Sontek. Steve said he has a program for 20 ADVs next year. He will use the existing data-acquisition system at SIO and will not use the Sontek RS-485 system. The Sontek system uses a 16-conductor cable to shore with Impulse fittings. The dummy plugs cost $400/pair. Steve tried to get Sontek to use Brantner connectors, but he was unsuccessful.
- Guy Gelfenbaum, USGS
  ⇒ Is using 7 Ocean ADVs with a 485 data link. They are positioned at the north end of the FRF.
- Dan Haines, USGS
  ⇒ Has two Ocean ADVs at Duck.
- WES
  ⇒ Has a new array of 10 ADVs for use in their laboratory.
- John Trowbridge, WHOI
  ⇒ He has a frame with 5 Sontek ADVs placed in 4 m of water. Currents are about 100 cm/sec.
- Ib Svendsen and Dave Aubrey, U. of Del and WHOI
  ⇒ They will install three stand-alone ADVs at Duck.
- FRF
  ⇒ Kent Hathaway has a set of three ADVs on a single post. The data from these sensors come back to a single Tattletale 8 and then to shore. The sensor cables lead back to individual electronics boxes, and these lead back to another pressure vessel with the Tattletale in it. From there, the data go to shore in a single **RS-422** data stream. Kent is using 7-conductor armored cable to shore: 2 transmit, 2 receive, 2 power, 1 ground.

1.2.2.7 Miscellaneous

- Bill Birkemeier suggested we collect our own barometer data since there can be as much as 20mb (approx 20cm) changes in a few hours.
- However, budget constraints leave us with asking the FRF to deploy and collect data from our 4 Marsh McBirney CMs placed in a cross-shore array in the surf zone. Therefore, the barometer data could also be collected by them.
- Chuck Long said that critter growth on the orifice of the pressure sensors causes offsets. Can use copper paint, etc., but it is highly toxic.
- Sand screens on the pressure orifices are also recommended. Scripps divers stick their fingers in the orifice and sweep the orifice clean. Sand screens seem to be a good idea for that reason as well.
- Steve Elgar believes the Setra pressure sensor with temperature compensation algorithms can be as accurate as the Paros sensor. He has software that corrects for temperature-induced fluctuations and believes he is getting order cm accuracy now. If his sensors were below sand, he believes he could be getting even better (without the Bernoulli effect) and use these sensors for set up and set down studies (order less than cm accuracy).
- Sontek has moved to new offices in April 97. It still is in the same part of town. October is particularly busy for Sontek – they could not visit here but we could visit there.

1.2.3 The August 1997 Copalis Field Test

In this section, the initial ocean testing of BPS equipment is described. The field test took place from 16 through 21 August 97 at a location near Copalis, Washington, on the state's Pacific Coast.

1.2.3.1 Objectives of Field Test

The objectives of the field test were as follows:

1. Verify the acquisition, transmittal, and recording of pressure and current data obtained from a pair of BPS Sensor Packages in a nearshore wave environment.
2. Test the suitability of the Sensor Package design and the mooring methodology for BPS field operations.
3. Verify the transfer to battery operation and internal recording when the connection to shore is disconnected.
4. Train the BPS team on the installation, operation, and recovery of the BPS equipment.

1.2.3.2 Test Site Description

The test site was on the Washington State Pacific Coast, approximately 2 km south of the town of Copalis Beach. Units at the Surfcrest Timeshare Condominium were used to house the field team. One unit served as a base of operations where the Array Controller and the Onshore

Processor computers were placed. The distance from the high water line to the condominiums is about 400 m. It is approximately another 350 m from the high water line to the point of the lowest tide we saw during the tests (Figure 1.2-2). One can easily walk on various paths from the condominiums over the sand dunes to the shoreline, but there is no direct vehicular access to the water from the Surfcrest. Vehicles can enter the beach at a point 1.5 km south of the resort. During the time of our field test, the beach north of the vehicle access point was closed to general vehicular traffic. We obtained special permission to have our vehicles on the beach.

The beach sand is fine to medium grain. The sand base is greater than the three-meter depth to which we jetted our mooring pipes. The beach slope is very gentle, at a ratio of approximately 1:100. The beach is remarkable in its uniformity with no headlands or rock outcrops or significant change in beach slope for several kilometers both north and south of the site. Conner Creek is located approximately 20 meters east of the condominiums, and runs in a north-northwest direction until it empties into the ocean about 2 km north of the test site.

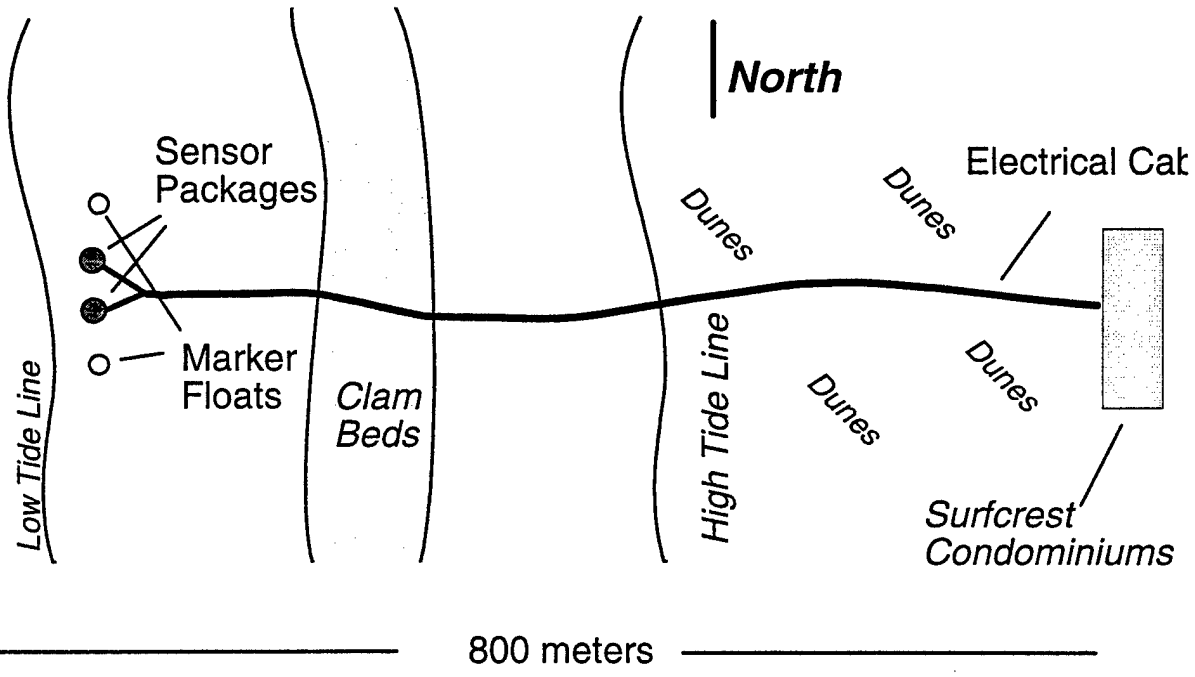

Figure 1.2-2. Plan view of the Copalis Beach field site.

The tidal range during the test period, 17 to 21 August 97, was approximately 3 meters. Table 1.2-1 contains tide high and low information for Pacific Beach, which is 14 km north of the test site. It is from a commercially available "Tide Guide" (Evergreen Pacific, 1996) which states, "These Tide Tables have been computed from the latest available NOAA data." The Pacific Beach data were obtained from the Aberdeen, WA, tidal data by applying the correction provided in the "Tide Guide."

Table 1.2-1. Tidal data for Pacific Beach, WA.

Day	Time, meters	Time, meters	Time, meters	Time, meters
17 Aug	--	06:11 -0.5m	12:47 2.2m	18:21 0.2m
18 Aug	00:24 2.6m	06:57 -0.6m	13:31 2.3m	19:11 0.1m
19 Aug	01:16 2.6m	07:42 -1.0m	14:14 2.4m	20:01 0.0m
20 Aug	02:08 2.5m	08:26 -0.5m	14:57 2.5m	20:51 -0.1m
21 Aug	03:00 2.5m	09:10 -0.3m	15:39 2.5m	21:41 -0.1m

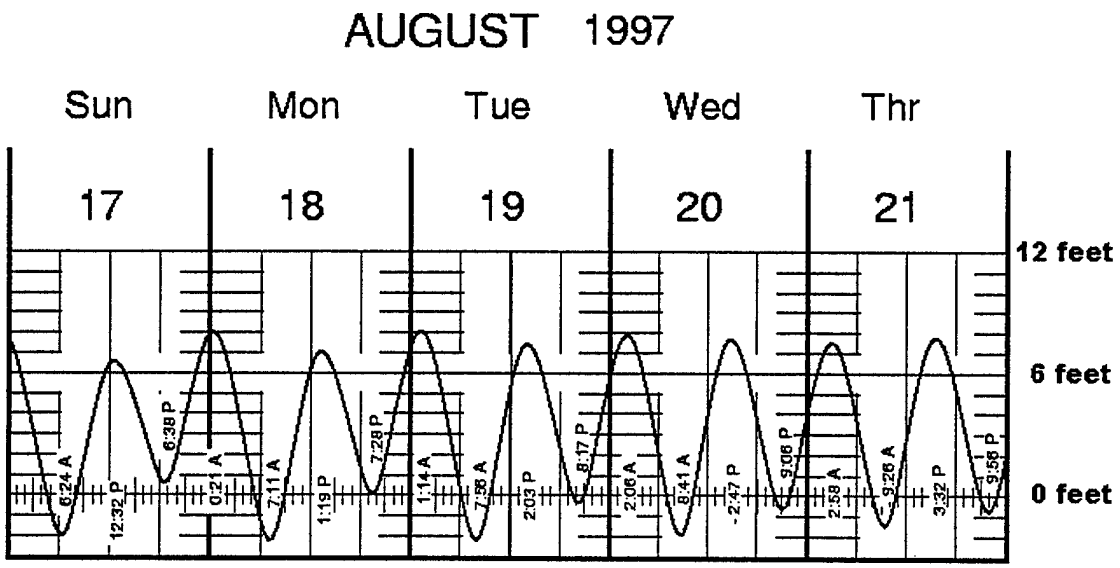

Figure 1.2-3. Tidal predictions for Pacific Beach during the period of the field experiment.

Figure 1.2-3 shows the tidal forecast for the period August 17 to 21 for Pacific Beach. It was generated using NOAA tidal constants for Aberdeen, WA, and using offsets specified for Pacific Beach. In general, these low times are 10 to 15 minutes later than in the Table. The times of high water are 2 to 13 minutes earlier.

1.2.3.3 Equipment and Logistics

Equipment used in the field program included the following:

- Two Sensor Packages (SP): each was equipped with a Sontek ADVOcean current meter, a Setra 270 pressure sensor, a Precision Navigation Model TCM2 compass/tiltmeter, and an Onset Tattletale 8 with flash memory. Additionally, one of the packages was equipped with a salinity/temperature sensor. The SPs contained internal batteries, which

automatically came on line in case power from the shore was lost.

- An in-water Junction Box to combine the electrical cables from the Sensor Packages into a single electrical cable back to the base station at the Surfcrest.
- Non-armored (SOW) electrical cable, with eight 16-gauge conductors, connected the Sensor Packages to the Junction box.
- SOW cable with twenty 16-gauge conductors was used to connect the Junction box to the onshore Array Controller (AC). This 800-meter cable was cut into three lengths to facilitate deployment. The lengths were 400m, 200m and 200m.
- An onshore Array Controller consisting of a PC computer with a multiple serial input card. It was powered through an uninterruptable power supply to allow continuous operation through a short period of utility power outage. A backup AC was on site in case of failure of the primary AC.
- An Onshore Processor (OP), consisting of a PC computer, was connected to the AC. It contained preliminary analysis software.
- Two types of DC power supplies were placed at the base station. A 120 VAC-input, DC output power supply was used to energize the array with 72 volts DC. Additionally, a series of gel-cell batteries was held in reserve in case of a failure of the onshore DC power supply or a line voltage power outage.
- The Rickshaw Surf Zone Pump for jetting in the offshore moorings.
- Two rental trucks, one 15 ft and the other 25 feet long, were used to carry the equipment to the site. The larger truck was used for storage and staging at the condominiums. The smaller truck carried equipment to and from the beach. When used at the beach, only the equipment needed for that trip was carried by the small truck. This minimized the weight of the truck to limit the likelihood of getting the truck stuck in the sand.
- The onshore computers were housed in the base unit, #14, of the condominiums.
- A 2.5 kW gas-powered electrical generator was held as a backup AC power supply for the onshore computers. It also would serve as a portable electrical source for any repairs done on the beach.
- We obtained permission from the Ocean Shores Chief of Police, Michael F. Wilson [(206) 289-3331], to drive our vehicles on the beach. He has jurisdiction over the beach north of Ocean Shores to the mouth of Conner Creek.

A complete list of the equipment used on the field program is included as Appendix 1.2-A.

1.2.3.4 Field Methodology and Sensor Positioning

Field Methodology

The two Sensor Packages, the Junction Box, and the underwater cables were installed, serviced, and recovered at low tide, thereby obviating the need for divers.

A sketch of the field site is shown in Figure 1.2-2. From a topographic map of the area (USGS, 1994) the beach alongshore orientation, at mean high water, is 354 deg. true. Field compass measurements of the alongshore orientation, made when the shoreline was 40m offshore of the high-tide line, 50m offshore of the high-tide line, and at the low-tide point on the morning of 18 August, were all within two degrees of 356 deg. true.

Laying cable from the condominiums to the low-tide deployment site was hampered by two physical features of the beach. Between the condominiums and the high tide line is a 350m stretch of partially vegetated dunes. Only footpaths crossed this area. Use of a 4-wheel drive vehicle, such as a pickup truck, would damage the vegetation. The second feature was the clam beds, which could be identified by the many holes in the sand. The beds were a swath approximately 50 m wide, about half way between the high and low tides. We could not drive a vehicle across this region without damaging the beds. Cable installation over these two regions was done by hand.

The cable from the Junction Box to shore was 800 meters long and weighed a total of 430 kg. Because of its weight, a continuous lay of this cable would be physically difficult. We chose to break the cable into three sections, each terminated with underwater connectors. One 200m section was pulled from the condominiums to midway through the dunes. The second 200m section was pulled from the high tide line back toward the condominiums, joining up with the first cable. The final 400m section was laid by truck from near the high tide line to the clam beds. From the clam beds to the low tide location, the cable was pulled by hand from the truck.

The mooring posts for the array were jetted in using the Rickshaw Surfzone Pump. At times, the pump provided low water flow or no water flow. This problem is described in the lessons learned section.

The sequence of the field activities is listed in Table 1.2-2.

Table 1.2-2. Sequence of Copalis Beach field events.

Activity	Time (PDT)	Date
Advance Team reported for duty at Surfcrest	17:00	16 Aug (Sat)
Prepared equipment for cable-laying next morning	18:00 – 19:00	
Laid 200 m cable from Base Unit toward ocean	08:00 – 10:00	17 Aug (Sun)
Placed BPS informational signs on beach	10:00 – 11:00	
Laid 200 m cable from high tide toward condominiums	10:00 – 12:00	
Lunch (Delivered to site)	12:00 – 13:00	
Follow-on Team reported for duty at Surfcrest	13:00	
Setup sighting poles onshore	14:00 – 15:00	
Installed cable posts toward low tide (at 18:38)	15:00 – 19:00	
Setup and Tested Computers in Base Unit.	14:00 – 16:00	
Tested 400 m cable, A/C and Sensor Packages	16:00 – 17:00	
Dinner (Delivered to site)	17:00 – 18:00	
Prepared equipment for Mon. AM installation	18:00 – 22:00	
Laid cable and placed J-Box at offshore-most location.	04:30 – 06:30	18 Aug (Mon)
Installed Sensor Packages	06:30 – 08:00	
Tested if Sensor Packages were up and communicating	08:00 – 09:00	
Secured cable from J-box-to-shore	08:00 – 12:00	
Evaluated output of Sensor Packages	10:00 – 16:00	
Determined current sensors were off-scale	16:00	
Attempted to recover Sensor Packages to reprogram	1800 - 20:30	
Recovered SPs, reprogrammed, and redeployed	06:00 - 09:00	19 Aug (Tu)
Recovered array and wet-end cables	06:00 – 12:00	20 Aug (Wed)
Recovered onshore cables	13:00 – 17:00	
Packed and loaded equipment	13:00 – 17:00	
Work at field site completed	17:00	

Sensor Positioning

The orientation of the Sensor Packages after the installation on 18 August was as follows:

Sensor Package #1

- This package was partially jetted into the sand. The distance from the sand to top of the package (the pressure sensor port) was 23 cm.
- The Sontek orientation mark (and the main probe line) was oriented 20 deg. true.
- The Conductivity and Temperature instrument was attached to this package.

Sensor Package #2

- This package also was partially jetted into the sand. The distance from the sand to top of the package (the pressure sensor port) was 19 cm.
- The Sontek orientation mark and main probe line was oriented at 356 deg. true.

Sensor Packages 1 and 2 Relative Orientation

- Package #1 was north of Package #2 on a 357 deg true line.
- There was a distance of 1.0 m between the centers of the two Sontek current meters.

The orientation, after the reinstallation on the morning of 19 August, is described below.

Sensor Package #1

- The distance from the sand to top of the package (the pressure sensor port) was 30 cm.
- The Sontek orientation mark and main probe line was oriented to point 337 deg. true.
- The Conductivity and Temperature instrument was attached to this package.

Sensor Package #2

- The distance from the sand to top of the package (the pressure sensor port) was 28 cm.
- The Sontek orientation mark and main probe line pointed 94 deg. true.

Sensor Packages 1 and 2 Relative Orientation

- Pkg #1 was north of Pkg #2 on a 353 deg. true line.
- Pkg #1 was 12.68 m north of Pkg #2.

1.2.3.5 Results

1.2.3.5.1 Data Acquired

Overview

The data are described in two time periods. Period 1 extends from installation at 0750 (PDT) on 18 August to the mid-experiment pulling at 0720, 19 August. The Sensor Packages were pulled on 18 August because the Sontek data did not appear correct, as observed onshore by the Onshore Processor. An improper dynamic range setting for both Sontek current meters was suggested as the cause of the poor data. Therefore, the Sensor Packages (SP1 and SP2) were pulled to reset the dynamic range of the Sonteks from 0 - 30cm/sec to 0 - 200cm/sec.

The second period, Period 2, spans from reinstallation at 0920 (PDT) on 19 August, with the new dynamic range settings, to recovery at 0750 on 20 August. The larger dynamic range setting appeared to improve data quality as observed onshore.

After the field test, it was ascertained that the Sontek on SP1 was misaligned from the Sensor Package compass by 16 degrees (counter clockwise). This error was determined by comparing field measurements of the Sontek x-axis receiver finger orientation on the Sontek probe, with the reading from the compass inside SP1. The PUV wave direction analysis from the two Sensor Packages further confirmed this misalignment; SP1 showed a 28-degree angle of incidence of the

wave train in the second collection period and SP2 showed a 12-degree angle of incidence.

In addition to the 16-degree misalignment of the SP1 Sontek with the internal compass, there may have been smaller orientation errors in both SP1 and SP2. It was noted in the field that the Sontek on SP2 was easily rotated by hand, indicating that the Sontek and its Sensor Package compass would not be tightly aligned. And the SP1 Sontek x-axis receiver finger appeared, on visual inspection, to be misaligned by a few degrees with the external markings on the package that marked the orientation of the internal compass.

The problems with Sontek orientation were many. We clearly need to re-engineer the Sontek attachment and alignment. This has been done in the new design of the Sensor Packages.

Data from Collection Period 1

Pressure, current, and conductivity/water temperature measurements were recorded on the compact flash memory in SP1 and SP2. There was incomplete data recorded onshore due to communication problems between the Sensor Packages and the Array Controller. No data were gathered onshore from Sensor Package 1 after 1848 (PDT) on 18 August. This was caused by a connector failure at the Junction Box.

During this period, most current measurements were offscale because of an improper setting of the dynamic range of the sensor (0 to 30cm/sec instead of 0 to 200cm/sec).

Data from Collection Period 2

Pressure, current, and conductivity/water temperature measurements were recorded on the compact flash memory in SP1 and SP2. There were incomplete data from SP2 recorded onshore due to communication problems between the SP2 and the Array Controller. No data from SP1 were received onshore during this period because of the connector failure at the Junction Box.

The change in the current meter dynamic range made after Period 1 to the Sontek software yielded good data.

Data Summary

Several plots of the data are presented below to summarize the data acquired. All data in these plots were extracted from the flashcard memory on each Sensor Package. Dates and times are displayed in time relative to UT (Universal Time, i.e., GMT or Zulu). The data were processed by Bob Bussey through the Array Controller and Onshore Processor software after the experiment.

Figure 1.2-4: Means from Entire Deployment

The two plots in this figure show the variation of the sub-interval (256sec) mean pressure and v-component of the Sontek data from SP1 and SP2 for the entire deployment. The v-component observations were not corrected for the 16-degree offset in SP1 noted post experiment. It is interesting to note that while the v-component data from both packages are in fair agreement during Period 1 (when the dynamic range was set too small), they diverge in Period 2. Perhaps the 16-degree misalignment of SP1 occurred only with the second deployment. Note that there

really are two time series plotted in the pressure plot; they just lie on top of one another.

Figure 1.2-5 through Figure 1.2-8: 2 Hz Time-Series Plots from Collection Period 2
These data from SP1 and SP2 are from the top-of-the-tide on 19 August at 20:26:04UT (Figures 1.1-5 and -6), and on 20 August at 08:39:01UT (Figures 1.1-7 and -8). The upper plot on each page are the pressure data, and the lower plot shows the u (solid curve) and v (dotted curve) components from the Sontek. The Sontek data have been transformed to beach coordinates (u perpendicular to the shore), and the SP1 Sontek data has been corrected for the 16-degree misalignment. These plots show the first two minutes of data in each of the two 1024sec sample periods.

These figures show that the data from SP1 and SP2 are in good agreement in both pressure and u,v velocity. SP1 leads SP2, which concurs with SP1 placement north of SP2 and the waves approaching the beach from the north-west quadrant.

A rough comparison between pressure and velocity magnitudes can be made using the shallow water equations. The approximate cross-shore velocity magnitude of a near normal wave is a function of the wave's phase speed, C_p, its surface elevation, η, and the depth, h as $u = C_p(\eta/h) = \eta(g/h)^{1/2}$, where g is the gravitational constant. From Figure 1.2-5, the first positive peak in u-velocity is approximately 60cm/sec. The associated pressure peak shows a water displacement of approximately 30cm in 230cm of depth water. Using the above relation we get a magnitude of u from η of 61cm/sec. Therefore, the pressure and current meter magnitudes are internally consistent for signals dominated by shallow water waves.

Figures 1.2-9 and 1.2-10: Power Density and Directional Spectra
These two figures show the pressure-sensor power-density spectra (PDS) and the PUV directional spectra calculated using the data partially shown in the time-series plots of Figures 1.2-5 through 1.2-8. The PDS are from an ensemble average of three 512-sec detrended, overlapping time-series sections with a Kaiser-Bessel window taper and five frequency-bins merged (merged bin-width is 0.00977 Hz). The PUV spectra were generated for the maximum frequency peak visible in the pressure PDS. Note that there are three directional spectra shown. The dotted line is the directional spectrum from SP1 before the 16-degree misalignment correction.

The two Sensor Packages are in excellent agreement. Pressure data from both packages show a noise floor of $1cm^2 \cdot sec$.

Figure 1.2-11: Pressure PDS at Different Stages of the Tide
This figure shows the effect of the rising (top plot) and ebbing (bottom plot) tide on the SP2 pressure PDS. The top-of-the-tide spectrum is shown as a heavy solid line; the rising or ebbing spectra are in light solid lines with the lowest tide spectra being indicated by light dotted lines. Every third 1024sec sample is plotted. The PDS spectra were generated as described for Figures 1.2-9 and 1.2-10.

The effect of low tide is a reduction of the energy in the wind wave frequency band (0.05 - 0.35Hz) and an increase in the 'noise floor' above 0.50Hz. At low tide the Sensor Packages are on the shoreward end of the 500^{+}m surf zone. This low-sloping beach (0.01) is dissipative so that the waves are almost completely broken at this shoreward location. Therefore the strong decrease in the wind wave energy is expected from high to low tide.

The likely source of increased energy above the wind wave band (>0.35Hz) is from the higher harmonics generated from the breaking waves. However, there is a little concern that it may be from vortex shedding off of the Sontek probe adjacent to the pressure port. The lower velocities of the flow around a cylinder, likely at low tide, generate lower-frequency vortices. A back-of-the-envelope calculation indicates that vortices with frequencies near the wind wave band could be generated.

We have chosen a 2Hz sampling rate, which yields a 1Hz Nyquist frequency. For the Setra pressure sensor, we have a 4-pole, 1Hz Butterworth filter on the pre-sampled data. These figures suggest that signals are approaching close to our Nyquist and filter cutoff at low tide!

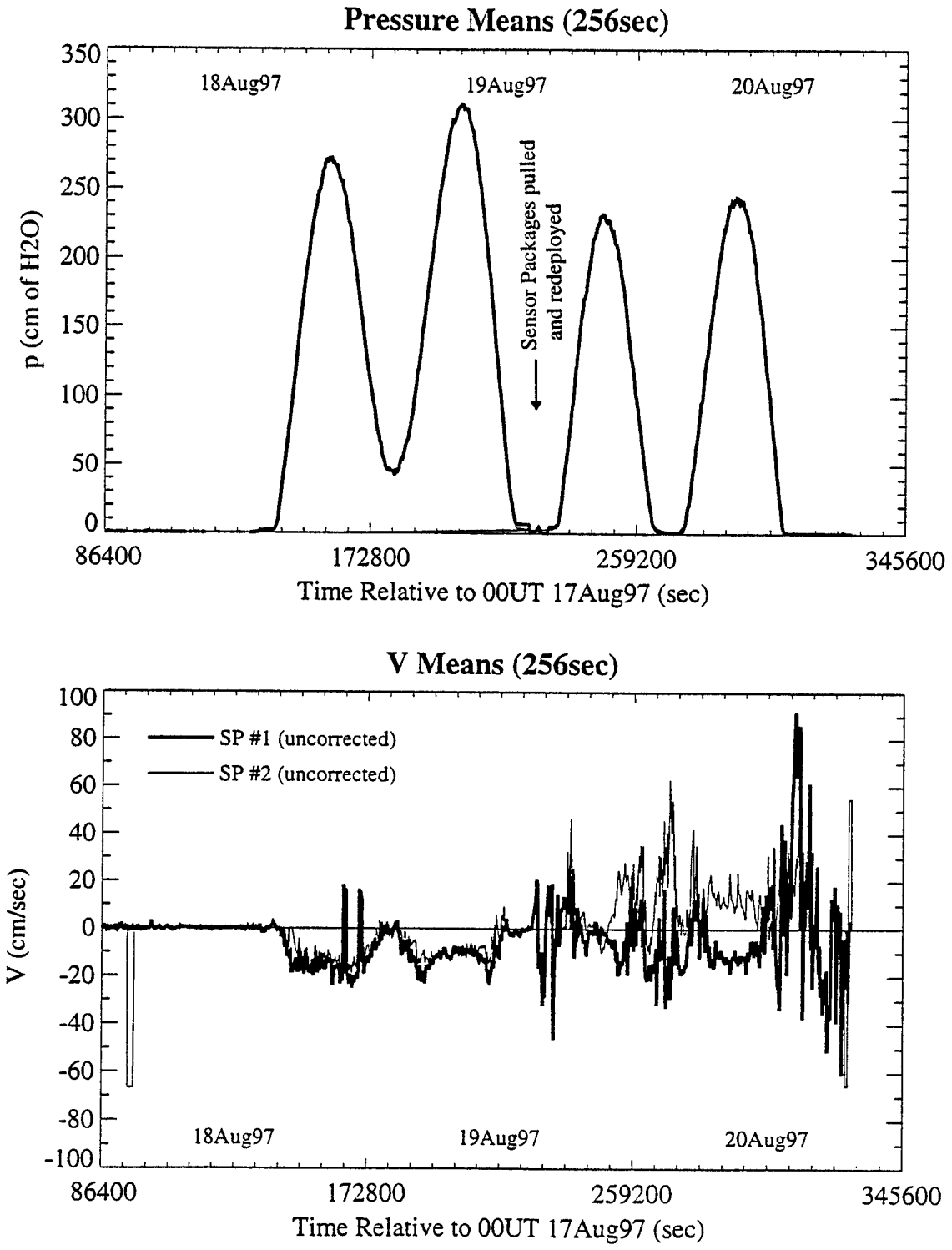

Figure 1.2-4. Pressure and velocity means for the entire deployment.

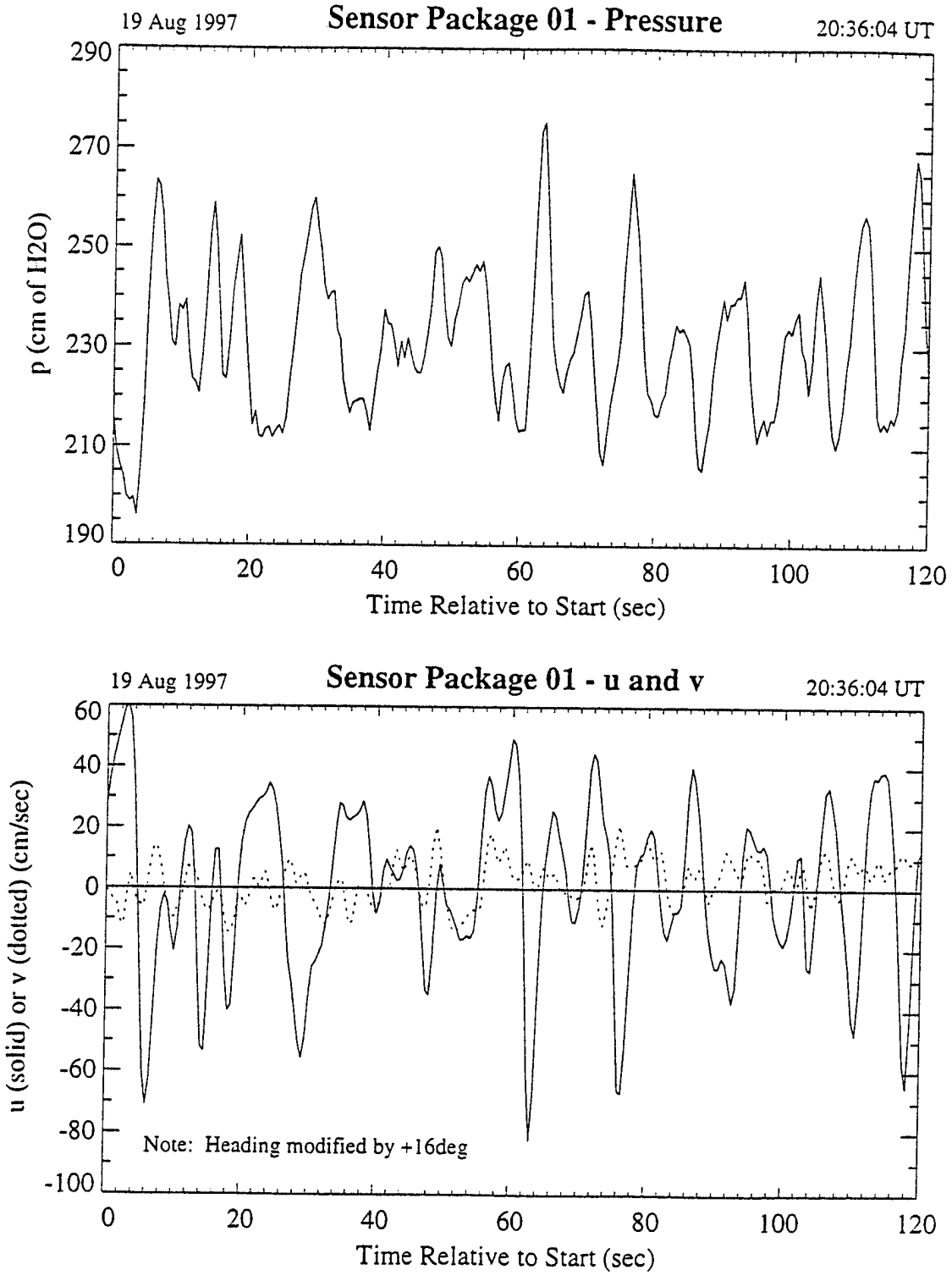

Figure 1.2-5. Sensor Package 1. Time-series plots of pressure and velocity from top of tide on 19 August 97 (2Hz sample rate).

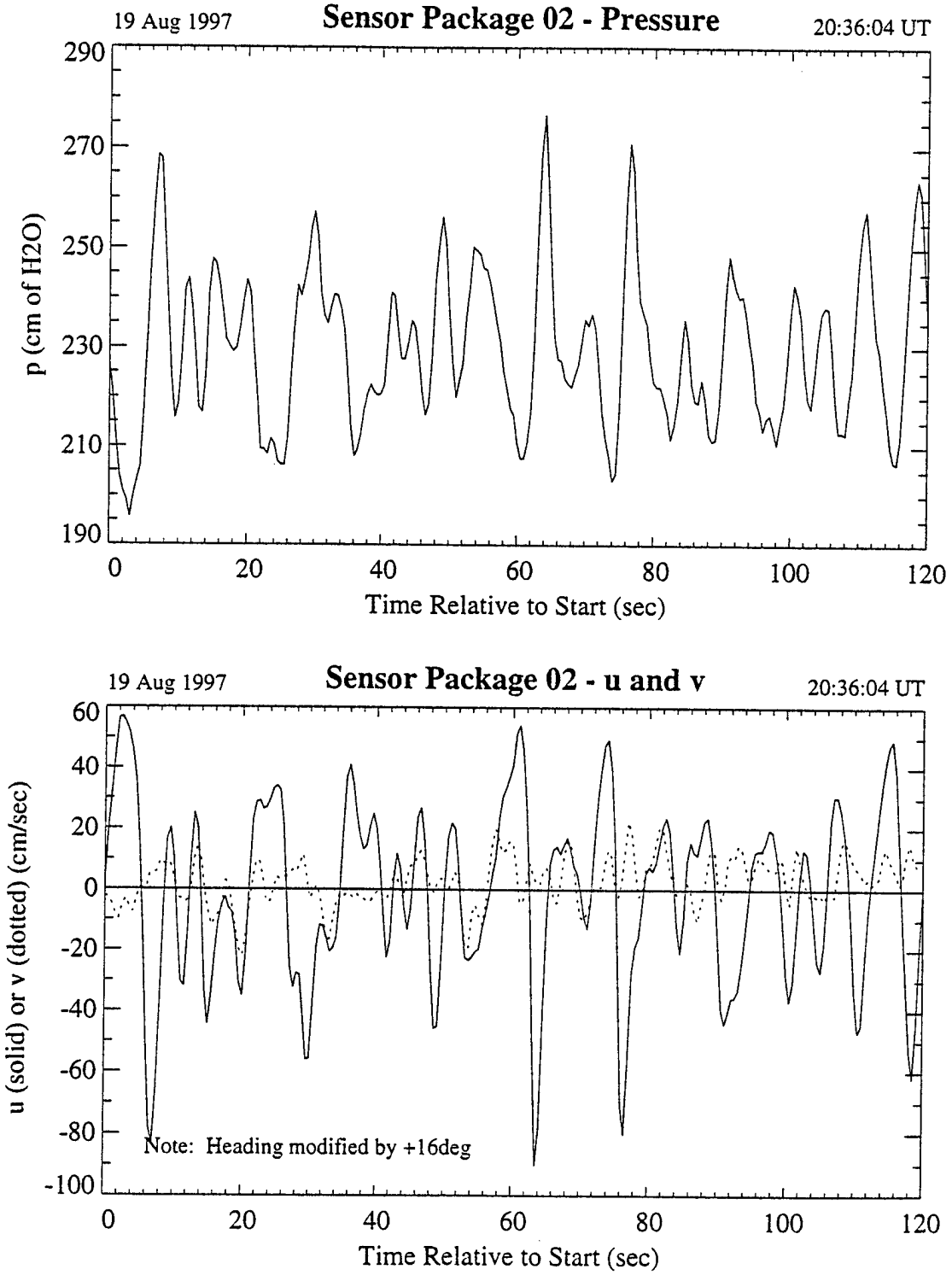

Figure 1.2-6. Sensor Package 2. Time-series plots of pressure and velocity from top of tide on 19 August 97 (2Hz sample rate).

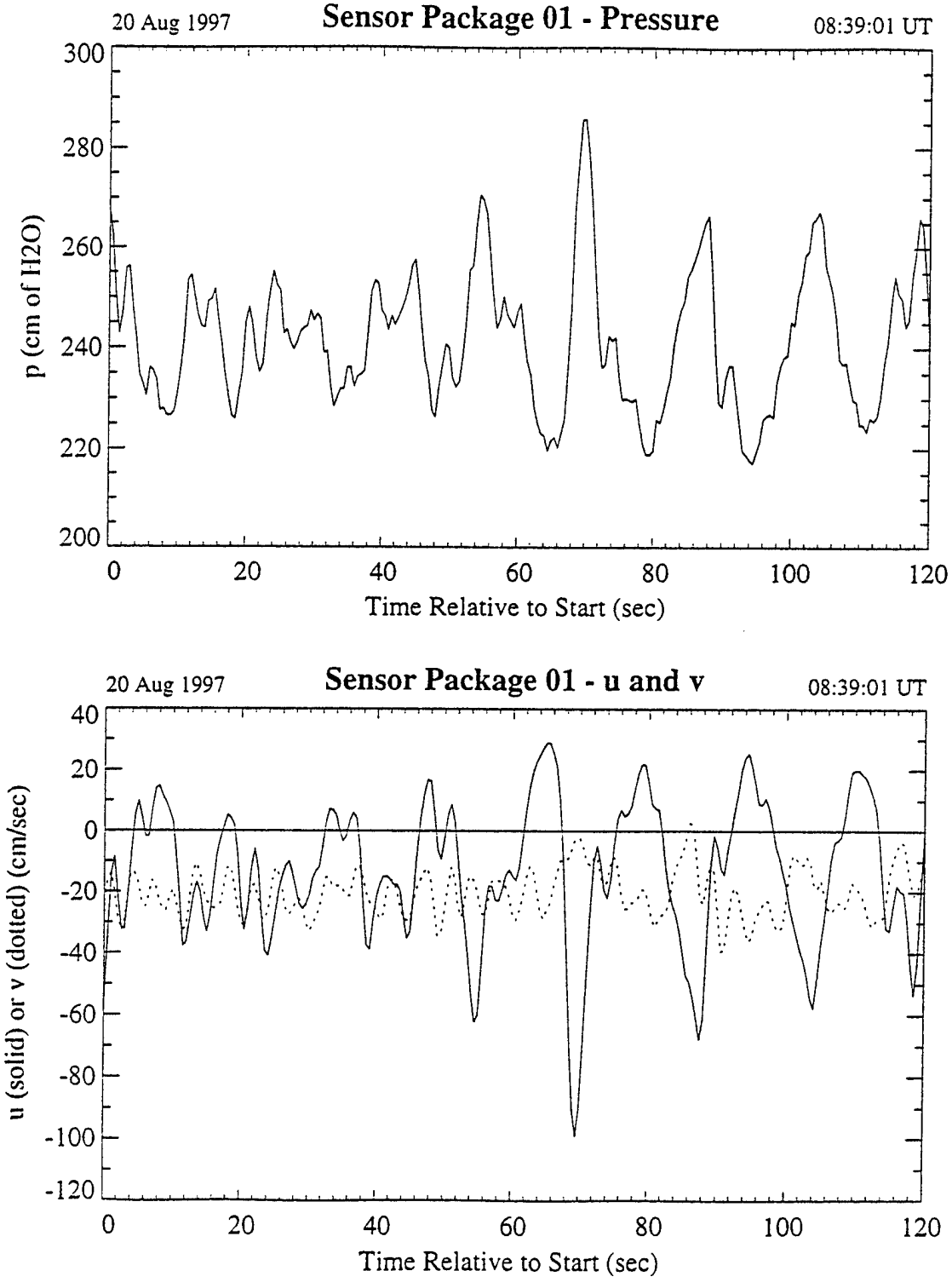

Figure 1.2-7. Sensor Package 1. Time-series plots of pressure and velocity from top of tide on 20 August 97 (2Hz sample rate).

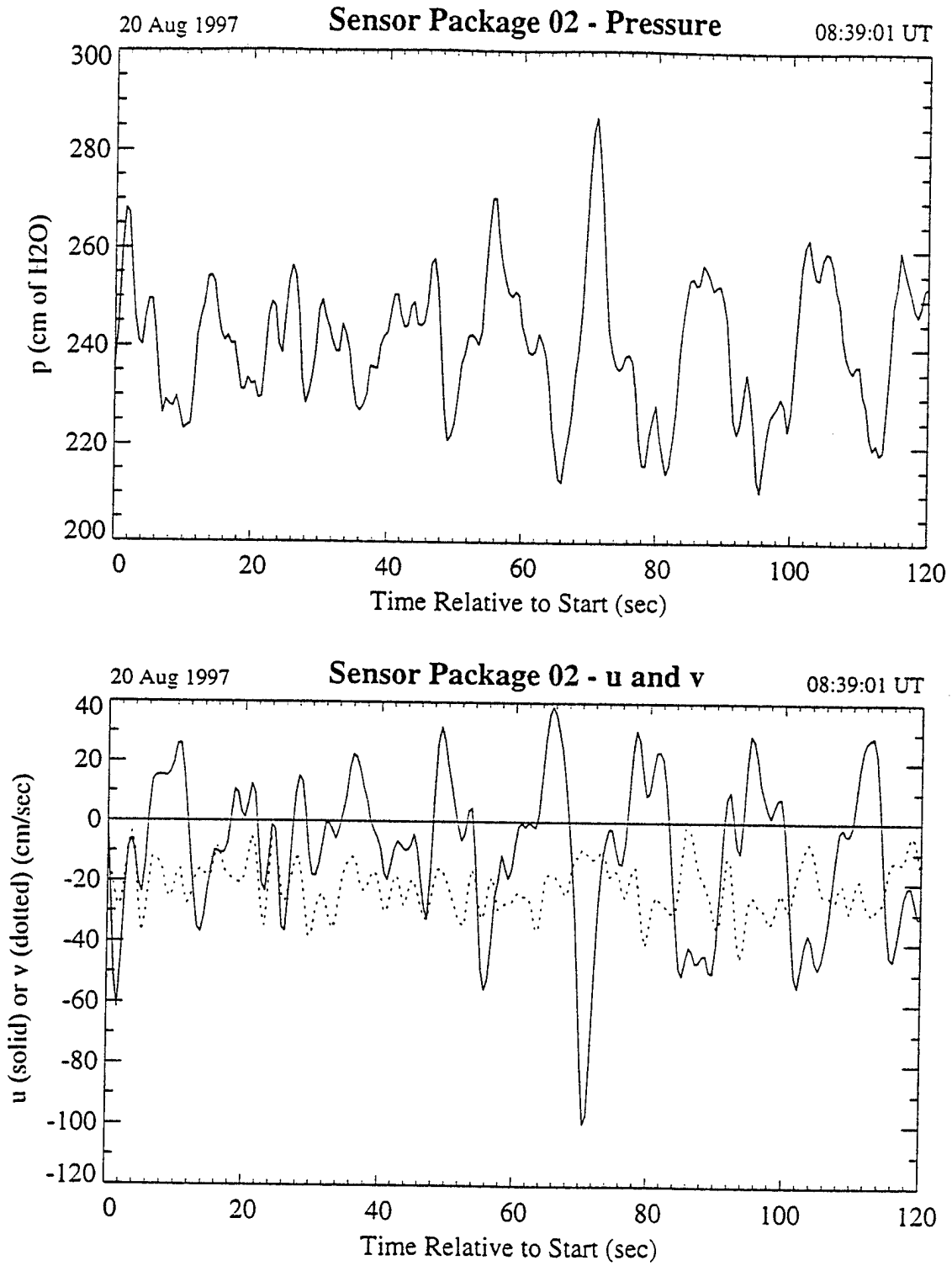

Figure 1.2-8. Sensor Package 2. Time-series plots of pressure and velocity from top of tide on 20 August 97 (2Hz sample rate).

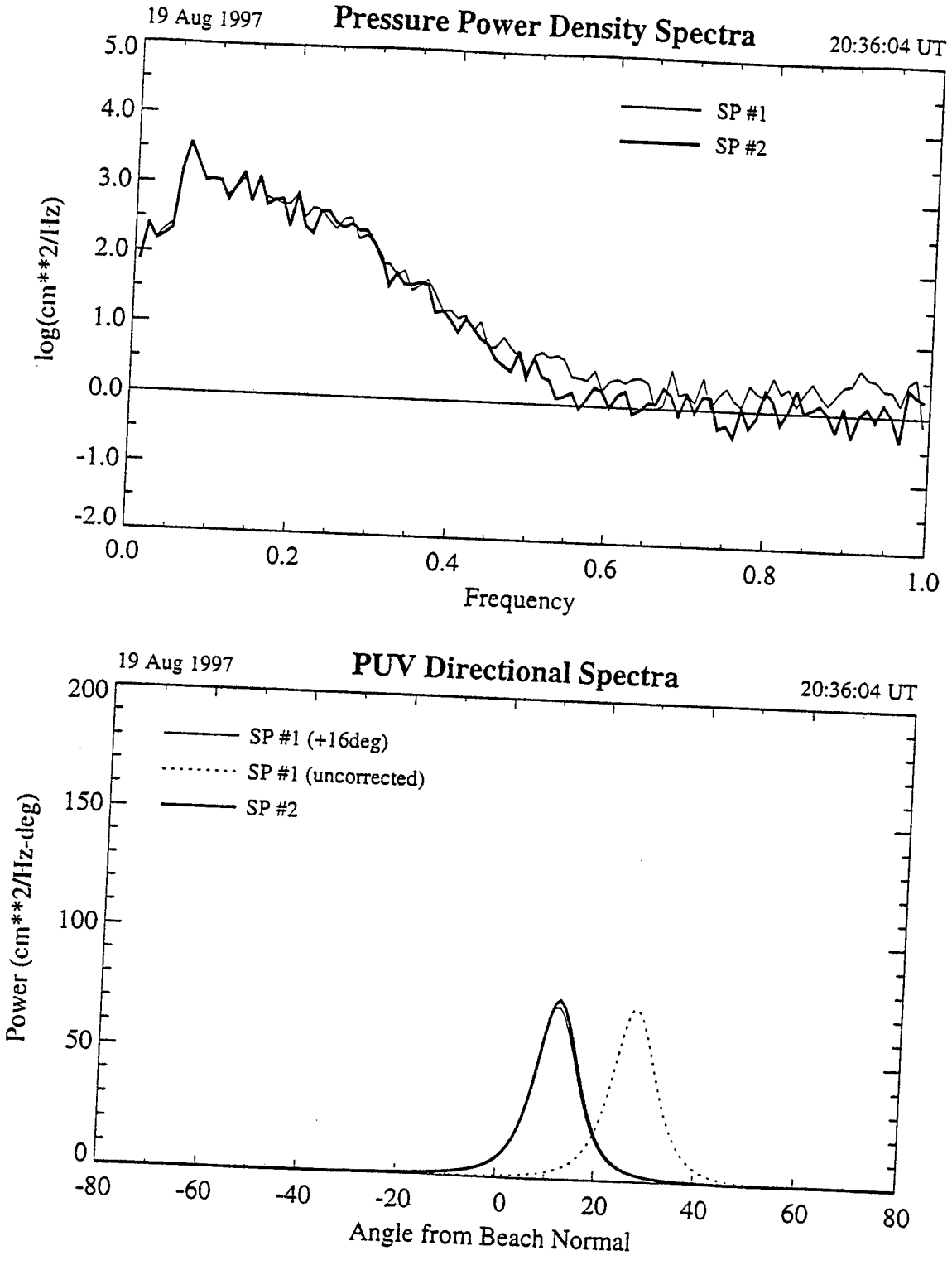

Figure 1.2-9. 19 August 97. Power density and directional spectra.

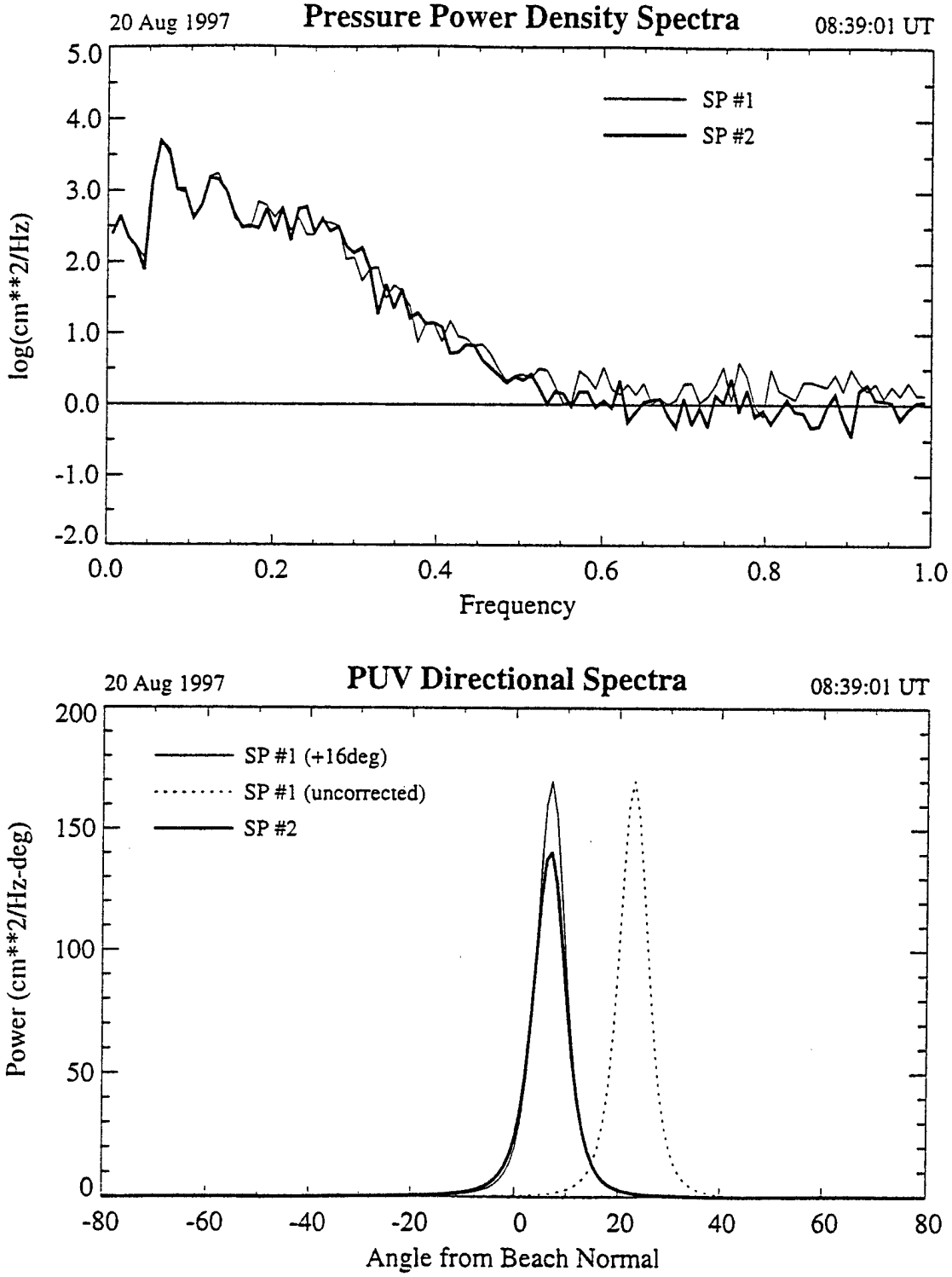

Figure 1.2-10. 20 August 97. Power density and directional spectra.

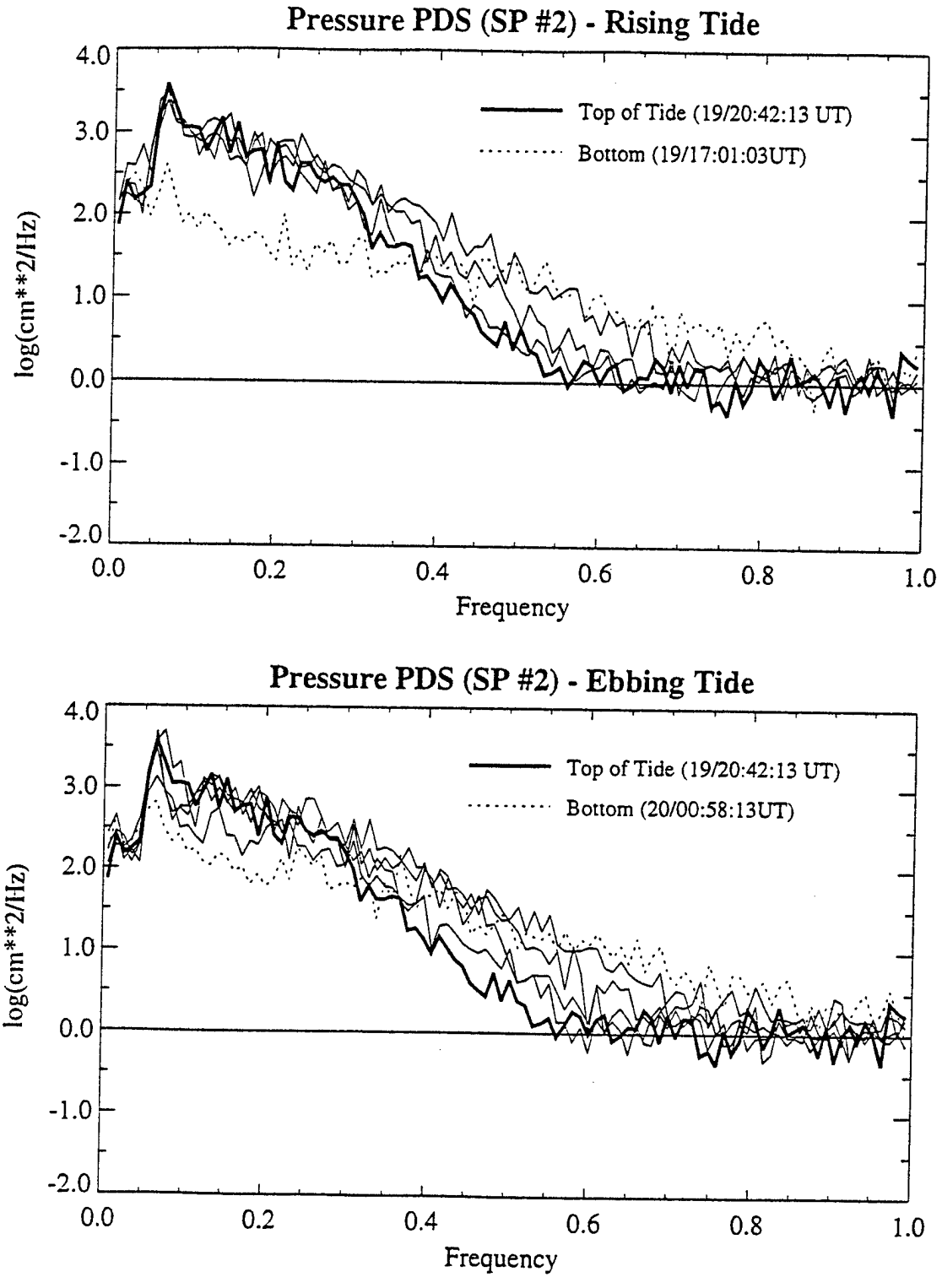

Figure 1.2-11. Power density spectra at different stages of the tide.

1.2.3.5.2 Achievement of Objectives

We met all four of our objectives for this field test. The work on each objective is described below.

Objective 1: Verify the acquisition, transmittal and recording of pressure and current data obtained from a BPS array in a nearshore wave environment.

Results: Data were acquired, transferred to shore, and were recorded on both the Array Controller and in the sensor packages. Some timing and communications problems were experienced. These are described in the "Lessons Learned" section of this report.

Objective 2: Test the suitability of the package design and mooring methodology for BPS Array field operations.

Results: From these tests we determined the cable strain relief on the sensor package requires modification. Additional details are contained in the Lessons Learned section of this report.

Objective 3: Verify the transfer-to-battery operation and internal recording when the connection to shore is disconnected.

Results: The battery operation and internal recording worked properly.

Objective 4: Train the BPS team on the installation, operation, and recovery of the BPS equipment.

Results: Accomplished – five NWRA employees and three consultants received training. The team actually received more training than originally planned because of the recovery and redeployment of the sensor packages in the middle of the experiment to reprogram the data loggers.

1.2.3.6 Problems and Lessons Learned

1.2.3.6.1 Sensor Package Hardware Design and Operation

- Problem: The connectors selected were not wet pluggable. Although we were not using divers during deployment, a problem occurred when we attempted to recover the Sensor Packages during the second low tide on 18 Aug. The bulkhead connector on the Junction Box (J-Box) became wet before the cable to shore was reconnected. The next morning during the recovery/reinstallation, one of the pins was severely corroded and was bent. This pin carried one of the RS422 wires, which led to Sensor Package 1. This conductor normally carried 5 VDC.

  Solution: We will upgrade to SeaCon wet mate-able connectors.

- Problem: The small, 8-pin Impulse connectors on the Sensor Packages and J-Box were hard to mate. We broke three of these bulkhead connectors just before or during the field operations.

  Solution: We will not use these connectors in the future (see above).

- Problem: The right-angle connectors on top of Sensor Packages caused orientation problems. We threaded the end cap instead of drilling a hole through the end cap and using a nut on the inside. Non-uniformity in the threads of the bulkhead connectors meant each hole had to be fitted to a particular connector to assure the right-angle plug could clear the probe shaft. Creep in the plastic threads or substitution of another bulkhead connector meant the alignment would be off.

  Solution: The upgrade to the SeaCon connectors will use right-angle connectors that penetrate the end cap and are fixed with a nut on the underside.

- Problem: The system used for orienting the Sontek probe with the package compass was not reliably accurate, and the probe was not positively indexed to maintain the alignment.

  Solution: The newer model Sontek probes have a re-designed probe case that will greatly ease the process of orienting the probe with the compass.

- Problem: Sensor Package #2 (SP2) had intermittent problems communicating with the Sontek current meter. Diagnostic tests back in the laboratory showed the Sontek circuit board was not operating. The probe head did function when attached to another set of circuit boards.

  Solution: Send circuit boards back to manufacturer for repair.

- Problem: When installed in the sand the morning of 17 August, two field team members in wetsuits received a shock when touching the Sontek probe on SP2. Individuals in normal clothes could not receive the shock. The shock was felt even with the shore power to the sensors turned off. No shock was found on SP1.

  Solution: The cause is not apparent. Sontek could also not understand how it was possible, but may be associated with the circuit board malfunction found in the previous problem.

1.2.3.6.2 Sensor Package Software Design

We identified a number of problems with the operation of the Sensor Packages that related to the software or a combination of hardware and software.

- Problem: When first tested, the time reset command only worked about 9 out of 10 times. Occasionally it would cause erratic behavior in the rest of the Tattletale program. We later learned that PIC-related procedures need to be single-threaded, that is, one clock-related function call cannot be interrupted by another. According to John Godley, of Peripheral Issues, this problem will result in silent failures (no notification) and indeterminate results. This is indeed what happened.

  Solution: Calls to real-time clock related routines are bracketed with commands to disable and enable interrupts.

- Problem: The clock errors were larger than had been expected; on the order of 200-300 milliseconds in the space of an hour on some occasions. Also, the difference from one unit to the next started out on 18 Aug to be as large as 26 milliseconds. This difference decreased

later in the afternoon. The largest expected difference, due to Tattletale considerations, was 2 to 3 milliseconds.

1) Explanation: A design flaw was discovered in the sensor package software that could delay servicing of an interrupt for up to 75 milliseconds.

   Solution: Redesign wait logic to enable interrupts once every millisecond.

2) Explanation: The phase-lock loop time base was cycle-slipping, causing Tattletale clocks to drift relative to each other.

   Solution: Improve the reliability of the Sensor Package time base.

3) Explanation: The Windows 95 system clock has a very coarse resolution - 18 milliseconds.

   Solution: Use the GPS board directly to drive the timing of interrupt pulses.

4) Explanation: Windows 95 employs preemptive multi-tasking. The array-controller process can be preempted by other system processes incurring delays in sending out the interrupt pulse. The average time slice on Windows 95 is 20 milliseconds. With 6 or 8 system processes running, delays of 120-160 milliseconds could be incurred.

   Solution: Increase the priority of the array-controller process to the highest possible value during the time it is waiting to send out an interrupt pulse. Microsoft provides a software interface for elevating a process to real-time status for time-critical operations.

- Problem: In one case there was no response from SP2 to a TIME_RESET message. It is possible there was a transmission error in sending this message to the Tattletale. Even a one-bit error would cause the CRC check to fail and the message would be ignored. Without a Laptop connected to the sensor package, we would not see any error messages issued.

  1) Explanation: A software delay is built into the array controller software to allow time for transmission and receipt of data before an interrupt is raised. Subsequent testing and inspection of the log files indicates that the delay was too short so that the interrupt was triggered before unit 2 had a chance to receive and process the message. In at least one case, a subsequent TIME_RESET message generated an interrupt, which completed the first transaction and forced the two units out of synchronization.

     Solution: Allow sufficient delay for all seven Sensor Packages to receive and process a TIME_RESET message before the interrupt is issued.

  2) Explanation: The time required to send out messages to all sensor packages was excessive. This was due to a particular setting in the Digiboard multiport driver.

     Solution: Change option in Digiboard driver from basic configuration 1 to basic configuration 0.

     Solution. We may want to have the Tattletale respond in some way to invalid messages.

- Problem: Buffers sent to the Array Controller would regularly be short some large number of characters.

Explanation: In several prototypes, excessive current drain was found to have resulted in low-voltage supply to the RS-422 driver chip. Examination of hexadecimal buffer contents showed contamination of groups of 40-50 bytes as well as the more obvious symptom of missing characters. This contamination could have caused short buffers as well as CRC errors.

Solution: Provide a separate regulated 5-volt power source for communication driver circuitry on the Sensor Package board.

- Problem: In one case, Vx, Vy, and Vz were all zero for an entire buffer at the onshore processor. This may be due to three buffers in a row that were short when they were received at the array controller or they had CRC errors.

  1) Explanation: The corroded connector may have caused intermittent shorts or noise on the RS-422 line.

     Solution: Wet-pluggable connectors should alleviate this problem.

  2) Explanation: see discussion of excessive current drain above.

- Problem: SP1 experienced repeated problems with buffers, which were one or two bytes short or had CRC errors. We had originally suspected that impedance mismatches in the cable was causing these errors. When we conducted the postmortem on unit 1, we found that these errors continued to occur even when the array controller was connected with a pigtail to the Sensor Package. Therefore, it appears that the cable is not the problem.

  Explanation: see discussion of short buffers above.

  Solution: We may want to revisit our decision not to retry following transmission errors.

- Problem: As a part of data evaluation, we wanted to zoom in on sections of a 17-minute time series. The Excel macro developed for this purpose turned out to be a cumbersome way to plot data.

  Solution: Have the onshore processor host Matlab plotting routines for the next field test.

1.2.3.6.3 Mooring

The attempted recovery of the Sensor Packages during the evening of 18 August identified a number of operational changes that should be made.

- Problem: The attempted recovery was done in knee-to-waist-deep water. The toolbox, approximately 200 feet away on the sand near the water's edge was not readily accessible.

  Solution: Each technician involved with installation, maintenance, or recovery should have available a basic set of tools in a fabric bag that can be strapped to his/her body. This bag would be used if the crew must operate while wading in the water.

- Problem: The wire rope strain relief for the electrical cable, between the sensor package and the junction box, was attached to the sensor package mooring post beneath the sensor

package. During deployment, the Sensor Packages were jetted about half way into the sand. This resulted in the wire rope being inaccessible during the attempted removal.

Solution: Attach the cable higher on the sensor package mooring pipe and be ready to cut the wire if it is buried in sand and otherwise cannot be removed.

- Problem: The electrical cable service-loop and strain-relief configuration at the Sensor Packages and junction box was not well defined before the field test. A makeshift arrangement, using copious quantities of tape and a wooden block, was put together the night before the deployment. The wood swelled in the water, blocking the unscrewing of a connector during the attempted recovery and thereby stalling the recovery.

  Solution: Design the strain relief as part of the revised package design. Test the revised design both in the lab and in the field prior to the next deployment.

1.2.3.6.4 Logistics

- Problem: We had little time at low tide to deploy or recover the instruments.

  Solution: We should install the Sensor Packages more shoreward of the maximum low tide line to be able to work at both ebb and flood tides with some breathing room.

- Problem: The length of the hose on the Rickshaw, 150 feet, was too short. We need more hose so we can operate at a greater shoreward distance from the water's edge.

  Solution: Mike Clifton said the unit could be operated with up to 400 feet of hose. We will have 400 feet for the next Copalis experiment.

- Problem: We found the low tide forecasts to be about 30 minutes late, relative to the data in Figure 1.2.3-1.

  Solution: We should plan accordingly.

- Problem: With the gas engine running the Rickshaw surfzone pump would occasionally cease pumping water. Water flow could be restarted for a minute by shaking the unit or could be restarted for a several minutes by moving it to a new location. We later found the bottom of the reservoir could deform upward, closing off the pump intake. This deformation was enhanced when the wheels sank into the sand, allowing the reservoir to rest on, and be pushed upward by, the sand.

  Solution: Reposition the intake farther from the bottom of the reservoir and then test the pump to verify operation.

1.2.4 The April 1998 Copalis Beach Field Test

Some elements of the BPS equipment design have changed since the August 1997 field test at Copalis Beach. These hardware changes include the mooring system, underwater connectors, the Sensor Package onboard clock, and the addition of the multiplexer electronics at the offshore J-box and on shore. Software changes in the Sensor Packages relate to communications and time coordination between Sensor Packages and the Array Controller.

Because of the above changes, we believe it prudent to perform an in-water test of the BPS system before the field program at Duck in September 1998. In addition, we want to obtain data suitable to test the analysis codes. Copalis Beach is again selected because of its accessibility from the Seattle area, the proximity of the condominiums to the water, and its relative lack of beach goers.

The objectives of the April 98 Copalis Beach tests are to:

1. Verify the acquisition, transmittal, and recording of pressure and current data obtained from a BPS array in a nearshore wave environment. The emphasis here is multiplexer function, system time coordination, and communications from five to seven Sensor Packages simultaneously.
2. Test the suitability of the new package design and mooring methodology for BPS Array field operations.
3. Obtain data to test the Onshore Processor's data analysis and inverse model software.
4. Provide additional field training for the BPS team on the installation, operation, and recovery of the BPS equipment.
5. Compare the level of biofouling and corrosion between different Sensor Package halo materials.
6. Test the sensitivity of the pressure sensor signal to vortex shedding off the Sontek probe and the halo structure.

The field methods and schedule will be similar to those used during the August 1997 tests:

- We will use two rental trucks for transport and onsite storage, one open bed (1-1/2 ton) truck, and one 15' closed truck.
- The work will be completed within a one-week lodging rental period.
- The data will be recorded and the system will be powered from one of the condominium units.

Significant differences from Copalis Beach 97 are:

- We will deploy five to seven Sensor Packages instead of two.
- Data analysis codes are further along for testing real-time processing.
- We are using new electric cable and plugs.
- We have a different mounting system design and a new Sensor Package clock.
- Sensor Package and Array Controller software bugs observed at Copalis 97 have been fixed.

APPENDIX 1.2-A

EQUIPMENT FOR BPS FIELD TEST, AUGUST 1997, COPALIS, WA

Item	Quantity
Sensor Package Systems	
Sensor Packages (one with CT sensor) with internal batteries	2
Cable, Tattletale to PC download	2
Battery pucks for SPs, spare	3
Junction Box	1
Onshore sensor package simulator	1
Onshore Power supplies, AC to DC	2
Onshore gelcell batteries, 12 V with harness to produce 72V	6
Chargers for gelcells	3
Memory, Compact flash, 15 MB	3
Underwater Cables	
Cable, JB to shore, 20 cond., w conn., 800 m (3 pieces)	1
Cables, SP to JB, 8 conductor, w connectors, coils	3
Cable, SP to CT sensor	1
Spare cables and connectors, set	1
Mooring Equipment	
Mooring posts for Sensor Package, Al. Channel, 8 ft	3
Rubber and hose clamps for Mooring posts	3
Mooring pipes for cable, 1.5" x 1.5 m, galvanized	7
Cable support grips,	8
3/16" dia aircraft cable (wire rope) between SP & JB. (strain relief)	2
Nicopress tool and spare sleeves for cables above	1
Marker Floats	7
Mooring pipes and attached mooring lines for floats	7
Installation Equipment	
Cable reel stand	2
Slide hammer (as backup)	1
Stuck-vehicle equipment	
Plywood sheets, come-along, sand anchors (2)	
Shovels (2), hand winch, set	1
2.5 KW generator to run heat gun and computers	1
Precision compass (pocket transit)	1
Garden Carts	3
Sighting Poles	2
BPS info signs and poles	6

Binoculars	1
Rickshaw and Related Equipment	
Rickshaw	1
Gasoline can	2
Ramps for pickup	2
Firehoses, 50 ft lengths	4
Wand, 1"dia. PVC sched. 80, 6 ft	1
Wand, 1"dia. PVC sched. 80, 8 ft	1
Wand, 1"dia. PVC sched. 80, 10 ft	1
Wand spare parts, set	1
Big pipe wrenches	2
20 W 50 motor oil, quarts	2
Rickshaw spare hardware bits	1
Array Controller and Onshore Processor Equipment	
Array controller computer with monitor, cables, and software	2
Array controller software, installed in above	2
Backup of array controller software, on floppy disks	1
Onshore Processor computer with monitor	1
Onshore Processor Software	1
Backup of Onshore Processor software, on floppy disks	1
Laptop with Zip drive and PCMCIA card reading software	1
Laptop with network capability	1
Printer, color (with paper and spare ink)	1
"T" Box to share printer, with 4 cables	1
Uninterruptable Power Supply	2
Zip Disks	10
Signal Generator	1
Set-up Tables (for computers)	2
Documentation for All equipment and Software, set	1
General Support Equipment	
Toolbox with tools	2
Heat gun	1
First aid kit	1
Truck, large, rental, 25 ft, for storage	1
Truck, small, rental, 14 ft, for beach	1
Stepladders, 3 and 5 ft tall	2
NWRA Phone list	each person
Garden/Work gloves, misc. sizes	12
Booties, wet suit, pairs	3
Surf suits	2
Tape measure, fiberglass, 50 ft and 100 ft	2

Radios, Walkie-talkie	3
Cell phone	1
Sledgehammer	1
Duct tape, rolls	2
Silicone Spray for connectors, can	3
O-ring grease, tube	2
WD-40 Penetrating oil	2
Scotch 33 tape, rolls	12
Tie wraps, 100 ea of 3 sizes	3
Driver Drill with bits	1
Hand truck	1
Dolly	1

1.3 Task 3: BPS Software Development and Testing

1.3.1 Overview

In the April 1997 Semi-Annual Report, we listed the Task-3 milestones and objectives to be met by the end of the six-month reporting period. These are listed again below.

1) Complete code implementation for the Sensor Package Field Tests (full implementation on the Sensor Package Controllers, partial implementation on the Array Controller and Onshore Processor).
2) Participate in the Sensor Package Field Tests. Modify code implementation and design as indicated by results of these tests.
3) Update Volumes 1 and 2 of the BPS Software Documentation, and create Volume 3 to cover description of the software implementation in the Array Controller (move sections from Volumes 1 and 2 which discuss the Array Controller software).

Presented below is a brief discussion of the status of these efforts with an outline of the results or a direction to the locations in this report with more detailed discussions.

1) Complete code implementation for the Sensor Package Field Tests, and
2) Participate in the Sensor Package Field Tests. Modify code implementation and design as indicated by results of these tests.

   Done. Code was in place to acquire data on the flash memory within each Sensor Package and to transmit and acquire data to both the Array Controller and Onshore Processor.

3) Update Volumes 1 and 2 of the BPS Software Documentation, and create Volume 3 to cover description of the software implementation in the Array Controller.

   Volume 1 has been updated, Volumes 2 and 3 will be updated this biennium. These documents are living documents in that they are expected to be continuously modified. Copies of these documents are available upon request.

1.4 Task 4: BPS Hardware Development and Testing

1.4.1 Overview

In the April 1997 Semi-Annual Report, we listed the Task-4 milestones and objectives to be met by the end of the six-month reporting period. These are listed again below.

1) Receive and test the *Rickshaw* jetting system.
2) Build two Sensor Packages, one Onshore Array Controller, and one Junction Box.
3) Integrate the Sensor Package hardware and software.
4) Perform bench tests and in-water tests of the Sensor Packages and Array Controller.

5) Update the BPS Hardware Documentation.

Presented below is a brief discussion of the status of these efforts with an outline of the results or a direction to the locations in this report with more detailed discussions.

1) Receive and test the *Rickshaw* jetting system.

The Rickshaw was delivered, tested at a local lake beach, and used to deploy instruments at the Copalis field test in August 1997. We had some problem with suction that was identified post experiment to be caused by the flexing of the reservoir pan and the concomitant sealing of the intake port. This design problem is understood and will be corrected before the April 1998 Copalis field test.

2) Build two Sensor Packages, one Onshore Array Controller, and one Junction Box.

Done. These packages were deployed at the August 1997 Copalis field test. Data were collected; packages were water tight. We nonetheless have made several design changes to the packages based on the test experience. These changes are presently being finalized and will be reported in the next semi-annual report.

3) Integrate the Sensor Package hardware and software.

Done. Data were both collected on flash memory within each Sensor Package and transmitted and collected at the onshore Array Controller.

4) Perform bench tests and in-water tests of the Sensor Packages and Array Controller.

Some bench tests were performed before deployment at the Copalis August 1997 field test. However, time constraints did not permit a full set of bench tests or in-water tests.

5) Update the BPS Hardware Documentation.

Postponed until the hardware design is finalized.

1.4.2 Sensor Package Hardware and Mounting-System Design

A number of design decisions were finalized during this reporting period. The experience gained at Copalis 97, the testing subsequent to that field test, and our visit to Sandy Duck 97 were used to re-evaluate the existing design. A schematic of the Sensor Package and mounting system design (as of Nov 97) is shown in Figure 1.4-1. Some minor changes made since this drawing will be presented at the next Advisory Panel meeting.

A brief summary of the major design decisions is presented below.

- We have decided to use the Sontek ADVO as our current meter instead of the Marsh-McBirney EMCM.

- We reaffirmed the single-package concept for the Sensor Packages. The alternative was a two-package concept, with the Sontek ADVO current probe mounted separately from the rest of the elements of the sensor package. The fewer number of cable connections (and therefore

potential failures), and the ease of installation and recovery of the single package were the major determinants of this package concept.

- The Sensor Packages will be mounted on steel pipe rather than the aluminum channel used at Copalis 97. This methodology, well tested at the FRF, allows installation by jetting through the mooring pipe. A section of non-magnetic stainless steel pipe may be used at the top of the mooring pipe to eliminate interference with the compass. We will test compass interference before finalizing this aspect of the design.

- We will not require the sensor packages be adjustable vertically on the mooring pipes after installation. If sand is eroded or deposited at the site sufficient to require vertical repositioning, the mooring pipe will be rejetted up or down. We were motivated in this direction by the simplicity of the mooring design that such a decision affords and by the concomitant robustness of the design (fewer potential failure points).

- The difficulties with the accuracy of the clock onboard the Sensor Packages observed at the Copalis 97 test motivated us to find a more reliable clock. We selected an ovenized clock. This clock will provide relative time-synchronization accuracy among an array to nominally 20msec over a period of three weeks. The increase in power consumption is not significant (it did not require a redesign of the power system). Additionally, we will retain the ability to reset the clocks from shore.

- The Sontek sensor probe will be protected by a "halo" similar to that used by Kent Hathaway at the FRF. However, our halo will be mounted to the body of the sensor package rather than to the probe shaft. This halo will provide further strength and also serve as our mounting frame.

- We will use underwater mateable connectors. The ones selected are the flat "All Wet" SeaCon series by Brantner.

- We will use polyurethane-covered electrical cable (0.5 inch diameter) to power and transmit data from the onshore Array Controller to the underwater Junction Box and between the Junction Box and the Sensor Packages. This cable is designed to our specification at a cost of $1.20/foot (similar to the cost of used steel-armoured cable). It has three twisted pairs of 22-gauge wires for data transmission and one twisted pair of 16-gauge wire for power. Surrounding the wires is woven Kevlar braid providing tensile strength on the order of 600 lbs. The Brantner connectors will be spliced onto this electrical cable. This cable is 40% lighter than armoured cable, thus allowing us to more easily handle it on a beach without the help of heavy equipment. Our testing showed that twisted pairs were necessary to multiplex the data at the Junction Box to the Array Controller; multiplexing was desired to reduce the number of wires. The more commonly used well-logging (armoured) cable and neoprene-covered "SO" cable do not have twisted pairs. The ability to specify twisted pairs and the lightness of the cable were the significant factors in our decision to use this cable.

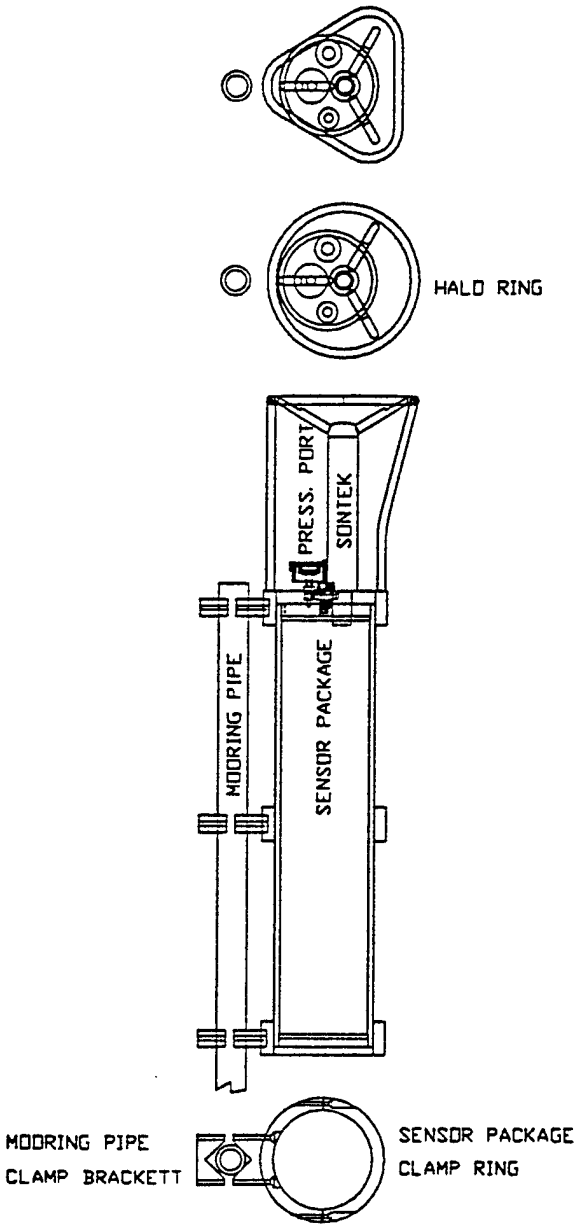

Figure 1.4-1. Schematic of the Sensor Package and mounting system design.

2.0 ANTICIPATED WORK DURING 1 OCTOBER 1997 – 30 MARCH 1998

2.1 Task 1: Concepts and Algorithm Development

- Expand the Template Matching Technique (TMT) library to include templates derived from two-slope depth profiles.
- Investigate, using simulated data, both the resolution of the beach slope estimates and the effects of nonplanar bathymetry on the two-slope beach estimation, its uniqueness, and its stability.
- Study the effect of array geometry on the solution.
- Compare the solution for edge wave analytic perturbation expansion against numerical solutions investigating issues such as the effect of the choice of the zeroth-order two-slope profile on the first-order correction.
- Prepare the wind wave analysis software for transition to the BPS Operation Software.
- Modify the TMT to allow for the presence of longshore currents.
- Design the array geometry and offshore placement for Copalis Beach field test and Field Campaign #1 (at Duck, NC).

2.2 Task 2: Field Campaign #1 – Depth Profile and Current Resolution

- Complete logistics preparation for the April 1998 Copalis Beach field test.
- Design the Duck Field Campaign sensor and cable layout.
- Coordinate with the FRF staff on cross-shore array deployment, data acquisition, and general support.

2.3 Task 3: BPS Software Development and Testing

- Finalize Sensor Package software design.
- Finalize Array Controller software design.
- Finalize Onshore Processor software design.
- Complete code implementation of the Onshore Processor QC up through and including basic statistics.
- Build a prototype QC display for the Copalis 98 field test.
- Update the BPS Software Documentation.

2.4 Task 4: BPS Hardware Development and Testing

- Finalize Sensor Package hardware design.
- Finalize Sensor Package mounting-system design.
- Purchase Sontek current meters and other Sensor Package components.
- Build two to five Sensor Packages and one junction box (for testing at the Copalis field site).
- Perform bench and in-water tests of the Sensor Packages and the Array Controllers.

2.5 Task 7: Management, Planning, and Reporting

- Monthly monitoring of milestones and expenditures.
- Weekly meetings with Task Leaders to maintain good communication and coordination among the tasks.
- Hold an Advisory Panel meeting to review methods and procedures before the Copalis (March 1998) experiment.